INFLUENCE OF CURVATURE UPON THE HEAT TRANSFER FROM CYLINDERS TO GAS STREAMS PARALLEL TO THE AXIS

WILLIAM TESSIN

Mont 28

Artisan Gold Lettering & Smith Bindery

593 - 15th Street · Oakland, Calif. GLencourt 1-9827

DIRECTIONS FOR BINDING

BIND IN
(CIRCLE ONE)

BUCKRAM
COLOR NO. 8854

FABRIKOID
COLOR

LEATHER
COLOR

OTHER INSTRUCTIONS

Letter in gold.
Letter on the front cover:

INFLUENCE OF CURVATURE UPON THE HEAT
TRANSFER FROM CYLINDERS TO GAS STREAMS
PARALLEL TO THE AXIS

WILLIAM TESSIN

shelf
LETTERING ON BACK TO BE EXACTLY AS PRINTED HERE.

TESSIN

1951

THESIS
T34

DUDLEY KNOX LIBRARY
NAVAL POSTGRADUATE SCHOOL
MONTEREY, CALIFORNIA 93943-5002

March 28
8554

Library
U. S. Naval Postgraduate School
Annapolis, Md.

Library
U. S. Navy Postgraduate School
Monterey, Calif.

ILLINOIS INSTITUTE OF TECHNOLOGY

INFLUENCE OF CURVATURE UPON THE HEAT TRANSFER FROM CYLINDERS TO GAS STREAMS PARALLEL TO THE AXIS

BY

WILLIAM TESSIN
Commander, U.S. Navy

Submitted in Partial Fulfillment of the
Requirements for the Degree of
Doctor of Philosophy in Mechanical Engineering
in the Graduate School of
Illinois Institute of Technology

CHICAGO, ILLINOIS

June, 1951

T34

14829

ACKNOWLEDGEMENT

My debt to the United States Navy and my gratitude to Dr. Max Jakob are hereby acknowledged.

William Tessin

TABLE OF CONTENTS

		Page
ACKNOWLEDGEMENT		iii
LIST OF TABLES		v
LIST OF ILLUSTRATIONS		vii
NOMENCLATURE		x
Chapter I.	INTRODUCTION	1
II.	THEORETICAL CONSIDERATIONS	4
III.	PREVIOUS INVESTIGATIONS	11
IV.	APPARATUS AND INSTRUMENTATION	20
V.	PRELIMINARY TESTS AND INVESTIGATIONS	38
VI.	EXPERIMENTATION AND DATA	44
VII.	PHYSICAL PROPERTIES AND OTHER CONSTANTS	66
VIII.	METHOD OF CALCULATION	68
IX.	EXPERIMENTAL RESULTS	92
X.	CORRELATION FOR THE MEAN SURFACE COEFFICIENT	125
XI.	THE LOCAL SURFACE COEFFICIENT	139
XII.	THE EFFECT OF SURFACE CURVATURE	148
XIII.	SUMMARY AND CONCLUSIONS	153
Appendix I.	VOLT BOX MODIFICATION	156
II.	CALIBRATION OF WESTON SHUNT	159
III.	CALIBRATION OF THERMOCOUPLES	163
IV.	CALROD SURFACE TEMPERATURE EXPLORATION	164
BIBLIOGRAPHY		171

LIST OF TABLES

Table		Page
I.	Critical Reynolds Number for Flat Plates....	11
II.	Exponent for Prandtl Number.....	12
III.	Exponent for Reynolds Number.....	13
IV.	Values of C_o' for Air.....	16
V.	Summary of Previous Investigations.....	17
VI.	Impressed Heater Voltage.....	50
VII.	Electric Heating Current.....	51
VIII.	Initial Air Stream Velocity Data.....	52
IX.	Initial Air Stream Temperature Data.....	53
X.	Temperature Distribution Data.....	54
XI.	Total Heat Input.....	69
XII.	Hydrodynamic Starting Lengths.....	83
XIII.	Corrected Temperature Distribution Data.....	85
XIV.	Calculation of Vibration Data.....	98
XV.	Comparison of Vibration and Parallel Flow Results.....	95
XVI.	Experimental Results, Series A Runs.....	115
XVII.	Experimental Results, Series B Runs.....	117
XVIII.	Experimental Results, Series C Runs.....	119
XIX.	Experimental Results, Series D Runs.....	120
XX.	Experimental Results, Series E Runs.....	121
XXI.	Experimental Results, Series X Runs.....	122
XXII.	Experimental Results, Series V Runs.....	124
XXIII.	Calculated Results for Correlation Purposes.....	129
XXIV.	Comparison of Surface Configuration Function Values.....	128

LIST OF TABLES, Continued

Table		Page
XXV.	Comparison of Local Surface Coefficients....	145
XXVI.	Comparison of Surface Configuration Functions.....	147
XXVII.	Deviation of Surface Configuration Functions.....	147

LIST OF ILLUSTRATIONS

Figure		Page
1.	Illustration of Boundary Layers	9
2.	Arrangement of Apparatus	23
3.	Vibration Controls	24
4.	Fabrication of Heat Transfer Surface	25
5.	Heat Transfer Element Details	30
6.	Centering Device	37
7.	Calrod Heater Test Data	43
8.	Temperature Distribution Data, Series A Runs	61
9.	Temperature Distribution Data, Series B Runs	62
10.	Temperature Distribution Data, Series C Runs	63
11.	Temperature Distribution Data, Series D Runs	64
12.	Temperature Distribution Data, Series E Runs	65
13.	Experimental Results, Thermal Length of Four Inches	99
14.	Experimental Results, Thermal Length of Eight Inches	100
15.	Experimental Results, Thermal Length of Twelve Inches	101
16.	Experimental Results, Thermal Length of Sixteen Inches	102
17.	Experimental Results, Thermal Length of Twenty Inches	103
18.	Experimental Results, Thermal Length of Twenty-four Inches	104
19.	Experimental Results, Thermal Length of Twenty-eight Inches	105

LIST OF ILLUSTRATIONS, Continued

Figure		Page
20.	Experimental Results for Starting Length of 0.49 Inches, Laminar Flow	106
21.	Experimental Results for Oblique Cross Flow, Thermal Length of Sixteen Inches	107
22.	Experimental Results for Vibrations, Thermal Length of Sixteen Inches	108
23.	Comparison of Vibration and Oblique Cross Flow Data for Thermal Length of Four Inches	109
24.	Comparison of Vibration and Oblique Cross Flow Data for Thermal Length of Eight Inches	110
25.	Comparison of Vibration and Oblique Cross Flow Data for Thermal Length of Twelve Inches	111
26.	Comparison of Vibration and Oblique Cross Flow Data for Thermal Length of Sixteen Inches	112
27.	Comparison of Vibration and Oblique Cross Flow Data for Thermal Length of Twenty Inches	113
28.	Comparison of Vibration and Oblique Cross Flow Data for Thermal Length of Twenty-four Inches	114
29.	Surface Configuration Data	130
30.	Correlation Results for Thermal Length of Four Inches	131
31.	Correlation Results for Thermal Length of Eight Inches	132
32.	Correlation Results for Thermal Length of Twelve Inches	133
33.	Correlation Results for Thermal Length of Sixteen Inches	134
34.	Correlation Results for Thermal Length of Twenty Inches	135
35.	Correlation Results for Thermal Length of Twenty-four Inches	136
36.	Correlation Results for Thermal Length of Twenty-eight Inches	137

LIST OF ILLUSTRATIONS, Continued

Figure Page

37. Correlation of all Results..... 138

38. Influence of Curvature..... 150

NOMENCLATURE

LATIN LETTER SYMBOLS

Symbol	Definition	Unit
A	Area of a cross-section	ft^2
a_A	Equation constant	
a_B	Equation constant	
a_k	Equation constant	
a_o	Equation constant	
B_o	Corrected barometric height	in. of Hg
b	Boundary layer thickness	ft
b_A	Equation constant	
b_B	Equation constant	
b_k	Equation constant	
b_K	Equation constant	
b_o	Equation constant	
C	Circumference	ft
C_o	Equation constant	none
C_o'	Equation constant	none
C_o''	Equation constant	none
C_s	Equation constant	none
c	Specific heat at constant pressure	B $lb^{-1}F^{-1}$
F	Curvature correction factor applied to results for a flat plate	none
F_x	Heat release correction factor for computation of h_m	none
F_x'	Heat release correction factor for computation of h	none

Symbol	Definition	Unit
H	Velocity head	in. of water
h	Local surface coefficient of heat transfer by convection	B $hr^{-1}ft^{-2}F^{-1}$
h_m	Mean surface coefficient of heat transfer by convection	B $hr^{-1}ft^{-2}F^{-1}$
h_r	Surface coefficient of heat transfer by radiation	B $hr^{-1}ft^{-2}F^{-1}$
K	Curvature	ft^{-1}
k	Thermal conductivity of air	B $hr^{-1}ft^{-1}F^{-1}$
k_w	Thermal conductivity of a tube-wall material	B $hr^{-1}ft^{-1}F^{-1}$
k_x	Thermal conductivity of the material of a cross-section	B $hr^{-1}ft^{-1}F^{-1}$
L	Total characteristic length	ft or in.
L'_a	Illustrative length	
L'_b	Illustrative length	
L_c	Illustrative length	
L_n	Nosepiece length measured between perpendiculars	ft or in.
L_t	Length of a tube	ft.
M	Heat release length of a heating coil	in.
m	Exponent for a surface configuration function	none
N_{Nu}	Nusselt number in general	none
$(N_{Nu})_L$	Nusselt number, $(h_m L)/(k)$	none
$(N_{Nu})'_L$	Nusselt number, $(hL)/(k)$	none
$(N_{Nu})_x$	Nusselt number, $(h_m x)/(k)$	none
$(N_{Nu})'_x$	Nusselt number, $(hx)/(k)$	none

Symbol	Definition	Unit
(N_{Pr})	Prandtl number, $(c\mu)/(k)$	none
N_{Re}	Reynolds number in general	none
$(N_{Re})_c$	Upper critical Reynolds number	none
$(N_{Re})'_c$	Lower critical Reynolds number	none
$(N_{Re})_L$	Reynolds number, $(v_o L)/(\nu_o)$	none
$(N_{Re})_x$	Reynolds number, $(v_o x)/(\nu_o)$	none
n	Exponent for Reynolds number	none
n	Exponent for velocity distribution	none
p	Exponent for Prandtl number	none
q	Heat transferred by convection	B hr^{-1}
q'	Heat transferred by convection	B $hr^{-1}ft^{-1}$
q"	Heat transferred by convection	B $hr^{-1}ft^{-2}$
q_c	Heat transferred by conduction	B hr^{-1}
$q_{c,o}$	Heat transferred by conduction at x_i-1	B hr^{-1}
$q_{c,2}$	Heat transferred by conduction at x_i+1	B hr^{-1}
q_e	Heat lost through downstream end	B hr^{-1}
q_i	Actual heat released by electric heater	B hr^{-1}
q_M	Total heat released by electric heater from energy input measurements	B hr^{-1}
q_n	Heat lost to nosepiece	B hr^{-1}
q_r	Heat transferred by radiation	B hr^{-1}
r	Radius of heat transfer surface	ft
r_1	Inside radius of a tube	ft
r_2	Outside radius of a tube	ft
S	Surface area	ft^2

Symbol	Definition	Unit
S_i	Surface area from $x = 0$ to $x = x_i$	ft^2
s	Hydrodynamic starting length	ft or in.
T_e	Absolute temperature of environment	degrees Rankine
T_o	Absolute temperature of initial air stream	degrees Rankine
T_s	Absolute surface temperature	degrees Rankine
t_1	Temperature of inside surface of a tube	°F
t_2	Temperature of outside surface of a tube	°F
t_f	Film temperature using Θ	°F
t_f'	Film temperature using Θ_m	°F
t_o	Temperature of initial air stream	°F
t_s	Temperature of heat transfer surface	°F
t_w	Temperature within a tube wall	°F
U_o	Initial stream velocity	
V_o	Initial stream velocity	
v_o	Initial stream velocity	ft sec^{-1}
v	Velocity at a place inside the boundary layer	ft sec^{-1}
W_o	Initial stream velocity	
x	Thermal length	ft or in.
x_i	Thermal length between $x = 0$ and $x = x_i$, where i assumes the values 0,2,4,6,etc., so that $x = x_4$ means $x = 4$ in.	in.
x_{i-2}	$x_i - 2$	in.
x_{i+2}	$x_i + 2$	in.
Y	Parameter, defined as $(N_{Nu})x/(x/L)^{0.91}$	none

Symbol	Definition	Unit
y	Distance along a normal from the surface	ft.
z	Distance along unmodified Calrod heater	in.

GREEK LETTER SYMBOLS

γ	Specific weight	lt ft^{-3}
ϵ	Radiation emissivity	none
θ	Temperature difference, $t_s - t_o$	F
θ_i	θ at $x = x_i$	F
θ_{i-2}	θ at x_{i-2}	F
θ_{i+2}	θ at x_{i+2}	F
θ_m	Mean temperature difference	F
θ_A	Temperature excess of Calrod heater	F
θ_B	Temperature excess of Calrod heater	F
ν_o	Kinematic viscosity	$ft^2 sec^{-1}$ or $ft^2 hr^{-1}$
μ	Viscosity	lb $hr^{-1} ft^{-1}$
ϕ	Surface configuration	none

DIMENSIONLESS GROUPS

Units are chosen for terms from the nomenclature so that the following dimensionless groups may result. They are: $(N_{Nu})_L$, $(N_{Nu})'_L$, $(N_{Nu})_x$, $(N_{Nu})'_x$, (N_{Pr}), $(N_{Re})_c$, $(N_{Re})'_c$, $(N_{Re})_L$, $(N_{Re})_x$, s/L, x/L, y/b, b/r, b_K/r, Y, θ/θ_m, x_i/M.

GENERAL

A place on a temperature scale is expressed as °F or °R, degrees Fahrenheit or degrees Rankine, respectively. The temperature difference between places on a temperature scale is expressed as F.

CHAPTER I

INTRODUCTION

It is recognized that there exist two modes of transferring heat between a surface and a flowing fluid. In the one mode, heat energy is transported by the fluid which is caused to move as a consequence of the heat energy it is transporting. The hotter and less dense portions displace overlying layers of colder and more dense portions and the fluid begins to flow. Natural convection occurs when heat is transferred by such a process.

In the other mode, an external influence is introduced so that there is relative motion between the surface and the fluid whether heat is transferred or not. Forced convection occurs when heat is transferred.

When a heated pipe is supported in still air with the pipe axis in a vertical position, heat is transferred from the pipe to the air by natural convection. The air moves upward near the pipe wall; the motion of the air is in a direction parallel to the pipe surface generators. Measurements by Koch (1)[1] show that the diameter of the pipe has an effect on the heat transfer; the heat transfer increases as the pipe diameter is decreased.

A conjecture on the effect of diameter upon the heat transfer in forced convection when the fluid flows parallel to the surface generators has been made by Jakob and Dow (2).

[1] References are correspondingly numbered in the Bibliography.

Their theoretical reasoning, supported by measurements, shows that an increase in heat transfer may be expected as the diameter of the pipe is decreased.

A distinction is required when heat is transferred by forced convection with the fluid flowing outside and parallel to the surface generators. One possibility is the case where the pipe is placed in a fluid stream bounded by the walls of a duct or other enclosure; the other is the case where such an enclosure does not exist.

This distinction arises from the concept of boundary layers as envisaged by Prandtl (3). It is postulated that a boundary layer of fluid is formed on any surface in contact with the flowing fluid. The main characteristic of the boundary layer is that the velocity of the fluid within the boundary layer is less than that of the main stream outside the layer, becoming zero at the surface. If a pipe is placed inside a duct, a boundary layer will form on the walls of the duct and on the pipe surface. It is obvious that the boundary layer forms only upon the pipe surface in the absence of such a duct or enclosure.

When fluids flow inside pipes, it is known that the boundary layer thickness eventually becomes equal to the pipe radius at a certain point, the point depending on specific flow characteristics. With this point fixed, the flow conditions are similar at places downstream from the point and all the fluid is in the boundary layer. At places upstream from the point, portions of the fluid are inside the

boundary layer and the remainder is outside the boundary layer; the relative proportions change from place to place.

Theory and experiment show that heat transfer for fluids flowing inside pipes is dependent upon the described boundary layer patterns, and it may be expected that similar problems are presented when the fluid is flowing outside the pipe. The presence of a duct or enclosure poses conditions that differ from the conditions in the absence of one.

It is the purpose of this work to determine the effect of curvature of a round cylindrical surface not surrounded by an enclosure, with the fluid flowing parallel to the surface generators, on the heat transfer by forced convection.

CHAPTER II

THEORETICAL CONSIDERATIONS

When heat is transferred by convection, the process is mathematically expressed as:

$$\frac{dq}{dS} = h\theta, \text{ or } h = \frac{1}{\theta}\frac{dq}{dS} \qquad \text{II-1}$$

This differential expression shows that the local surface coefficient and the local temperature difference are taken at a particular point on the surface.

The expression may be integrated when it is known how θ and h vary with S. This operation gives the total heat transferred as:

$$q = \int_0^S h\theta \, dS \qquad \text{II-2}$$

On the other hand, the total heat transferred may be written as:

$$q = h_m \theta_m S, \text{ or } h_m = \frac{q}{\theta_m S} \qquad \text{II-3}$$

Substitution from Equation II-2 into Equation II-3 yields:

$$h_m = \frac{1}{\theta_m S} \int_0^S h\theta \, dS \qquad \text{II-4}$$

Inspection of Equation II-3 shows that the choice of θ_m will influence the value of h_m, for the product $h_m\theta_m$ is constant for fixed values of q and S.

Thus θ_m requires definition, and may be defined as:

$$\theta_m = \frac{1}{S} \int_0^S \theta \, dS \qquad \text{II-5}$$

Substitution from Equation II-5 into Equation II-4 yields:

$$h_m = \frac{\int_0^S h\theta \, dS}{\int_0^S \theta \, dS} \qquad \text{II-6}$$

The above developed relations are simple ones. The effects of fluid properties, velocity of flow, and arrangement of surface are not readily apparent. Nor is the relationship among these effects apparent. Since Equation II-1 is used to define the local surface coefficient, it is expected that the coefficient is dependent upon these effects.

The determination of these effects upon the coefficient is an enormous task. Many variables are required to express the fluid properties and the surface arrangement. They may include such properties as density, specific heat, viscosity, and thermal conductivity. The surface may be the interior or exterior of a pipe, or a flat plate. There may be an adiabatic section of surface preceding. The flow direction may be parallel to the surface generators or at some angle to them.

The application of the theory of similarity to heat transfer problems by Nusselt (4) brought order from chaos. The procedures of dimensional analysis supplemented his work. In essence, these methods serve to assemble the many variables into dimensionless groups and have the effect of reducing the number of variables to be studied. An excellent treatment of these methods may be found in Jakob (5).

A practical result of Nusselt's work may be illustrated by the equation:

$$N_{Nu} = f(N_{Re}, N_{Pr}, \emptyset) \qquad \text{II-7}$$

that is, the Nusselt number is expected to be a function of Reynolds number, Prandtl number, and surface configuration. Other groups may be present.

The application of dimensional analysis to the heat transfer problem requires that the form of the function of Equation II-7 be a power function. This form is illustrated as:

$$N_{Nu} = C_o'' (N_{Re})^n (N_{Pr})^p \emptyset^m \qquad \text{II-8}$$

where C_o'', n, p, and m are determined by experiments.

The importance of Nusselt's work becomes more apparent when it is realized that the values of C_o'', n, p, and m remain constant for almost all fluids when the flow configuration remains the same. The major changes in these values occur when the flow configuration changes.

In general, three flow configurations are recognized.

They are termed laminar, transitional, and turbulent. Laminar flow along an immersed surface is characterized by the absence of a velocity component normal to the surface. The direction of the velocity is always parallel to the surface. Investigation of the velocity shows that it has a value of zero at the surface and increases in accordance with the principles of viscous motion until the magnitude equals that of the main stream. It may be noted that a boundary layer has been indirectly described. The place in the fluid where the velocity of the fluid in the layer is practically equal in magnitude to that of the main stream describes a boundary layer thickness.

There is no such orderly motion in turbulent flow. Except for a postulated thin laminar sublayer at the surface of the body, the fluid supports velocity components in a direction normal to the surface, and actual transport of material in this normal direction takes place. Investigation of the velocity component parallel to the surface shows that it increases with distance from the surface until it is practically that of the main stream. A boundary layer thickness is again described.

Transitional flow is the regime described when neither laminar nor turbulent flow occurs. This kind of flow is considered to exist in the region between laminar and turbulent flows.

These concepts are more clearly illustrated in Figure 1. In Illustration (A), the velocity U_o, and the length of the

surface L_a', are such that a laminar boundary layer is formed on the whole plate surface. If the velocity is increased to V_o, a place L_b' occurs wherein the boundary layer preceding this place is laminar, and a transition flow occurs following this place, shown in Illustration (B). If the velocity is increased further to W_o, all three kinds of boundary layers may occur as shown in Illustration (C). Illustration (D) shows how the velocity may be distributed within the boundary layers.

These concepts are of great importance in heat transfer. In the case of laminar flow, where a velocity component normal to the surface is lacking, heat energy is transferred similar to the heat conduction process. In turbulent flow, where a transport of material normal to the surface occurs, heat energy is transferred along with the material transport.

In the preceding discussion of the velocity distribution within the boundary layer, it was noted that the velocity of the fluid at the surface is zero. This means that some particles of the fluid having the velocity of the main stream have lost that velocity. The kinetic energy associated with the velocity has been dissipated. This phenomenon is known as aerodynamic heating; the temperature of an adiabatic surface acquires a value greater than that of the free stream. As may be expected, this effect requires attention in heat transfer problems.

A description has been given about the formation of boundary layers, and it has been indicated how the character

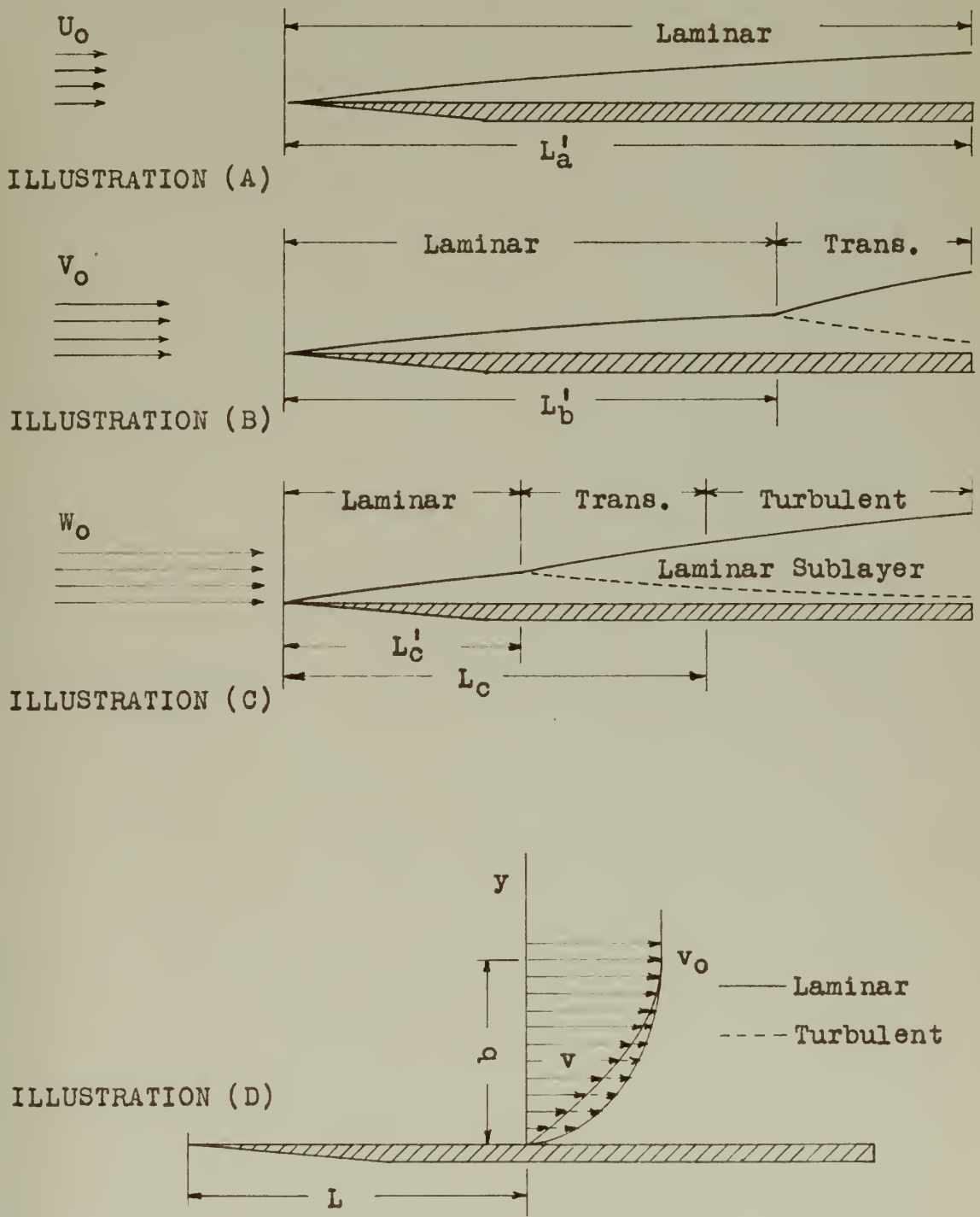


FIGURE 1. ILLUSTRATION OF BOUNDARY LAYERS

of the layers may change. Another effect may arise, for the heat transfer may or may not occur over the whole surface. The whole surface may be the heat transfer surface or the heat transfer surface may be preceded by an adiabatic section of surface. These considerations also require attention; for the boundary layer at the place which marks the beginning of heat transfer may be of different thickness or character, depending upon the choice of the length of the adiabatic section preceding the heat transfer section.

CHAPTER III

PREVIOUS INVESTIGATIONS

The description of the flow configuration is given most remarkably by the Reynolds number. Reynolds (7) and subsequent observers established the existence of upper and lower critical Reynolds numbers, $(N_{Re})_c$ and $(N_{Re})'_c$, respectively. For $N_{Re} \leq (N_{Re})'_c$, the flow was found to be laminar; for $N_{Re} \geq (N_{Re})_c$ the flow was found to be turbulent. Further, the values of $(N_{Re})_c$ and $(N_{Re})'_c$ are unique for all fluids usually encountered. By referring to Figure 1, this may be illustrated as:

$$(N_{Re})'_c = \frac{V_o L'_b}{\nu_o} = \frac{V_o L'_c}{\nu_o}, \text{ a constant.}$$

Moreover:

$$(N_{Re})_c = \frac{V_o L_c}{\nu_o}, \text{ another constant.}$$

The results of experimental determination of these constants is given in Table I.

TABLE I

CRITICAL REYNOLDS NUMBER FOR FLAT PLATES

(All data reduced to basis of total length)

Source	$(N_{Re})'_c$	$(N_{Re})_c$
Eckert (1)	3×10^4	5×10^5
Dodge and Thompson (8)	--	5×10^5
Ellis (9)	--	3.6×10^5
Ten Bosch (11)	1×10^4	5×10^5
FOR CYLINDER, HEMISPHERICAL NOSETIP		
Jakob and Dow (2)	5×10^4	3×10^5

Élias arrived at his value by judging from measured velocity profiles. Ten Bosch, according to Seibert (32), states that $(N_{Re})'_c = 1 \times 10^4$ may occur in the event of major disturbance; that both critical Reynolds numbers may be zero with a blunt leading edge; and that the transitional region may extend from $1 \times 10^4 \leq N_{Re} \leq 2 \times 10^7$ for sharpened leading edges and steadied flow.

The selection of the characteristic length in defining Reynolds number is significant. Élias based his observation on the thermal length and judged $(N_{Re})_c = 3 \times 10^5$. This has the effect of neglecting the boundary layer that has been formed on the preceding unheated starting length. The value from Élias listed in Table I has been corrected to include the starting length; the starting length was ten centimeters and the thermal length was fifty centimeters.

The value for the exponent p in Equation II-8 is given in Table II.

TABLE II

EXPONENT FOR PRANDTL NUMBER

Laminar and Turbulent Flow

Source	Surface	Exponent p
McAdams (6)	Tubes and Plates	0.4 - 0.3
Colburn (14)	Plates	1/3
Pohlhausen (12)	Plates	1/3
Latzko (13)	Plates	1

The values for p given by McAdams are the result after summarizing the work of many investigators. He attributes the variation to viscosity effects arising from heating the

fluid in one case and from cooling in the other, and recommends a value of 1/3 for fluids of low viscosity or if viscosity effects are considered by addition of another term to Equation II-8. Colburn's value is an assumed value arising from an effective correlation of heat transfer data and comparison with fluid friction. Pohlhausen's value is theoretically derived for laminar flow. Latzko's value is theoretically derived for turbulent flow over the whole plate surface. It may be noted that if the Prandtl number is near unity, then the effect of the exponent is small.

Values for n in Equation II-8 are given in Table III.

TABLE III

EXPONENT FOR REYNOLDS NUMBER

Source	Surface	Exponent
	Laminar Flow	
Colburn (14)	Plate	0.5
Pohlhausen (12)	Plate	0.5
Jakob and Dow (2)	Cylinder	0.5
Fisher and Norris (18)	Cone and Cylinder	0.5
	Turbulent Flow	
Colburn (14)	Plate	0.8
Juerges (19)	Plate	0.775
Elias (9)	Plate	Greater than 0.8
Latzko (13)	Plate	0.8
Griffiths and Awberry (20)	Cylinder	1.0
Jakob and Dow (2)	Cylinder	0.8
Fisher and Norris (18)	Cone and Cylinder	0.8

Referring to Table III, Colburn's values result from a summary of various investigators work. Pohlhausen's value comes from theoretical considerations. The values reported by Elias and Griffiths and Awberry are probably due to a

lack of fully developed turbulence. The data of the other observers listed are reasonably well correlated by the reported value for n.

The selection of the characteristic length for defining Reynolds number is not significant with respect to the value of n. The transformation of the characteristic length from thermal length to total length and vice versa, for example, is accomplished by a length ratio which does not affect the value of the exponent. To illustrate, let

$$N_{Nu} = C''_o \, (N_{Re})^n_L \quad . \quad . \quad . \quad .$$

and

$$(N_{Nu})_L = C''_o \left(\frac{v_o \, L}{\nu_o} \right)^n \quad . \quad . \quad . \quad .$$

$$= C''_o \left(\frac{v_o \, L}{\nu_o} \, \frac{x}{x} \right)^n \quad . \quad . \quad . \quad .$$

or

$$(N_{Nu})_L = C''_o \left(\frac{v_o \, x}{\nu_o} \right)^n \left(\frac{L}{x} \right)^n \quad . \quad . \quad . \quad .$$

Therefore, the exponent for Reynolds number is the same irrespective of the characteristic length used in definition as long as the selection is consistent for any given case.

Investigation of the function ϕ^m is a relatively recent occurrence. The first conclusive evidence of considering a starting length function is offered by Jakob and Dow (2). Using the mean surface coefficient, and the total length in both Nusselt and Reynolds numbers, they arrive at the expression:

$$\phi^m = 1 + 0.40 \, (s/L)^{2.75} \quad , \quad 0.101 \leq (s/L) \leq 0.606 \qquad \text{III-1}$$

for turbulent and laminar flow. This result was determined experimentally by heat transfer measurements with unheated starting lengths. Also, they offer a result when the Nusselt number is computed with the local surface coefficient, obtained by differentiation. With certain restrictions, they report:

$$\phi^{m} = 0.8 + 0.2(s/L) - 0.78(s/L)^{2.75} + 1.18(s/L)^{3.75} \qquad \text{III-2}$$

Another experimental result was recently offered by Maisel and Sherwood (16). Using the local surface coefficient, and total length in both Nusselt and Reynolds numbers, they report:

$$\phi^{m} = \left[1 - (s/L)^{0.8}\right] - 0.11, \quad 0.46 \leq (s/L) \leq 0.95 \qquad \text{III-3}$$

for turbulent flow. This result comes from investigating mass transfer and the starting length may be considered to be adiabatic.

Theoretical results have been reported. Using the local surface coefficient, and total length in both Nusselt and Reynolds numbers, Eckert (10) and Rubesin (15) each report:

$$\phi^{m} = \left[1 - (s/L)^{3/4}\right] - 1/3, \text{ for all } (s/L), \qquad \text{III-4}$$

for laminar flow.

A theoretical result for turbulent flow is due to Rubesin (15). With local coefficients and characteristic lengths as before, he gives:

$$\phi^m = \left[1 - (s/L)^{39/40}\right] - 7/39, \text{ for all } (s/L). \qquad \text{III-5}$$

Comparing these equations, it is seen that the expressions in Equations III-3, III-4, III-5, tend to become infinite as (s/L) becomes unity, whereas the expression in Equation III-2 approaches the finite value 1.40. Concerning Equation III-2, Jakob and Dow (2) state: "However, since differentiation of an empirical equation is a delicate matter, the accuracy of the result should not be overestimated.".

The expression $C_o''\ (N_{Pr})^p$, of Equation II-8, may be given by another constant C_o', which assumes different values according to the fluid properties. Values of C_o' for air at atmospheric pressures and about 68°F are given in Table IV, according to Jakob and Dow. The values in the table are corrected for the ratio (s/L) according to Equation III-1.

TABLE IV

VALUES OF C_o' FOR AIR (FROM JAKOB AND DOW)

Atmospheric pressure and about 68°F.

Source	Surface	C_o'
	Laminar flow, n = 0.50	
Pohlhausen	Plane	0.592
Fage and Falkner	Plane	0.750
Jakob and Dow	Cylinder	0.590
	Turbulent flow, n = 0.80	
Latzko	Plane	0.0253
Juerges	Plane	0.0322
Colburn	Plane	0.0320
Seibert	Plane	0.0349
Jakob and Dow	Cylinder	0.0280

Results recently obtained by Berman (21) may be added to this table. He reports $C_o' = 0.37$ for laminar flow. This result comes from mass transfer measurements from cylinders of ice having hemispherical nosetips and with cylinder diameters from 2.22 inches to 3.79 inches.

The effects of aerodynamic heating on heat transfer have been studied and a summary of results is given by Johnson and Rubesin (17). The summary shows how heat transfer results obtained at low fluid velocities, wherein the effect of aerodynamic heating may be neglected, can be applied to measurements where the flow velocity is large and may be greater than the speed of sound.

A summary of the foregoing brief review of previous investigations is presented in Table V.

TABLE V

SUMMARY OF PREVIOUS INVESTIGATIONS

Quantity	Approximate Value
$(N_{Re})_c'$	5×10^4
$(N_{Re})_c$	5×10^5
p	1/3
n, laminar	0.50
n, turbulent	0.80
ϕ^m	Discussed below
C_o	" "
K	" "

Although the function ϕ^m may appear to have inconclusive forms, it is noted that Laisel and Sherwood reported that the Jakob and Dow form gave a good correlation for their data also. This problem will be discussed in more detail later.

When one of the groups on the right side of Equation II-8 is held constant, the effect of that group is absorbed, giving a new equation constant. This was illustrated in the presentation of Table V in which the expression $C_o'' (N_{Pr})^p$ was replaced by C_o'. A similar effect may be expected with respect to a curvature factor.

The Jakob and Dow result for laminar flow agrees with a theoretical result for a plane. However, the theoretical result for a plane has an intermediate value between experimental results for a plane and a cylinder. Therefore, the effect of curvature is not too clear, although the theoretical reasoning of Jakob and Dow indicates that results for a plane may apply to results for a cylinder of 1.3 inches diameter.

For turbulent flow, the Jakob and Dow result is between a theoretical one and experimental ones. If their theoretical reasoning regarding curvature is correct, then there is strong indication that the theoretical value for a plane is nearly correct. If their theoretical reasoning is incorrect, then comparison of the experimental values indicates that the effect of curvature may be to reduce the heat transfer as curvature increases. Therefore, the effect of curvature is in doubt for both turbulent flow and laminar flow.

The above considerations indicate a plan for experimental attack;

(a) the curvature must be made great enough so that a comparison with the flat plate and a cylinder 1.3 inches diameter

- that of Jakob and Dow - may be made;

(b) a series of nosepieces should be used so that the results may be extrapolated to zero starting length; and

(c) varying thermal lengths should be used to determine if the function ϕ^m is valid for variable thermal length as well as variable starting length.

CHAPTER IV

APPARATUS AND INSTRUMENTATION

It is desirable to express heat transfer data by a relation as Equation II-8, for the equation is based upon the powerful tool supplied by the theory of similarity. The application of such an equation to the flow of fluids in pipes, for example, shows the effectiveness of the theory over a very wide range of variables. Consequently, Equation II-8 is to be used to express the results of this work.

Proceeding term by term, it is seen the Nusselt number requires measurement of a surface coefficient of heat transfer, a characteristic length, and the thermal conductivity of the fluid. Reynolds number requires the relative velocity between fluid and surface, a characteristic length, and the kinematic viscosity of the fluid. Prandtl number requires the specific heat, viscosity, and the thermal conductivity of the fluid. The function $\emptyset$ requires two characteristic lengths of the surface.

The measurement of the surface coefficient of heat transfer may not be made directly. Referring to either definition, Equation II-1 or Equation II-3, it is seen that a knowledge is required of the heat transferred, the temperature difference between fluid and surface, and the heat transfer surface area.

Fluid properties as thermal conductivity, specific heat, viscosity, kinematic viscosity, density, and others are required. A knowledge of any two properties, such as

temperature and pressure, serves to determine all others.

Bernoulli's Theorem affords a simple method to determine the fluid velocity. A knowledge is required of the fluid pressure, specific weight and the local gravitational constant.

The heat transfer apparatus is illustrated in Figure 2. Heat is transferred from the long slender element to an air stream flowing parallel to the long axis. A hemispherical nosetip is observed at the upstream end. The downstream end is clamped to a vertical stanchion which is mounted on a wood base. The stanchion is braced by guy wires attached to the base.

Vibration insulation of the base from the floor of the laboratory is accomplished by the use of shear-type rubber shock mounts. A vibration absorber is provided by the weight and rod fastened to the stanchion. These vibration controls are illustrated in Figure 3.

The heat transfer element consists of an outer tube, an inner tube, an electric heater, and selected nosepieces. The outer surface of the outer tube provides the heat transfer surface. The inner tube, which slides into the outer tube and surrounds the heater, is used for fastening the nosepieces to the outer tube.

The outer tube was fabricated from brass tubing, seventy per cent copper and thirty per cent zinc. Three lengthwise holes, one-sixteenth of an inch square, located at 120° intervals, were provided for insertion of thermocouples.

Fabrication of the outer tube is illustrated in Figure 4. The tube was annealed by heating at 750°F for one-half hour, prior to machining. The machining process consisted of cutting grooves one-sixteenth of an inch wide by three-thirty seconds of an inch deep followed by cutting second grooves, centered over the first, one-eighth of an inch wide by one-thirty second of an inch deep. The upper groove surfaces and strips of brass rod, one-eighth of an inch square, were tinned with soft solder - sixty per cent lead and forty per cent tin. The strips were placed over the grooves and clamped to the tube at two-inch intervals. The sweating operation was accomplished by using an electric heater inserted into the bore of the tube. After cooling, the protruding portions of the brass strips were machined away. The surface was highly polished, bright chromium plated, and finally repolished.

The interiors of the square holes were cleaned and polished. This was done by sliding and rotating steel drill rods, coated with valve grinding compound, in the holes. Another piece of drill rod was used as a gauge and the holes were judged to be clean when the gauge rod could slip easily through the holes.

It is realized that the continuity of the sweated joints is of great importance, and that a thermal bond must exist along the whole joint. It is reasonable to assume that a thermal bond was obtained for the reasons following:
(a) It was necessary to perform the sweating operation many



FIGURE 2. ARRANGEMENT OF APPARATUS

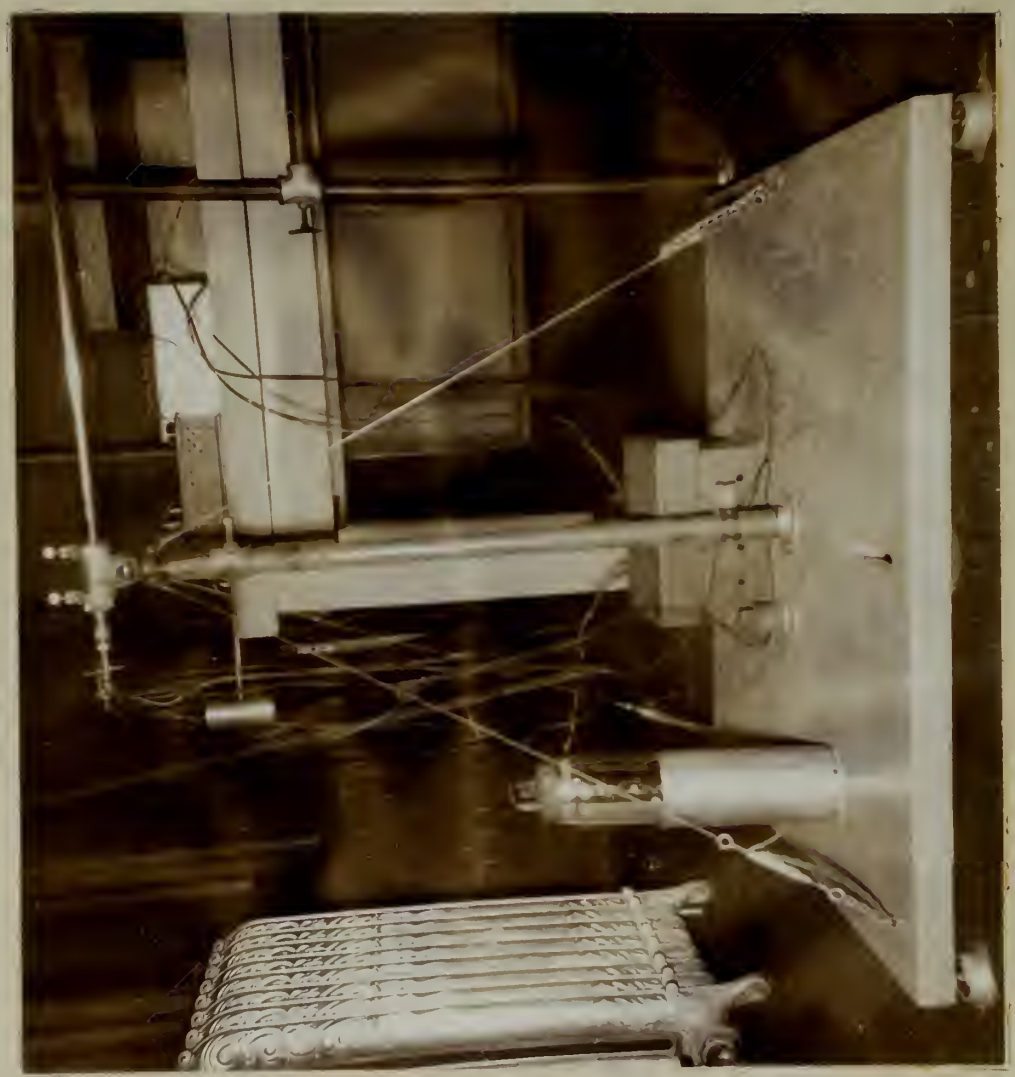
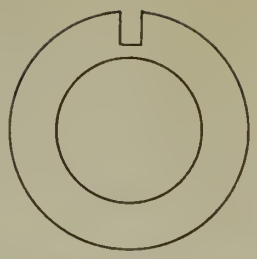
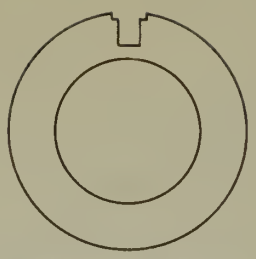


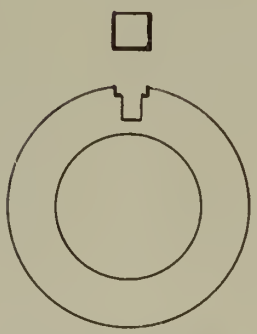
FIGURE 3. VIBRATION CONTROLS



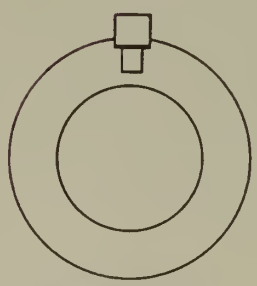
(a) First Groove



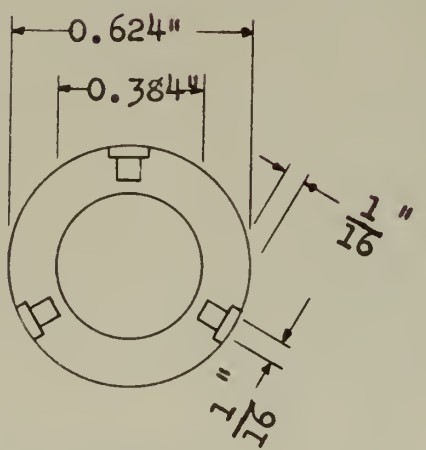
(b) Second Groove



(c) Tinning



(d) Sweating



(e) Completed

FIGURE 4. FABRICATION OF HEAT TRANSFER SURFACE
(SCALE: 2"=1")

times before it was found how to prevent the solder from filling the holes. Each time the parts were separated, the surface showed that a good bond had existed.

(b) A piece of finished tubing, about one inch long, was cut from one end. The cut was made at the middle of the first clamp interval. Mechanical destruction of this piece showed complete bonding had occurred.

The outside diameter of the finished outer tube was found to be 0.624 in., plus or minus 0.002 in. The inside diameter was measured to be 0.384 in. The tube was thirty-five inches long. A surface plate was used to determine longitudinal eccentricity; this was found to have a maximum of one-sixty fourth of an inch located eleven inches from the end subsequently used as the downstream end.

The inner tube was of brass, seventy per cent copper and thirty per cent zinc, and was not annealed. This tube had an outside diameter of 0.376 in., and an inside diameter of 0.326 in. One end was closed with a brass plug, one-eighth of an inch thick, silver soldered to the tube. The plug was drilled and tapped for a Number 10-32 machine screw.

At the plugged end, the outside diameter of the tube was reduced to 0.346 in. for a distance of one-fourth of an inch by cutting away the metal. This device serves to reduce heat conduction to the end plug.

The plugged end of the inner tube was designed to extend one-fourth of an inch beyond the upstream end of the outer tube. The other end of the inner tube extended beyond the

downstream end of the outer tube and was flared to fit a compression tube-fitting assembly. This assembly served as a device for tightening nosepieces to the outer tube. A set screw was provided in the assembly to anchor the electric heater.

The electric heater was a General Electric Company tubular Calrod heater (22), rated at 1500 watts, 230 volts. This element consists of an outer heat-resisting steel sheath surrounding the heating element wire which is embedded in magnesium oxide insulation.

Initially, the outer sheath was forty-eight inches long between terminals and was insulated from them with mica washers. The active heating length was located within the middle thirty-six inches, leaving six inches at each end unheated.

Modification of the heater was accomplished by cutting ten inches from an end. This cut exposed the heating element cross section. Here, the outer sheath was cut and filed longitudinally to form four gores so that a closed hemispherical tip could be shaped at the cut. The wire of the internal heating coil was placed into these cuts while forming was in progress. The wire was firmly pinched and held by elastic forces to the outer metal sheath. Care was taken during the shaping process to prevent loss of insulation.

This construction served to make a heating element with one terminal as originally provided and with any place on the outer sheath to be used for location of the other

terminal. In effect, the outer metal sheath was converted to an electric conductor to complete the heater circuit. As modified, a terminal lug was soldered to the sheath adjacent to the other terminal.

The portion of the Calrod heater cut off was used to establish pertinent dimensions for the heater. These were as follows:

Outside diameter of outer metal sheath	0.316 in.
Inside diameter of outer metal sheath	0.252 in.
Heating coil wire diameter	0.020 in.
Unheated length	6.25 in.

From this information and by measurements, the modified heater was thirty-eight inches long. The active heating length was thirty-one and three-fourths inches long, beginning at the formed end.

Five nosepieces were made of sugar maple dowel stock. All had hemispherical nosetips. They were carefully cut and sanded so that the final diameter was the same as that of the outer tube.

A hole, twenty-three sixty-fourths of an inch in diameter by one and one-half inches deep, was drilled into the bases of four nosepieces. Another hole, one-eighth of an inch in diameter, was drilled along a nosepiece diameter one inch from the base. A glued maple pin was driven into this hole and through the eye of a linking device inside the nosepiece. The pin was dressed to size and smoothed to the nosepiece surface.

A lip cut into the nosepiece base served as a locating device. The lip engaged into a recess in the outer tube.

The linking device was made of brass wire, one-sixteenth of an inch in diameter. An eye was formed at one end and the other end was silver soldered to a brass stud. The stud was threaded to fit the plug in the inner tube.

The four nosepieces constructed this way were five and one-fourth inches, twelve and one-sixteenth inches, eighteen and one-sixteenth inches, and twenty four inches long, respectively, measured from the joint with the outer tube to the tangent plane at the nosetip.

The fifth nosepiece, five-sixteenths of an inch long, required different construction. The hole in the base was one-eighth of an inch deep and a one-eighth of an inch hole was counterbored to a depth of one-eighth of an inch. The linking device was a brass stud with a Number 52 hole drilled along a diameter at one end. A corresponding hole was drilled along a nosepiece diameter and the linking device assembled with a brass wire.

The details of these assemblies are illustrated in Figure 5.

Upon assembly of the nosepieces to the outer tube, the mating surfaces were coated with Duco Household Cement. After assembly, when the cement had dried, any cement that had oozed from the joint was removed. The nosepiece and a portion of the outer tube were given two coats of lacquer and then smoothed with fine steel wool and rubbed with Duco

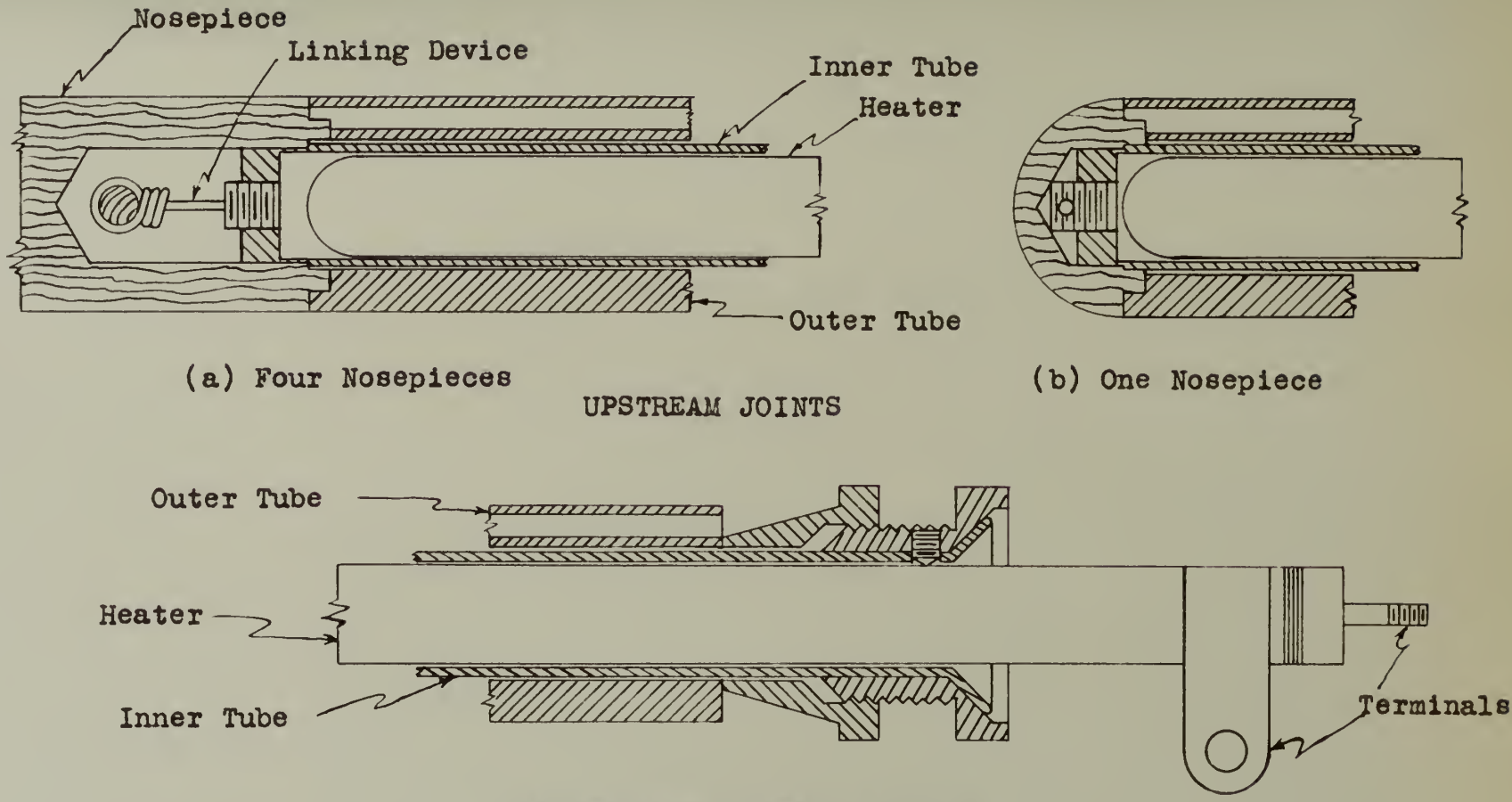


FIGURE 5. HEAT TRANSFER ELEMENT DETAILS
(NOT TO SCALE)

Rubbing Compound until a smooth joint was obtained and no lacquer remained on the outer tube.

Each joint was tested for smoothness. This was done by placing the assembly in V-blocks upon a surface plate. A machinist's dial-indicator was used to test the joint. Any joint imperfections were treated with lacquer and re-polished until the dial indicator showed zero deflection at the joint.

Before assembling the electric heater to the outer tube-nosepiece assembly, a mark was made on the heater surface. This mark served to set the insertion depth so that the heater tip would be in the plane of the outer tube-nosepiece joint. The heater was inserted to the established mark and then locked in place with a set screw.

The heat transfer element was electrically insulated from the stanchion. A smoothly bored one-inch IPS pipe tee at the top of the stanchion was split horizontally and each half was lined with insulating paper. A finned spacing device was used as a filler piece between the heat transfer element and the pipe tee. The finned spacing device also served as a cooling element. Hose clamps were used to hold the assembly.

Direct current was used as the source of heat energy. The current was provided by a motor-generator set equipped with a General Electric Company alternating current induction motor, rated at fifteen horsepower at 1200 revolutions per minute. The motor was connected to an Electro Dynamic

Company direct current generator rated at 0-110 volts, 115 amperes, at 1200 revolutions per minute, and to a Leece-Neville Company twenty-four volt aircraft-type generator. This latter machine was used as an exciter.

An aircraft-type voltage regulator was modified so that the voltage output of the main generator could be controlled over the full rated voltage range.

The relatively high mechanical inertia of the motor-generator set in conjunction with the modified voltage regulator gave good regulation. The voltage variation did not exceed one-half of one per cent for the current magnitudes used.

The heater power consumption was obtained by measuring the voltage drop between the heater terminals and by measuring the electric current. The voltage drop was measured by installing a modified Leeds and Northrup Company volt box in parallel with the heater. The current was measured by using a Weston Instrument Company shunt in series with the heater. Both measuring elements were connected to a Leeds and Northrup Company portable precision potentiometer through a rotary switch.

A blower and duct system served to provide an air stream. The blower was a Power Engineering Company Type HS machine, driven through a Reeves Vari-Speed drive, by a five horsepower induction motor.

The straight duct system was connected to the blower by means of a transition piece and terminated with a nozzle

at the open end. The duct system was fourteen inches in diameter and twenty-nine feet long, measured between the blower discharge flange and the nozzle mouth. The nozzle was nine and seven-eighths inches in diameter.

Control of air velocity was obtained with the Reeves drive and a set of removable dampers at the blower inlet. The blower inlet, equipped with a psychrometer, was in the laboratory room.

The measurement of velocity head was accomplished with an impact tube placed into the duct three feet ahead of the nozzle mouth. Two Ellison Draft Gages (23) were used for indicating the velocity head. The low-range gage was used for velocity heads below 0.5 in. of water. The scale was ten inches long graduated to 0.005 in. of water. The high-range gage, to five inches of water, was thirty inches long graduated to 0.1 in. of water.

Measurement of the air stream temperature and estimation of the heat transfer surface temperature was accomplished with seven thermocouples. The thermocouples were of Leeds and Northrup Company copper and constantan wires, Number 30 Brown and Sharpe Gauge, 1938 Calibration.

Four thermocouples were used to indicate air temperature. These thermocouples were enamelled, single cotton covered wires, connected in series. The hot junctions were located at four equidistant places around the nozzle circumference. They extended into the air stream one inch away from the wall and were parallel to the air stream a distance

of one and one-half inches pointing upstream. The cold junctions were inserted into glass tubing wells immersed in a mixture of melting ice and water in Dewar flasks.

The combined thermo-electromotive force of the four thermocouples was measured with a Leeds and Northrup Company Speedomax Indicator-Recorder. The indicator scale was divided into tenths of a millivolt for a range of six millivolts. A vernier was fabricated and mounted on the pointer to permit reading to 0.01 millivolts.

A switching arrangement provided a means to check the Speedomax operation with the portable precision potentiometer.

Three independent thermocouples were used for estimating surface temperature. These thermocouples were enamelled, double wrap glass fiber covered wires. They were twisted with a one-half inch pitch and then dipped in lacquer and dried several times. Paint marks were added at intervals of two inches beginning at the hot junction, and the dipping and drying process repeated. The dipping process served to stiffen the wires for easy insertion into the heat transfer element holes. The cold junctions of these thermocouples were placed in an ice-water mixture as previously described.

A ten-point Leeds and Northrup Company rotary switch was used for selectively connecting the electromotive forces from the volt box, shunt, Speedomax, and the three thermocouples above to the portable precision potentiometer. This

instrument was provided with two scales. Electric potentials of sixteen millivolts and less could be read to 0.01 mv. and estimated to 0.001 mv. Potentials greater than sixteen millivolts could be read to 0.1 mv. and estimated to 0.01 mv.

A mercury barometer was used to determine atmospheric pressures.

An impact tube probe device was used to locate the heat transfer element in the air stream. The device, illustrated in Figure 6, was made by soft soldering two brass tubes to a split sleeve. The tubes were located one-half of an inch and one inch, respectively, from the surface and parallel to it, pointing upstream. A draft gage served to indicate velocity head. The sleeve was made to slip over the element and was provided with a clamp.

The heat transfer element was judged to be centrally located and parallel to the air stream when rotation of the device around the element showed no change in the velocity head. The device proved to be highly sensitive when located near the supporting stanchion as shown in Figure 6. The device was removed when making heat transfer measurements.

A system for measuring vibrations of the heat transfer element was provided. This system consisted of a motion picture projector equipped with speed control, erected to cast a shadow of the heat transfer element tip upon a ground glass screen. The system provided a magnification factor of 2.9. Amplitudes of vibration were measured from the

screen and frequency was measured with a tachometer driven by the projector.

The apparatus enabled experimentation within the following limits:

Heat transfer element diameter	0.624 in.
Nosepiece lengths	0.31, 5.25, 12.06, 18.06, and 24.00 inches
Thermal length	to 30 in.
Ratio, x/L	0.14 to 0.98
Air stream velocity	9.9 to 123.6 ft sec^{-1} .



FIGURE 6. CENTERING DEVICE

CHAPTER V

PRELIMINARY TESTS AND INVESTIGATIONS

The method of measuring power consumption has been described, and it was noted that a modified volt box and shunt were used in conjunction with a potentiometer. The volt box was modified and tested as described in Appendix I, with test results as:

Range, volts	Multiplier, volts per millivolt
0 - 15	0.1992
0 - 150	1.992
0 - 300	3.984

The shunt was calibrated against a standard resistance as described in Appendix II, with test results as follows:

Range, amperes	Multiplier, amperes per millivolt
0 - 5	0.04340
0 - 20	0.1844

The thermocouples were calibrated as described in Appendix III, and were found to be within 0.3 F of the calculated temperature of condensing steam at prevailing atmospheric pressure. The three used in the heat transfer element differed from the others by 0.2 F. The thermocouples were calibrated in place after all wiring connections were made so that any effects of switches and lead wires might be included.

The electrical resistance of the modified heating element was measured with a Wheatstone bridge with results as follows:

Part	Resistance, ohms, at 90°F.
Heating coil	32.34
Outer sheath	0.060

These data show that the error made by considering all the heat as coming from the coil may be negligible. Also, since the heating element was not insulated from the inner and outer tubes, the electric resistance attributed to the outer sheath may be reduced to some smaller value because of possible parallel paths for the electric current.

The impact tube located in the duct was compared with a pitot tube of Prandtl's design (24). During testing, the pitot tube was located twelve inches downstream from the nozzle mouth in the center of the stream. Assuming that the velocity coefficient for the pitot tube is unity, it was found that the velocity head obtained with the impact tube multiplied by 1.03 would equal the velocity head obtained with the pitot tube. All subsequent measurements for stream velocity were made with the impact tube in the duct and corrected accordingly.

An exploration of the jet without the heat transfer element in the stream was made with the pitot tube. Downstream stations were selected at six inch intervals beginning one inch from the nozzle mouth. Traverses were made at intervals of one inch horizontally and vertically at these stations. This procedure was followed in detail for a nominal jet velocity of 107.8 ft per sec. Explorations in less detail were made at other velocities. The results

of these explorations for a central core of four inches in diameter are:

Distance from Nozzle mouth, inches	Loss of velocity, per cent
37	0
43	1
49	5

The exploration was repeated with the heat transfer element in place and with the tip located five inches downstream from the nozzle mouth. The results for a central core four inches in diameter are:

Distance from Nozzle mouth, inches	Loss of velocity, per cent
37	1
43	2
49	10

As a consequence of these data, all heat transfer measurements were limited to the portion of the jet included between five inches from the nozzle mouth to forty-three inches from the nozzle mouth.

The Calrod heater was tested for uniformity of heat generation prior to modification. An estimate of the uniformity was obtained by inference from surface temperature measurements. The method is based on the supposition that the surface coefficient of heat transfer in free convection may be assumed to be constant for small changes of surface temperature. Therefore, variations in surface temperature indicate variations in heat generation as expressed by Equation II-1.

These tests are described in Appendix IV and the

results are illustrated in Figure 7. It is noted that the Calrod heater was hotter at one end. It is assumed that the test results are expressed reasonably well by a linear relation with respect to length. The equations of such relations, obtained by the method of least squares, are:

$\theta_A = 307.1 - 0.43\ z$, F, at 125 watts input. (Appendix IV, Part A).

$\theta_B = 160.4 - 0.19\ z$, F, at 41.2 watts input. (Appendix IV, Part B).

These equations were derived for data within the middle twenty-four inches of the Calrod heater.

It was noted in Chapter III that heat transfer results for forced convection with turbulent flow between a flat plate and an air stream may be expressed as:

$$(N_{Nu})_L = C_o' (N_{Re})_L^{0.80}$$

or

$$h_m = C_o' (k/L) (N_{Re})_L^{0.80}$$

$$= C_o' k (v_o/\nu_o)^{0.80} (1/L)^{0.20}$$

It is seen, therefore, that the surface coefficient becomes smaller as L becomes larger, other conditions remaining unchanged. Hence, if a plate is constructed so that the heat transferred per unit area is constant over the whole area, then the temperature difference between the plate and environment must increase as L increases.

As a consequence of the above discussion, consideration of the temperature difference of the Calrod heater as tested and the plate as predicted resulted in the conclusion that

the modified end of the heater should be the hotter end. A partial compensation for temperature difference in order to approach an isothermal heat transfer surface was effected when the heater was cut accordingly.

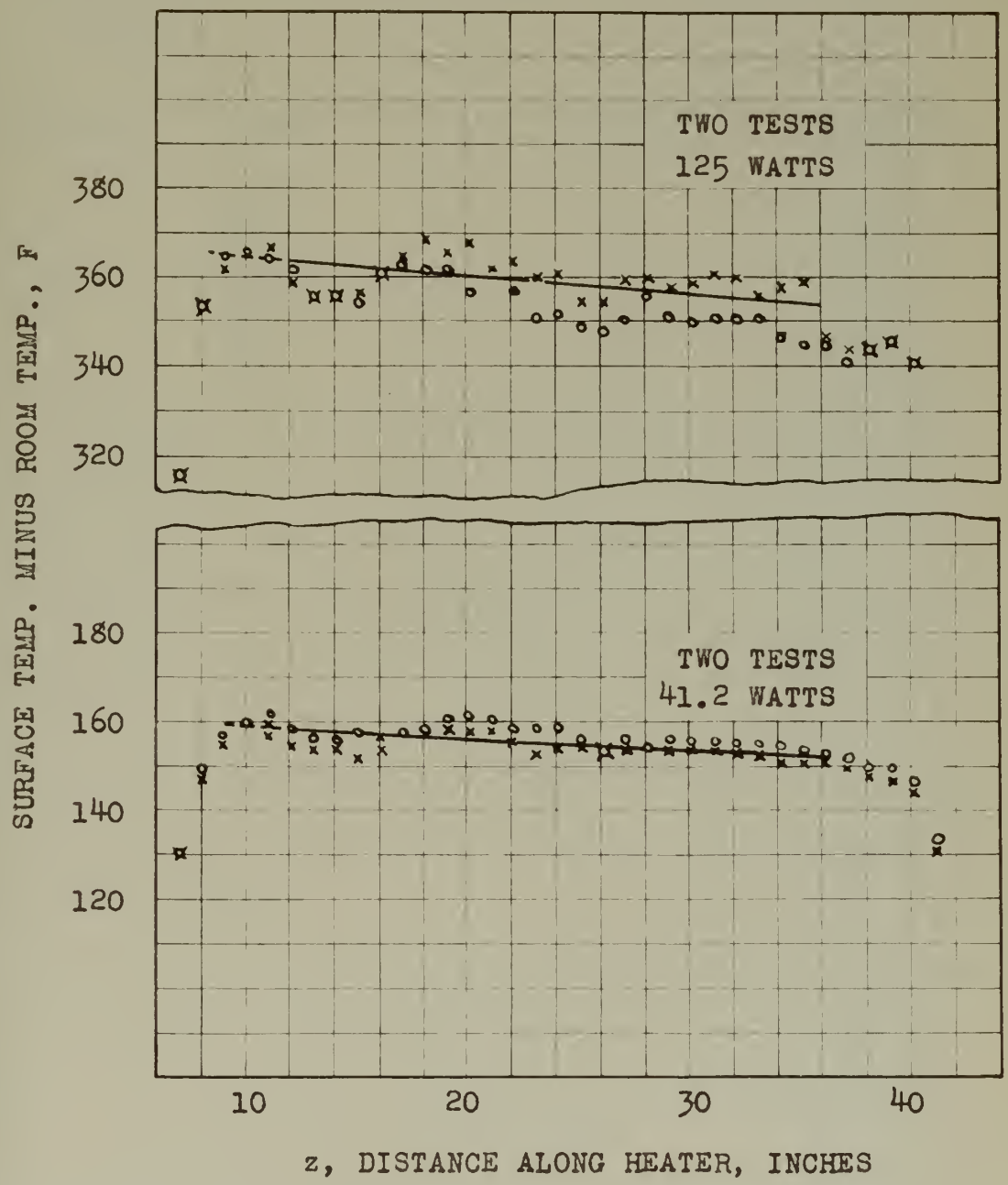


FIGURE 7. CALROD HEATER TEST DATA. SOLID LINES ARE LEAST SQUARES LINES FOR 12 - 36 INCHES, INCLUSIVE

CHAPTER VI

EXPERIMENTATION AND DATA

The experiments were classified into seven series of runs as follows:

Series Designation	Nosepiece Length, inches	Angle to Stream, degrees	Vibration controls
A	0.31	0	Yes
B	5.25	0	Yes
C	12.06	0	Yes
D	18.06	0	Yes
E	24.00	0	Yes
X	5.25	3	Yes
V	5.25	0	No

A run of any series consisted of making a temperature traverse along the heat transfer element at intervals of two inches after a steady state was judged to prevail. Power input and air stream velocity were the controlled variables for a given series. Variables as humidity, air temperature, and barometric pressure were uncontrolled variables. The steady state was judged to prevail when the temperature difference between the air and the nosepiece joint remained steady.

A run was not started or was discarded if the Speedomax record of air temperature showed instantaneous variations exceeding 0.5°F or if the average air stream temperature rise was in excess of 1°F in ten minutes.

The temperature traverse was made by moving the thermocouples from place to place along the heat transfer element length beginning at the nosepiece joint. Preliminary tests revealed that the thermocouples reached relative equilibrium

within one minute after being moved. To provide an ample margin, data for the temperature traverses and corresponding air temperature were taken at intervals of three minutes.

It may be demonstrated that the surface temperature, the heat conducted to the nosepiece, and the accuracy of the determination of temperature difference increases with power input, whereas the accuracy of the surface temperature measurement decreases with power input. It was shown previously that if the unit surface heat generation is constant, a rise in surface temperature with length may be expected. On the other hand, a thermocouple does not yield reliable results unless the wires are in an isothermal zone for a distance depending upon the wire size and temperature gradient. As a compromise, therefore, the power input for a run was adjusted so that the maximum temperature gradient along the heat transfer element in the region of the nosepiece joint was in the neighborhood of one degree Fahrenheit per inch.

In all except Series V runs, vibration control was obtained by changing the absorber weight or length. Amplitudes could be limited to less than one-sixteenth of an inch in most cases and were about one thirty-second of an inch generally. The vibrations encountered were of sporadic nature and probably caused by nearby vehicular traffic. In the Series V runs, the shock mounts and vibration absorber were removed and the base was clamped to the laboratory

floor.

Readings for power input determination were made four times per run and other readings were made once per run excepting surface and air temperature measurements.

The basic data are given in Tables VI to X, inclusive, and represent ninety-two runs. A total of ninety-five runs were made and three runs were rejected because of failure to take complete data.

The data of Table VI, Impressed Heater Voltage, are derived from the 0 - 150 volts range of the volt box.

The data in Table VII, Electric Heating Current, are derived from the 0 - 5 ampere range of the shunt and includes the current passing through the volt box. The data of Appendix I show that the maximum current passing through the volt box is 0.005 amperes with rated voltage impressed on the terminals used here. Examination of Table VI shows that the maximum impressed voltage was 43.6 volts. The corresponding current is (43.6 x 0.005)/150 equal to 0.0015 amperes. By Table VII, the total current for this voltage is 1.338 amperes of which 0.0015 amperes is one-tenth of one per cent, approximately. A computation with the minimum values yields a similar result. Therefore, no correction was made and the data in Table VII are used directly.

A check between corresponding values of Tables VI and VII is provided by use of Ohm's Law and the measured electric resistance of the modified heater.

The data in Table VIII, Initial Air Stream Velocity,

are the result from considering the observed impact tube velocity head corrected by the multiplier previously described, corrected barometer observations, and the air stream temperature. To facilitate computations, the conversion tables of the Ellison Draft Gage Company (23) were used. The tables are based on the formula:

$$v_o = 15.85 \sqrt{\frac{T_o \, H}{B_o}} \quad \text{ft sec.}^{-1}$$

The maximum relative humidity at the blower inlet was thirty-five per cent, hence the air was assumed to be dry and no correction for humidity was made in the velocity determination.

The temperature data in Tables IX and X are uncorrected for the steam point deviation found in Appendix III. The agreement between the thermocouples used for air temperature measurement and the computed steam point temperature is such that correction is not required.

Comparison of the air temperature thermocouples with those used in the heat transfer element shows a deviation of 0.2 F at the steam point. Examination of Table X shows a maximum temperature difference of thirty-one degrees Fahrenheit, approximately. If it is assumed that the deviation of the thermocouples is a linear function of the temperature above the ice point, then the probable deviation between the thermocouples may be a maximum of (31 x 0.2)/180 equal to 0.034 F, and is considered to be negligible.

Of the data in Table X, Temperature Distribution Data,

it is assumed that the measured wall temperature is at a place corresponding to half the outer tube wall thickness. No correction is made for conduction of heat along the thermocouple wires because of the small wire size and the relatively small temperature gradient. The computed wall temperature is the average of the observations from the three traverse thermocouples.

The Leeds and Northrup Company Temperature Conversion Tables, Standard 31031, were used. For purposes of interpolation, the ratio of temperature difference above the ice point to the corresponding potential difference versus potential difference was plotted. A smooth curve was drawn through the plotted points and a new conversion table prepared for immediate purposes. A cross check between the standard established the acceptability of the new table.

Some of the data of Table X are shown graphically in Figures 8, 9, 10, 11, and 12. Runs having nearly the same velocities were selected for the figures so that a visual comparison may be made.

Vibration data gathered from the Series V runs are:

Run Nos.	Amplitude, inches	Revolutions per minute
1,2	1/16	440
3,4,5	0	-
6,7,8	1/8	440

Comparative data from the Series B runs are:

Run Nos.	Amplitude, inches	Revolutions per minute
1,2,3,4,5	1/16	520
6,7,8,9	1/32	520
10,11,12,13,14,15	1/16	520

The data for both series do not include sporadic vibrations because the duration was too short to accomplish measurement.

TABLE VI

IMPRESSED HEATER VOLTAGE

(Body of table is volts)

Run No.	Run Series A	B	C	D	E	X	V
1	14.98	19.48	22.3	22.6	23.6	19.48	20.6
2	16.12	20.3	23.6	23.5	23.6	20.6	20.6
3	18.09	21.4	23.4	23.4	23.6	21.6	24.0
4	18.07	21.4	24.5	24.4	23.7	22.6	26.1
5	18.90	22.2	26.6	26.4	23.6	23.6	29.2
6	19.89	22.2	27.6	27.6	23.6	25.4	32.3
7	20.0	23.4	29.6	28.7	23.4	27.6	35.3
8	22.2	23.3	31.6	28.6	27.4	30.6	40.4
9	25.6	25.4	33.6	31.6	30.5	34.6	-
10	26.8	27.4	35.6	32.4	32.6	39.7	-
11	28.8	29.6	36.4	34.8	34.6	-	-
12	30.2	31.4	38.3	37.7	36.4	-	-
13	31.1	33.3	40.3	40.5	39.6	-	-
14	33.4	35.3	41.6	43.6	-	-	-
15	35.4	37.4	43.6	-	-	-	-
16	37.6	38.8	-	-	-	-	-

TABLE VII

ELECTRIC HEATING CURRENT

(Body of table is amperes)

Run No.	Run Series A	B	C	D	E	X	V
1	0.462	0.600	0.688	0.695	0.727	0.601	0.636
2	0.496	0.625	0.728	0.724	0.727	0.636	0.636
3	0.557	0.659	0.721	0.722	0.727	0.665	0.739
4	0.557	0.657	0.756	0.755	0.732	0.686	0.805
5	0.583	0.684	0.820	0.814	0.730	0.726	0.900
6	0.613	0.685	0.849	0.852	0.727	0.783	0.994
7	0.613	0.721	0.912	0.884	0.725	0.849	1.085
8	0.677	0.718	0.972	0.881	0.844	0.943	1.242
9	0.787	0.784	1.034	0.973	0.940	1.062	-
10	0.825	0.843	1.097	0.997	1.002	1.219	-
11	0.889	0.913	1.121	1.071	1.068	-	-
12	0.930	0.966	1.178	1.158	1.125	-	-
13	0.958	1.023	1.238	1.240	1.220	-	-
14	1.028	1.087	1.280	1.338	-	-	-
15	1.090	1.149	1.341	-	-	-	-
16	1.155	1.194	-	-	-	-	-

TABLE VIII

INITIAL AIR STREAM VELOCITY DATA

(Body of table is velocity, feet per second)

Run No.	Run Series A	B	C	D	E	X	V
1	11.5	9.9	14.8	14.6	16.4	13.0	13.2
2	14.3	15.5	17.6	17.5	19.6	15.9	19.1
3	17.6	17.8	20.1	20.3	22.4	20.4	26.2
4	20.5	20.9	23.6	23.4	26.0	27.4	34.9
5	23.5	22.8	27.7	28.0	30.2	33.8	48.6
6	27.8	28.2	31.6	32.1	35.1	44.8	67.7
7	30.9	31.7	36.3	36.8	42.8	55.3	88.8
8	36.0	34.2	43.4	42.9	55.6	79.1	120.8
9	42.9	44.3	50.0	56.8	67.5	101.6	-
10	49.9	55.5	58.2	65.9	78.3	123.6	-
11	58.3	67.8	66.8	78.2	89.2	-	-
12	66.3	78.0	78.9	88.5	111.9	-	-
13	78.6	89.7	89.6	104.2	122.7	-	-
14	90.2	101.0	106.0	122.8	-	-	-
15	106.7	112.0	122.7	-	-	-	-
16	122.2	122.2	-	-	-	-	-

TABLE IX

INITIAL AIR STREAM TEMPERATURE DATA

(Body of table is degrees Fahrenheit)

Run No.	Run Series A	B	C	D	E	X	V
1	66.6	78.0	80.3	68.1	66.1	78.0	62.7
2	64.9	77.4	79.9	68.3	65.9	78.3	64.0
3	80.1	77.4	79.1	69.3	66.0	78.2	66.0
4	79.1	77.2	79.2	70.7	66.7	77.8	69.0
5	78.6	69.7	79.1	71.8	66.3	76.2	69.4
6	78.5	70.8	79.0	73.4	67.6	77.7	70.4
7	78.0	70.8	78.5	74.4	71.0	78.4	71.4
8	77.0	72.5	78.0	74.6	76.0	79.6	75.2
9	74.2	71.3	77.9	72.8	76.8	81.5	-
10	81.5	74.2	77.8	72.1	71.3	84.2	-
11	83.4	72.8	77.1	74.4	75.1	-	-
12	84.3	72.5	78.1	76.1	78.3	-	-
13	84.3	76.4	77.6	77.6	77.9	-	-
14	83.6	79.5	75.9	78.6	-	-	-
15	82.9	80.3	75.8	-	-	-	-
16	81.4	80.3	-	-	-	-	-

TABLE X

TEMPERATURE DISTRIBUTION DATA, SERIES A RUNS

(Body of table is $t_w - t_o$, F)

x, in.	Run No. 1	2	3	4	5	6	7	8	9
0	12.9	13.3	15.0	13.6	13.7	13.2	12.2	13.6	14.8
2	14.4	14.8	17.3	15.4	15.5	15.3	13.8	15.8	17.2
4	15.9	16.4	19.0	17.1	17.2	16.6	15.1	17.4	18.5
6	16.7	17.1	20.1	18.2	18.1	17.6	15.9	18.3	19.3
8	17.2	17.4	20.6	18.7	18.5	18.1	16.2	18.5	19.5
10	17.6	18.2	20.7	18.8	18.8	18.4	16.5	18.6	19.9
12	17.7	18.4	20.5	18.7	18.6	18.4	16.5	18.1	19.6
14	17.7	18.0	20.4	18.6	18.4	18.4	16.5	18.2	19.7
16	17.5	17.9	20.2	18.3	18.2	18.4	16.4	18.0	19.8
18	16.9	17.3	19.6	17.9	17.7	17.9	16.1	17.6	19.4
20	16.6	16.9	18.9	17.3	17.1	17.4	15.8	17.3	19.3
22	15.7	16.4	18.1	16.3	16.2	16.7	15.3	16.6	19.1
24	14.7	15.0	17.1	15.4	15.5	15.9	14.5	16.3	18.7
26	13.5	13.7	15.7	14.2	14.3	14.8	13.6	15.2	17.9
28	11.6	12.1	13.4	12.3	12.4	12.8	12.1	13.5	16.0
30	10.0	9.0	10.2	9.2	9.4	9.7	8.8	10.2	12.2

x, in.	Run No. 10	11	12	13	14	15	16
0	15.3	14.6	13.1	11.2	11.1	10.6	10.1
2	17.5	16.9	15.3	13.2	13.3	12.9	12.6
4	19.1	18.0	16.6	14.7	14.9	14.6	14.7
6	19.7	18.5	17.4	15.8	16.1	15.7	15.9
8	19.7	18.7	17.5	16.1	16.4	16.7	16.7
10	19.9	19.2	18.3	17.1	17.4	17.6	17.7
12	19.8	19.2	18.4	17.1	17.4	17.5	17.2
14	19.8	19.5	18.9	17.3	18.0	17.8	17.7
16	20.1	19.9	19.3	18.1	18.4	18.4	18.3
18	19.8	19.7	19.4	18.1	18.4	18.2	18.4
20	19.7	19.7	19.3	17.8	18.4	18.2	18.3
22	19.3	19.5	19.0	17.7	18.1	18.2	17.7
24	18.9	19.2	18.7	17.3	18.1	17.9	17.8
26	18.3	18.7	18.3	17.0	18.1	17.7	17.6
28	16.4	17.0	17.0	16.1	16.7	16.4	16.5
30	12.7	13.3	12.3	12.2	13.1	13.2	13.0

TABLE X, Continued

TEMPERATURE DISTRIBUTION DATA, SERIES B RUNS

(Body of table is $t_w - t_o$, F)

x, in.	Run No. 1	2	3	4	5	6	7	8	9
0	24.4	22.7	21.7	18.9	17.8	16.2	15.8	14.5	12.7
2	26.6	24.8	23.8	20.5	19.4	17.8	17.4	16.2	13.9
4	28.3	26.6	25.4	21.8	20.9	19.2	19.1	17.7	15.5
6	29.7	27.4	26.2	23.2	21.7	20.1	20.0	18.7	16.4
8	30.5	27.8	26.7	23.7	22.5	20.6	20.6	19.3	17.0
10	31.1	28.0	27.4	24.1	22.9	21.2	20.9	19.8	17.8
12	31.2	28.0	27.3	24.1	22.9	21.4	21.1	19.9	18.0
14	31.1	28.0	27.4	24.2	23.1	21.4	21.6	20.2	18.7
16	30.7	27.7	26.9	23.9	23.1	21.1	21.4	20.3	18.8
18	29.8	27.2	26.2	23.3	22.6	21.0	21.4	20.2	18.8
20	28.9	26.5	25.5	22.9	22.1	20.7	20.9	20.1	18.7
22	27.5	25.4	24.4	21.8	21.2	19.9	19.9	19.7	18.4
24	26.0	23.9	23.2	20.5	20.4	18.9	19.6	19.0	18.1
26	23.2	21.9	20.7	18.4	18.5	17.4	17.9	17.4	17.1
28	19.7	18.3	17.7	16.0	15.9	15.2	15.7	15.5	15.0
30	-	12.9	12.5	11.0	11.1	10.5	11.1	10.8	10.6

x, in.	Run No. 10	11	12	13	14	15	16
0	11.4	11.1	10.5	10.9	12.0	12.9	12.8
2	12.9	13.2	12.5	12.8	14.0	14.6	14.9
4	14.8	14.7	14.0	14.7	15.3	16.5	16.6
6	15.2	15.7	15.0	15.4	16.3	17.5	17.7
8	16.1	16.0	15.9	15.9	17.0	17.8	18.0
10	16.8	17.1	16.4	16.5	17.8	18.8	18.8
12	16.8	17.1	16.3	16.5	17.8	18.7	18.8
14	17.3	17.5	17.2	17.1	18.2	19.6	19.6
16	17.6	17.5	17.3	17.1	18.4	19.9	19.7
18	17.7	17.6	17.1	17.0	18.3	19.6	19.4
20	17.8	17.9	17.0	17.8	18.6	19.8	20.0
22	17.4	17.8	17.2	17.3	18.4	19.5	19.6
24	17.2	17.4	17.0	16.9	18.1	19.1	20.0
26	16.4	15.4	16.4	16.2	17.5	18.4	18.7
28	15.1	14.8	15.0	15.0	16.4	17.2	18.1
30	10.7	10.5	11.0	10.9	14.9	13.4	14.1

TABLE X, Continued

TEMPERATURE DISTRIBUTION DATA, SERIES C RUNS

(Body of table is $t_w - t_o$, F)

x, in.	Run No. 1	2	3	4	5	6	7	8	9
0	25.4	24.4	22.1	21.5	22.0	21.1	21.2	20.3	20.7
2	27.2	25.9	23.6	23.1	23.6	22.7	23.1	22.3	22.7
4	29.0	27.7	25.3	24.6	25.6	24.4	25.0	24.1	24.5
6	30.0	28.9	26.2	25.9	26.8	25.6	26.2	25.4	26.1
8	30.7	29.6	26.7	26.4	27.6	26.4	27.1	26.1	27.0
10	31.4	30.3	27.5	27.2	28.6	27.4	28.4	27.5	28.5
12	30.9	30.0	27.0	26.8	28.5	27.2	28.4	27.7	28.5
14	30.4	29.4	26.4	26.3	28.2	26.9	28.1	27.7	28.6
16	29.2	28.3	25.5	25.7	27.4	26.4	27.8	27.6	28.4
18	27.4	27.1	24.2	24.3	26.1	25.3	26.8	26.8	27.8
20	24.8	24.5	22.0	22.2	23.9	23.2	24.8	25.0	26.1
22	20.4	20.0	17.9	18.2	19.6	19.0	20.5	21.0	21.8

x, in.	Run No. 10	11	12	13	14	15
0	20.7	19.8	19.4	19.5	18.1	17.9
2	22.6	21.5	21.0	21.0	19.1	19.2
4	24.5	23.4	22.7	22.9	21.0	20.8
6	25.9	24.4	23.6	24.0	22.5	21.7
8	26.6	25.3	24.4	24.4	22.7	22.5
10	27.8	26.7	26.0	25.9	24.3	24.0
12	28.4	26.6	25.8	26.3	24.2	23.7
14	28.5	26.7	25.8	26.1	23.8	23.6
16	27.8	26.7	25.9	26.1	23.8	23.8
18	-	26.3	25.8	26.1	23.7	23.6
20	26.5	25.0	24.8	24.9	23.4	23.2
22	23.1	21.3	21.0	21.3	20.2	20.5

TABLE X, Continued

TEMPERATURE DISTRIBUTION DATA, SERIES D RUNS

(Body of table is $t_w - t_o$, F)

x, in.	Run No. 1	2	3	4	5	6	7	8	9
0	25.0	23.9	21.4	21.2	22.0	21.6	20.8	17.4	17.0
2	26.7	25.8	23.1	22.7	23.9	23.4	22.8	19.0	18.6
4	28.6	27.5	24.6	24.2	25.6	25.5	24.7	20.8	20.4
6	29.8	28.8	25.5	25.3	26.6	26.6	25.8	21.8	21.4
8	30.3	29.2	25.9	25.7	27.0	27.1	26.5	22.3	21.9
10	31.1	29.8	26.6	26.3	27.5	27.7	27.2	23.2	23.1
12	30.9	29.8	26.4	26.0	27.0	27.6	27.0	23.0	23.2
14	30.7	29.5	25.9	25.6	26.8	26.9	26.8	23.0	23.3
16	30.1	29.2	25.5	25.3	26.5	27.0	26.3	23.5	23.5
18	29.5	28.9	25.3	24.9	26.0	26.7	26.1	23.1	23.9

x, in.	Run No. 10	11	12	13	14
0	16.1	15.6	16.8	16.8	17.7
2	17.3	17.0	18.1	18.4	19.0
4	18.8	18.8	19.9	20.4	21.0
6	20.3	19.6	21.0	21.4	22.0
8	20.4	20.3	21.5	21.5	22.0
10	21.5	21.3	22.7	22.9	23.5
12	21.6	21.2	22.7	22.8	23.5
14	21.4	21.4	22.7	22.7	23.3
16	21.5	21.4	22.9	23.1	23.3
18	21.7	21.9	23.4	23.5	23.9

TABLE X, Continued

TEMPERATURE DISTRIBUTION DATA, SERIES E RUNS

(Body of table is $t_w - t_o$, F)

x, in.	Run No. 1	2	3	4	5	6	7	8	9
0	24.0	21.5	19.5	17.8	16.6	14.6	11.6	13.1	14.2
2	26.0	23.3	21.2	19.3	17.9	15.7	12.9	14.6	15.7
4	27.9	24.7	22.8	19.8	19.2	16.8	14.1	15.7	17.0
6	28.4	25.4	23.5	21.3	19.7	17.5	14.6	16.3	17.2
8	28.9	25.7	24.2	21.5	19.8	17.7	14.8	16.8	17.8
10	29.4	26.2	24.4	21.8	20.3	18.0	15.5	17.4	18.9
12	29.2	25.9	24.1	21.3	19.4	17.7	15.0	16.9	18.6
14	28.8	25.8	23.8	21.5	19.0	17.9	14.8	17.1	18.7
16	27.8	25.3	23.1	21.1	18.9	17.6	14.5	17.0	18.9
18	27.0	24.2	22.2	20.5	18.2	17.2	14.1	16.5	18.1

x, in.	Run No. 10	11	12	13
0	14.0	14.2	13.1	14.6
2	15.5	15.8	14.4	15.9
4	17.2	17.8	16.3	17.8
6	18.0	18.1	16.8	18.3
8	18.3	18.6	17.2	18.8
10	19.4	19.5	18.1	19.4
12	18.9	19.1	17.3	19.0
14	19.0	19.5	17.8	19.3
16	19.2	19.1	17.7	19.3
18	18.9	18.6	17.9	19.2

TABLE X, Continued

TEMPERATURE DISTRIBUTION DATA, SERIES X RUNS

(Body of table is $t_w - t_o$, F)

x, in.	Run No. 1	2	3	4	5	6	7	8	9
0	18.8	19.6	18.3	17.0	15.5	15.2	14.9	11.4	11.5
2	20.4	21.2	20.2	18.4	17.3	16.9	16.8	13.0	13.4
4	21.9	22.8	21.8	20.2	18.8	18.4	18.7	14.4	14.7
6	23.1	23.8	22.9	21.0	20.0	19.6	19.4	15.0	15.7
8	23.6	24.7	23.4	21.7	20.7	20.2	20.1	15.7	16.1
10	24.5	25.3	23.7	22.4	21.4	20.8	20.9	16.3	16.7
12	24.9	25.3	23.9	22.5	21.2	21.0	20.9	16.3	16.5
14	25.1	25.4	24.0	22.5	21.5	21.0	21.1	16.8	17.0
16	24.9	25.2	23.9	22.0	21.4	20.7	20.9	16.8	16.8
18	24.3	24.8	23.5	21.7	21.0	20.6	20.6	16.8	16.8
20	24.0	24.3	23.2	21.1	20.7	20.3	20.4	16.7	17.0
22	23.2	23.1	22.2	20.6	20.5	19.7	19.8	16.5	16.5
24	22.0	21.9	20.9	19.2	19.2	18.8	19.0	16.1	16.3
26	19.8	20.0	19.1	17.6	17.5	17.3	17.9	15.6	15.5
28	16.9	16.5	16.2	15.5	15.3	15.3	15.8	14.1	14.4
30	11.9	12.0	11.8	10.7	10.3	10.7	11.4	10.1	10.5

x, in.	Run No. 10
0	12.9
2	15.2
4	16.8
6	17.5
8	17.9
10	18.6
12	18.1
14	18.7
16	18.7
18	18.1
20	18.4
22	18.0
24	17.4
26	17.1
28	16.2
30	11.7

TABLE X, Continued

TEMPERATURE DISTRIBUTION DATA, SERIES V RUNS

(Body of table is $t_w - t_o$, F)

x, in.	Run No. 1	2	3	4	5	6	7	8
0	26.1	22.0	20.8	18.1	14.5	13.4	13.1	13.1
2	28.3	23.5	22.6	20.0	16.6	15.5	15.3	15.8
4	30.3	25.1	24.3	21.7	18.4	17.2	17.2	17.6
6	31.6	26.0	25.5	23.0	19.8	18.6	17.9	18.4
8	32.4	26.4	26.5	24.0	20.8	19.2	18.7	19.1
10	33.4	26.9	27.4	25.1	22.0	20.8	20.1	20.3
12	33.2	26.8	27.3	25.6	22.1	20.7	20.0	20.4
14	32.9	26.5	27.1	25.7	22.2	20.4	20.1	20.3
16	32.2	26.1	26.9	25.9	22.5	20.6	20.0	20.2
18	31.4	25.5	26.5	-	22.7	21.0	20.3	20.5
20	30.7	24.9	26.0	26.0	23.1	21.2	20.9	20.8
22	29.2	24.1	25.1	25.5	22.9	21.1	20.7	20.4
24	27.7	22.8	23.9	24.7	22.7	20.9	20.2	20.3
26	25.4	19.9	22.3	23.1	21.8	20.4	19.7	20.1
28	21.6	18.0	19.4	20.4	19.7	18.9	18.2	18.6
30	16.0	13.4	14.5	15.1	15.3	14.5	14.4	15.0

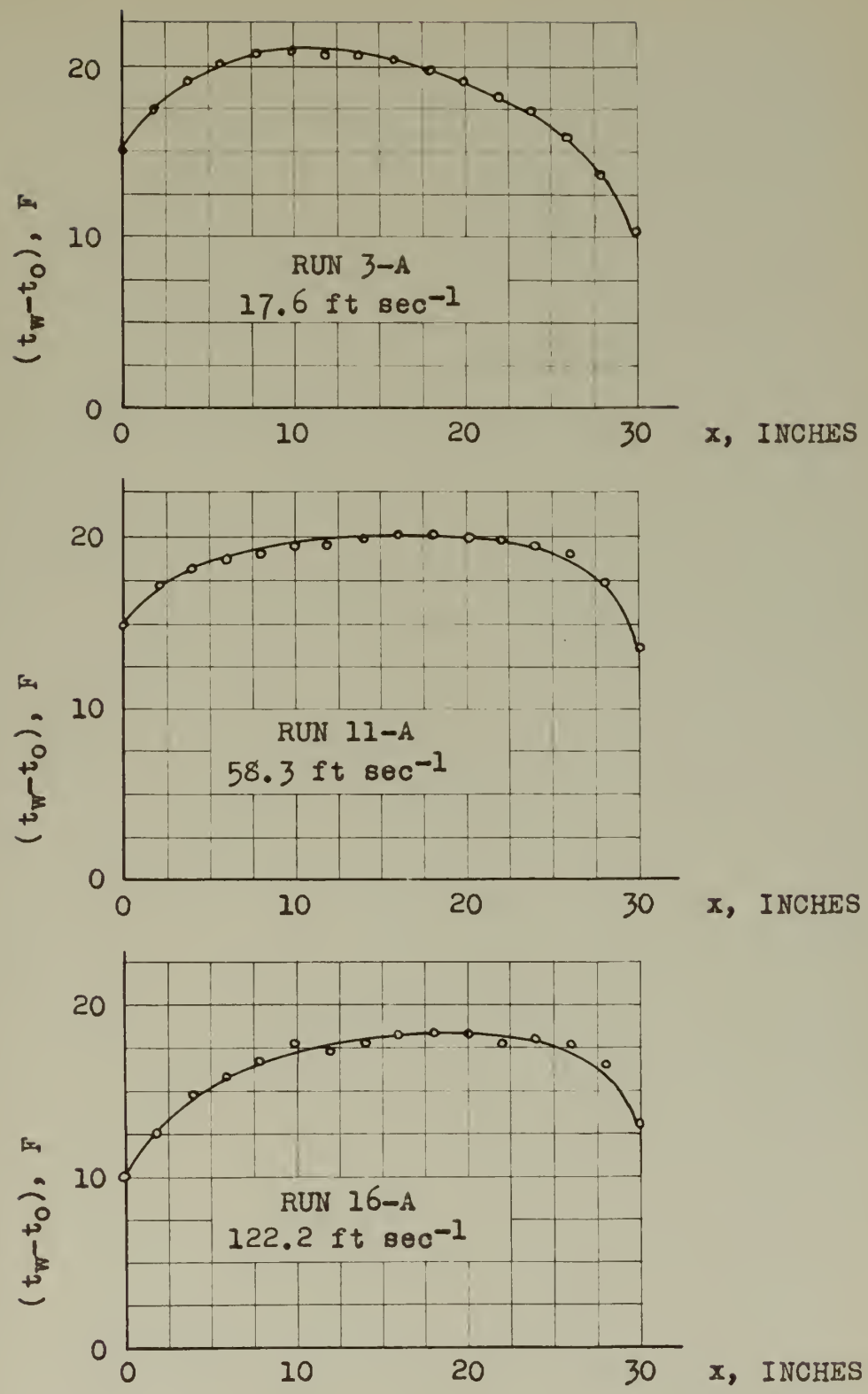


FIGURE 8. TEMPERATURE DISTRIBUTION DATA, SERIES A RUNS

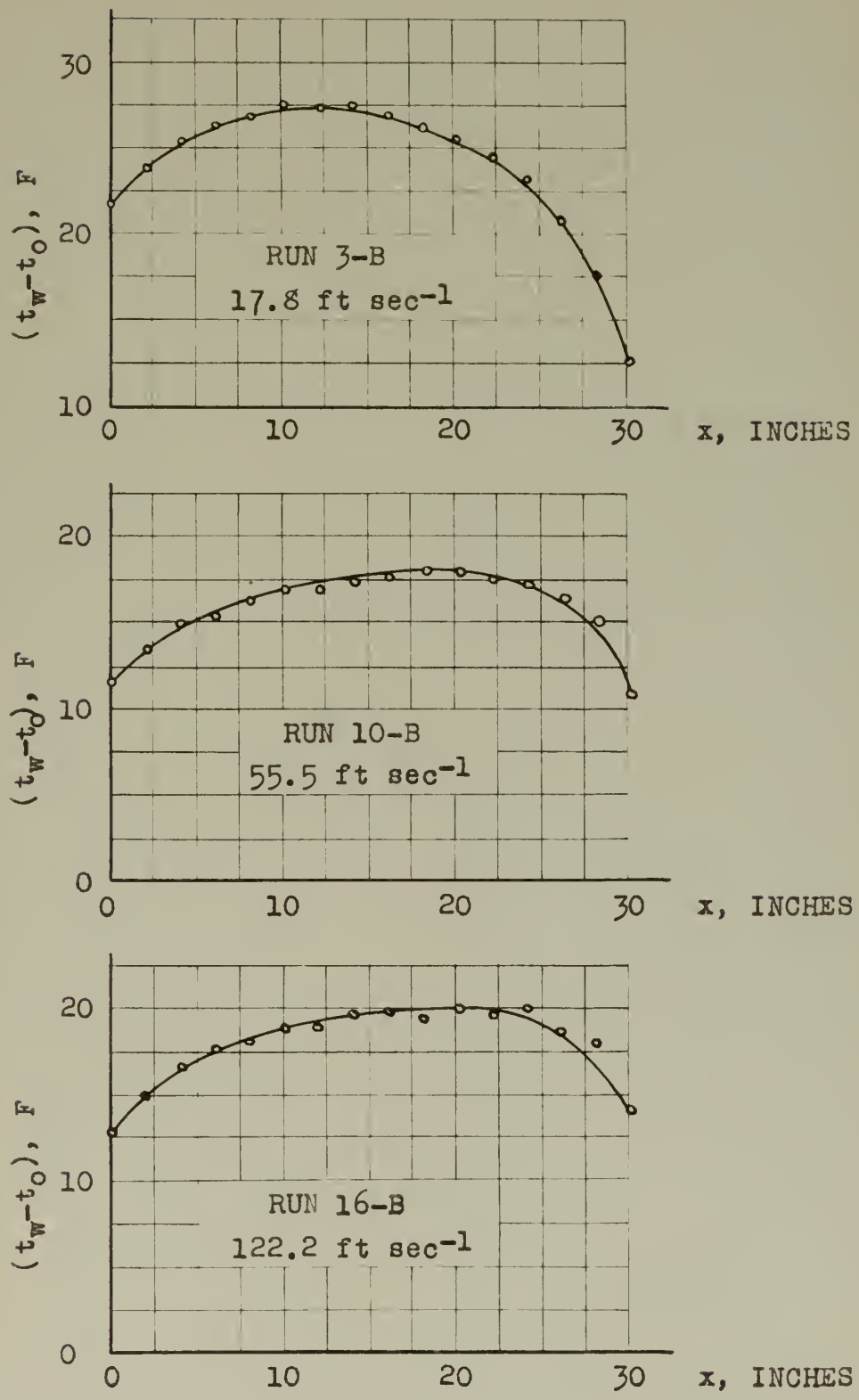


FIGURE 9. TEMPERATURE DISTRIBUTION DATA, SERIES B RUNS

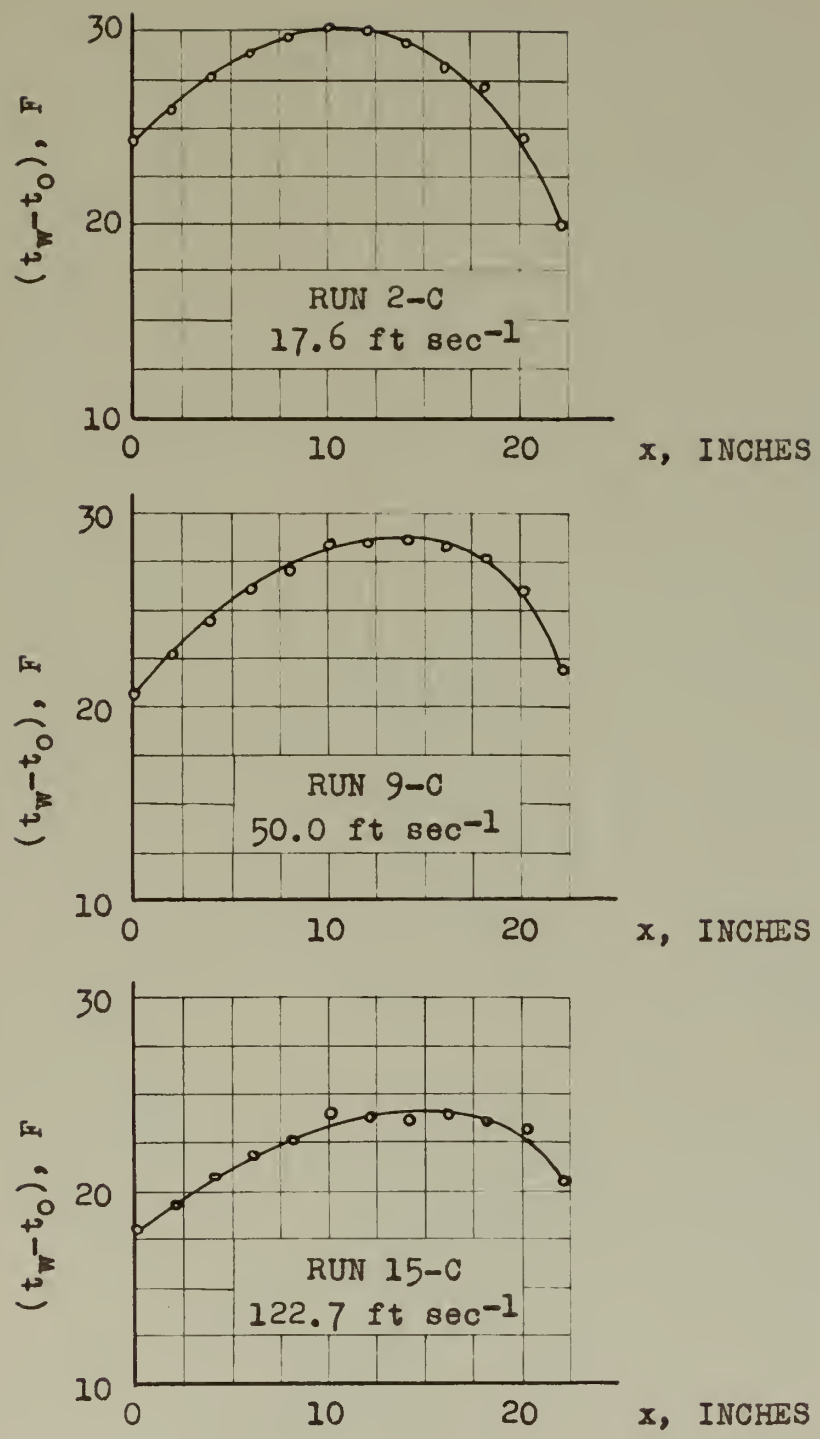


FIGURE 10. TEMPERATURE DISTRIBUTION DATA, SERIES C RUNS

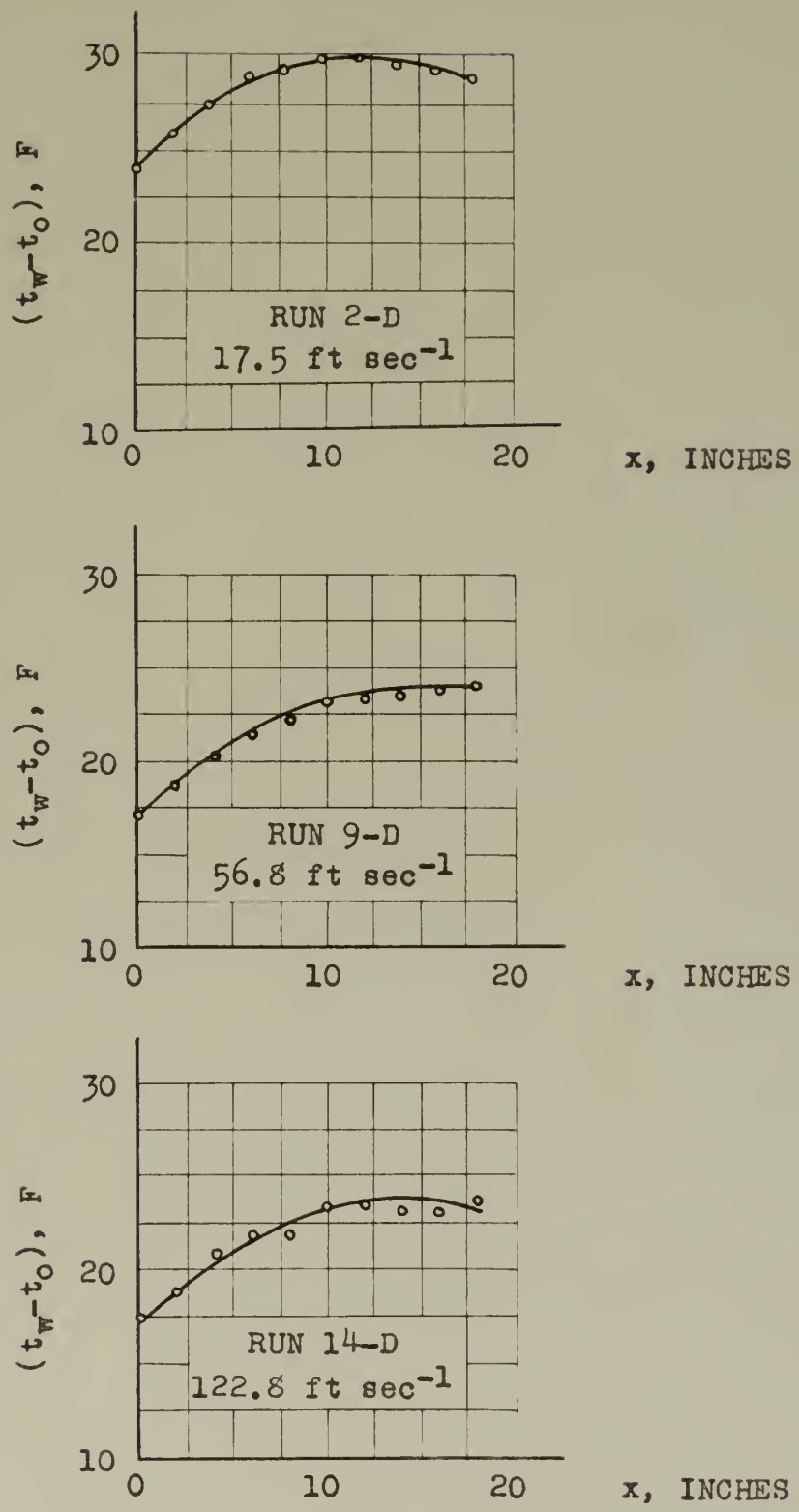


FIGURE 11. TEMPERATURE DISTRIBUTION DATA, SERIES D RUNS

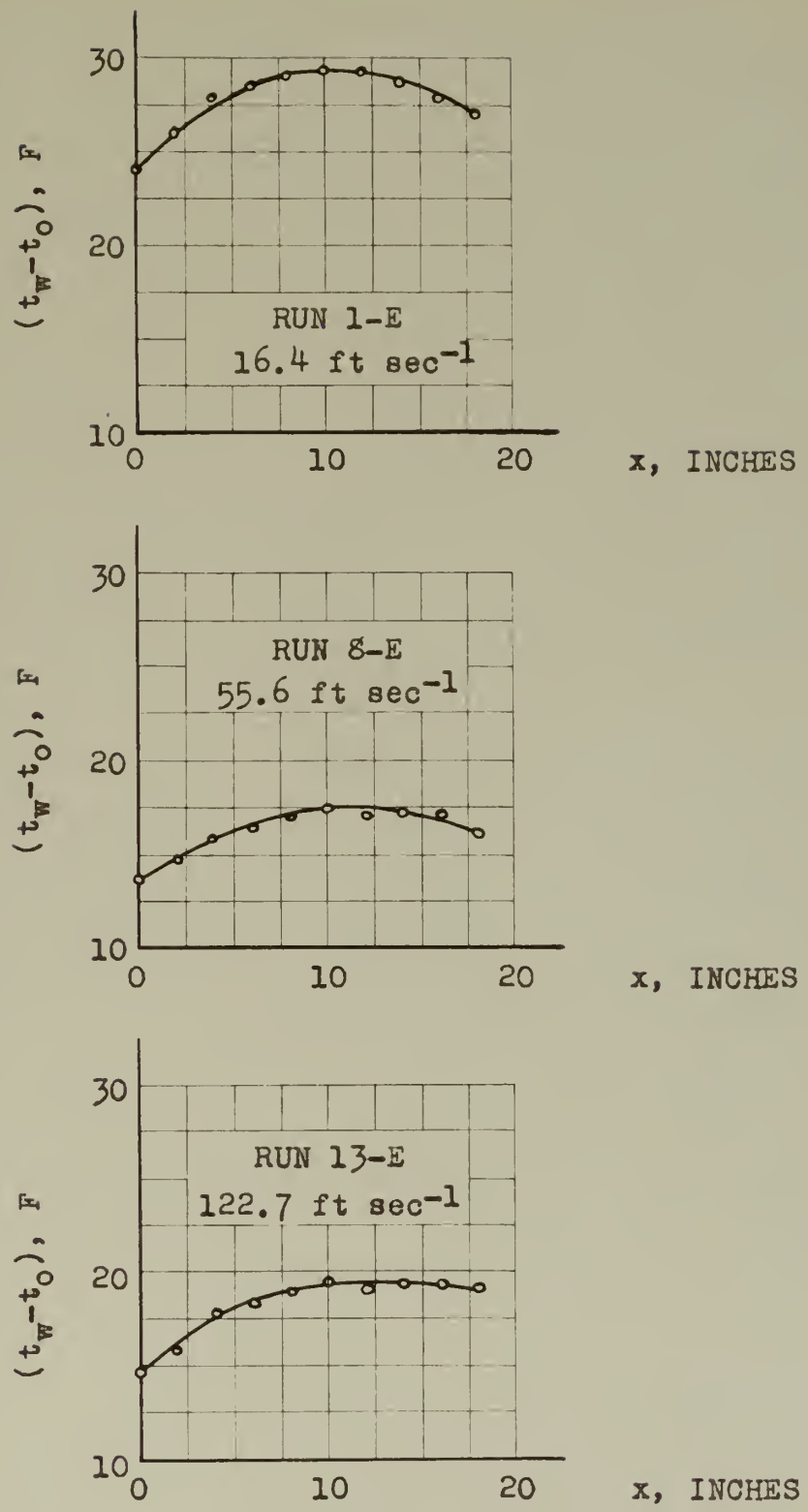


FIGURE 12. TEMPERATURE DISTRIBUTION DATA, SERIES E RUNS

CHAPTER VII

PHYSICAL PROPERTIES AND OTHER CONSTANTS

Physical properties and other constants are required in order to render the observed data into a more useful form. It was noted previously that the relative humidity of the air was a maximum of thirty-five per cent at the blower inlet. Such a relative humidity is small enough so that the air may be considered to be dry for present purposes. As a consequence, the properties of dry air were used and were obtained from the NBS-NACA Tables of Thermal Properties of Gases. These properties include kinematic viscosity (26), thermal conductivity (27), and Prandtl number (28).

An estimate of the thermal conductivity of the materials of construction is required also. The value chosen for the thermal conductivity of both inner and outer brass tubes is 59 B $hr^{-1}ft^{-1}F^{-1}$, according to Jakob (5). The value chosen for the thermal conductivity of the heat-resisting steel outer sheath of the Calrod heater is 15 B $hr^{-1}ft^{-1}F^{-1}$, according to Schack (29). The value chosen for the magnesium oxide insulation in the Calrod heater is 0.2 B $hr^{-1}ft^{-1}F^{-1}$, assumed to be equivalent to mica, according to Jakob (5).

Some of the heat transferred from the surface of the heat transfer element occurs by radiation to the surroundings. As the surface was bright chromium plated and then brightly polished, the value chosen for the hemispherical

emissivity is 0.07, from Jakob (5).

The heat energy conversion factor used was 3.413 B per watt-hour, according to Keenan and Keyes (25).

The computed areas of the various parts are:

Part	Area of cross-section, ft^2.
Outer tube, excluding holes	1.238×10^{-3}
Inner tube, excluding thinned section	1.914×10^{-4}
Calrod outer sheath and coil	2.09×10^{-4}
Calrod insulation	3.35×10^{-4}

The computed outer circumference of the outer tube is 0.1634 ft.

CHAPTER VIII

METHOD OF CALCULATION

The method of calculating the mean surface coefficient of heat transfer is based upon a heat balance and a defining equation. A heat balance may be written as:

$$q_i = q + q_r + q_n + q_e \text{ , or}$$

$$q = q_i - q_n - q_e - q_r \text{ .} \qquad \text{VIII-1}$$

Substitution from the defining equation, Equation II-3, yields:

$$h_m = \frac{q_i - q_n - q_e - q_r}{S_i \theta_m} \text{ ,}$$

$$= \frac{q_i - q_n - q_e - q_r}{C x_i \theta_m} \text{ ,} \qquad \text{VIII-2}$$

in which each term on the right must be evaluated.

The term q_i is the electrical heat energy released in the thermal length x_i. If the heating coil length is M, then the heat release per unit of length is (q_M/M) and the heat release for a length x_i is $(x_i q_M/M)$ for uniform heat release. A correction factor may be applied if the heat release is non-uniform. With such a factor, the heat release becomes:

$$q_i = \frac{F_x \, q_M \, x_i}{M} \text{ .} \qquad \text{VIII-3}$$

Values of q_M are given in Table XI. The data in the table come from multiplying the product of corresponding values in Tables VII and VIII, respectively, by the conversion factor 3.413 B per watt-hour.

TABLE XI

TOTAL HEAT INPUT

(Body of table is B hr^{-1})

Run No.	Run Series A	B	C	D	E	X	V
1	23.6	39.8	52.3	53.5	58.5	39.8	44.7
2	27.3	43.3	58.6	57.9	58.5	44.7	44.7
3	34.4	48.1	57.6	57.6	58.5	48.9	60.5
4	34.3	48.0	63.1	62.8	59.1	52.8	71.6
5	37.6	51.8	74.3	73.3	58.7	58.4	89.7
6	41.6	51.9	79.9	80.1	58.5	67.7	109.3
7	41.8	57.5	92.2	86.4	57.8	79.9	130.7
8	48.9	57.0	104.6	85.9	78.7	98.4	171.2
9	68.6	67.8	118.5	104.8	97.8	125.2	-
10	75.4	78.7	133.0	110.2	111.5	165.3	-
11	87.6	92.1	139.1	127.0	125.9	-	-
12	95.8	103.3	153.9	148.7	140.1	-	-
13	101.6	116.2	170.2	171.2	164.7	-	-
14	117.1	130.8	181.2	198.8	-	-	-
15	131.6	146.7	199.5	-	-	-	-
16	148.1	158.1	-	-	-	-	-

A coordinate system is chosen to describe other terms. The nosepiece joint is selected as the origin and the variable x is chosen to increase in a direction downstream from the joint along the heat transfer element.

The term Θ_m is defined by Equation II-5 and may be written as:

$$\Theta_m = (1/x_i) \int_0^{x_i} \Theta \, dx \quad . \qquad \text{VIII-4}$$

The term q_n is the heat lost to the nosepiece and may be written as:

$$q_n = k_x A \left(\frac{d\Theta}{dx} \right)_{x = 0} \quad . \qquad \text{VIII-5}$$

The term q_e is the heat passing along the heat transfer element downstream from the section located by x_i and may be written as:

$$q_e = -k_x A \left(\frac{d\Theta}{dx} \right)_{x = x_i} \quad . \qquad \text{VIII-6}$$

The term q_r accounts for the heat lost to the surroundings by radiation from the surface and may be written as:

$$q_r = h_r C x_i \Theta_m \quad . \qquad \text{VIII-7}$$

Data for Θ are not yet available. However, the data from Table X may serve for estimation purposes. Heat conduction through a round cylindrical wall may be expressed as:

$$q_c = - 2 \pi k_w L_t \frac{t_1 - t_2}{\ln (r_1/r_2)} \quad , \text{ or}$$

$$t_1 - t_2 = \frac{q_c \ln(r_2/r_1)}{2 \pi k_w L_t} \qquad \text{VIII-8}$$

For a fixed construction, Equation VIII-8 shows that the temperature difference is a maximum when q_c is a maximum. The maximum heat input in any run was 199.5 B hr^{-1}, found in Table XI. The ratio (r_2/r_1) may be written as (0.624/0.384). The value for k_w may be 59 B $hr^{-1}ft^{-1}F^{-1}$, and the value for L_t may be (31.75/12) ft.

Solution of Equation VIII-8 may be accomplished with the above values if it is assumed that all the heat generated passes through the wall. The solution yields t_1-t_2 to be 0.099 F as a maximum. On the other hand, the place of measuring the temperature was at half the wall thickness so that the temperature difference between the surface and the place of measurement is 0.05 F, approximately.

There is close geometrical similarity between the present instance and that of Jakob and Dow (2), and their study of the temperature field near the holes in the outer tube wall may be applicable. Their ratio of outside diameter to inside diameter is (1.3/0.95) equal to 1.37, the present one is (0.624/0.384) equal to 1.62; their ratio of wall thickness to hole height is (0.175/0.08) equal to 2.19, the present one is (0.120/0.0625) equal to 1.92.

It is considered that aerodynamic heating may not influence the temperature measurements. The relative velocity between the surface and the thermocouples used for measuring air stream temperature is zero. Both items have the same

general shape, that of a round cylindrical probe. Although the heating effect may have been as great as 1 F in some runs, it is considered that the effect on each item is the same and that the effect applied to the difference between the measurements is negligible.

As a consequence of the discussions above, the data of Table X are assumed to be applicable as measurements for surface temperature. The surface temperature may be found by adding corresponding values in Tables IX and X, respectively.

The values in Table X were plotted as a function of thermal length for all runs as illustrated in part in Figures 8-12, inclusive, to fair or smooth the data.

The irregularities in the data of Table X may be due to (a) hot spots, (b) air stream temperature stratification, (c) variations in thermocouple placement, and (d) the data are the difference between two magnitudes.

Most irregularities appear at high energy input rates. It is considered that hot spots are the probable cause of irregularities, because of the method of construction. The parts may touch at some places and may be entirely separated at others.

Stratification in the air stream was found to occur, the extent depending upon atmospheric conditions. This effect was the underlying reason for establishing temperature variation limits as recorded on the Speedomax, discussed in Chapter VI.

Variation in thermocouple location may have been one-eighth of an inch for it is assumed that placement was made to plus or minus one-sixteenth of an inch. An overall variation of placement of one-eighth of an inch could cause an irregularity of 0.1 F in the neighborhood of high temperature gradients along the element.

If it is assumed that the primary temperature determinations are within plus or minus 0.1 F then a difference of two such measurements could yield an irregularity of 0.2 F.

The smoothed data are found in Table XIII. The data from this table are used in subsequent calculations. Similarly, smoothed data for surface temperature may be obtained by adding corresponding values in Tables IX and XIII, respectively.

The mean temperature difference is found from Equation VIII-7 by applying Simpson's Rule for integration. Use of the rule affords progressive integration with ease and permits choosing thermal lengths in sequence at intervals of four inches. Several spot checks were made on the results of integration by using the data of Tables X and XIII, respectively. The difference between results did not exceed one per cent for the trial checks that were made.

The derivatives $\left(\frac{d\theta}{dx}\right)_{x=0}$ and $\left(\frac{d\theta}{dx}\right)_{x=x_i}$ are approximated by finite differences. The former derivative is approximated by $(\theta_2-\theta_0)/(x_2-x_0)$ equal to $6(\theta_2-\theta_0)$ F ft^{-1}, hence

$$q_n = 6k_x A(\theta_2-\theta_0) \text{ B } hr^{-1} \quad . \qquad \text{VIII-9}$$

The latter derivative is approximated by assuming that the best value is the average slope of the two secants joining the points (x_{i-2}, θ_{i-2}), (x_i, θ_i) and (x_i, θ_i), (x_{i+2}, θ_{i+2}), respectively. The slope of the one secant is $(\theta_i-\theta_{i-2})/(x_i-x_{i-2})$ equal to $6(\theta_i-\theta_{i-2})$ F ft^{-1}. Similarly, the slope of the other secant is $6(\theta_{i+2}-\theta_i)$ F ft^{-1}. The average of the slopes is $3(\theta_{i+2}-\theta_{i-2})$ F ft^{-1}, hence

$$q_e = -3k_xA(\theta_{i+2}-\theta_{i-2}) \text{ B } hr^{-1} . \qquad \text{VIII-10}$$

The evaluation of the product (k_xA) is based upon the assumption that the temperature gradients along the outer tube, inner tube, and heater are the same although the temperature level of each may be different. It may be supposed, as an example, that the parts are centered. The air space between the inner and outer tubes is 0.004 in. and is 0.005 in. between the inner tube and heater. The thermal conductivity of the air may be 0.0156 B $hr^{-1}ft^{-1}F^{-1}$ at 100°F and the maximum and minimum heat release rates from Table XI are 199.5 and 23.6 B hr^{-1}, respectively. With the aid of Equation VIII-8, there results:

Power Input B per hr	$t_1 - t_2$, F	
	0.004 in. space	0.005 in. space
199.5	16.0	23.5
23.6	1.9	2.8

The above data are indicative of the respective temperature levels.

The calculation of the product ($k_x A$) is as:

Part	k	A	kA	Per cent of Total
	B $hr^{-1}ft^{-1}F^{-1}$	ft^2	B ft $hr^{-1}F^{-1}$	
Outer tube	59	1.239×10^{-3}	73.1×10^{-3}	83.6
Inner tube	59	1.914×10^{-4}	11.3×10^{-3}	12.9
Calrod sheath	15	2.09×10^{-4}	3.1×10^{-3}	3.5
Calrod insulation	0.2	3.34×10^{-4}	0.06×10^{-3}	-
Total			87.5×10^{-3}	100.0

This result shows that 83.6 per cent of the heat conducted along the heat transfer element is conducted by the outer tube, if the temperature gradients are the same for each part.

An estimate of the consequences of the assumption is of interest. At the nosepiece joint, for example, the temperature gradient in the outer tube was limited to 1 F per inch or 12 F per foot, approximately. It may be supposed, for example, that the gradients along the inner tube and the heater are in the proportion 1:2:4. For these conditions, the ratio of the new kA product to that computed above is 1.24. With a heat input rate of 199.5 B hr^{-1}, the heat input to a length of four inches is 25.2 B hr^{-1}. The loss through the nosepiece in the one case is (12 x 0.0875) equal to 1.05 B hr^{-1}, or 4.17 per cent of the heat input. In the other case, the loss is (1.05 x 1.24) equal to 1.30 B hr^{-1}, or 5.15 per cent of the heat input. Thus the loss error is 0.98 per cent of the heat input.

The same calculation with the minimum heat input, 23.6 B hr^{-1}, yields 35.3 per cent and 43.6 per cent of the heat

input, respectively, and the loss error becomes 8.3 per cent.

The loss error is seen to decrease as the length is increased. At those places where the temperature gradient along the outer tube approaches zero, the basic assumption becomes more valid. As a consequence of the above discussions, the temperature gradients along the members are assumed to be the same as that along the outer tube.

The correction factor F_x may be estimated. Measurement of the heat input to a heating element is seen to yield the total value and no information as to release distribution can be obtained from such a measurement. Thus two coils having the same electric resistance may be wound with uniform wires so that the wires are bunched together in one coil and evenly spaced on the other; or, a uniform wire may be used on one coil and a tapered wire on the other. The measured heat input rate would be the same for all.

Let it be assumed that the temperature distribution along a coil of length M is given as $\Theta = a_o - b_o x$. The heat transferred is:

$$q = \int_0^M hC\Theta \, dx \text{ , and for constant h,}$$

$$q = hC\left(a_o M - \frac{b_o M^2}{2}\right),$$

and this is also the measured heat input, that is, $q = q_M$. If b_o is a small number, h may be assumed to be constant so

that $q = hC\Theta_m$. Substitution for q yields:

$$\Theta_m = a_o - \frac{b_o M}{2} .$$

When a distance x_i along the heater is considered, then:

$$q_i = \int_0^{x_i} hC\Theta \, dx$$

$$= hC \left(a_o x_i - \frac{b_o x_i^2}{2} \right).$$

The assumed heat input from input measurements may be $q_m = hCx_i\Theta_m$, which is less than q_i, becoming equal to it at $x_i = M$.

The factor F_x may be defined by the ratio (q_i/q_m). Then,

$$F_x = \frac{q_i}{q_m} ,$$

$$= \frac{a_o - \frac{b_o x_i}{2}}{a_o - \frac{b_o M}{2}} , \text{ or}$$

$$F_x = \frac{1 - \frac{b_o}{2a_o} x_i}{1 - \frac{b_o}{2a_o} M} \qquad \text{VIII-11}$$

It is recalled that the Calrod heater tests could be represented by the equations:

$$\theta_A = 367.1 - 0.43\ z, \text{ and}$$

$$\theta_B = 160.4 - 0.19\ z.$$

Figure 7 shows that the equations may be extended to the left beyond the middle twenty-four inches (z = 12 to 36 in.), the basis originally chosen.

The relation between z and x_i is given by $x_i = z - 10$. By substitution, there results:

$$\theta_A = 362.8 - 0.43\ x_i = a_A - b_A x, \text{ and}$$

$$\theta_B = 160.4 - 0.19\ x_i = a_B - b_B x.$$

The ratio $(b_o/2a_o)$ may be computed from these, for $(b_A/2a_A)$ is (0.43/362.8) equal to 0.000593 and $(b_B/2a_B)$ is (0.19/160.40 equal to 0.000599, with 0.000596 as the average.

Substitution of this result into Equation VIII-11 yields:

$$F_x = \frac{1 - 0.000596\ x_i}{0.981},$$

where M is 31.75 inches and x_i is in inches.

The correction factors for the calculation of the mean surface coefficient for the thermal lengths used are:

x_i	4	8	12	16	20	24	28
F_x	1.017	1.014	1.012	1.009	1.007	1.004	1.002

The heat transferred by radiation from a small body enclosed by a larger one is expressed by Stefan-Bolzmann's law and by Kirchoff's law as:

$$q_r = 0.174 \epsilon S \left[\left(\frac{T_s}{100}\right)^4 - \left(\frac{T_e}{100}\right)^4\right], \text{ B hr}^{-1}$$

$$= h_r S(T_s - T_e),$$

from which:

$$h_r = \frac{0.174 \epsilon \left[\left(\frac{T_s}{100}\right)^4 - \left(\frac{T_e}{100}\right)^4\right]}{T_s - T_e}, \text{ B hr}^{-1}\text{ft}^{-2}\text{F}^{-1}.$$

VIII-12

The order of magnitude of h_r is of interest. It may be supposed, for example, that $T_s = 572°R$, $T_e = 540°R$, and that $\epsilon = 0.07$. With the aid of Equation VIII-12, h_r is found to be 0.088 B $hr^{-1}ft^{-2}F^{-1}$. If it is supposed that $T_s = 538°R$, $T_e = 525°R$, with other values as before, the computation yields h_r to be 0.075 B $hr^{-1}ft^{-2}F^{-1}$. These results represent extreme values encountered in the experiments.

Also, the experiments were conducted during the winter season so that the temperature of the surrounding room walls was less than that of the air stream. As a consequence of the above discussions, a constant value of h_r is used in all calculations and is chosen to be 0.1 B $hr^{-1}ft^{-2}F^{-1}$.

Equation VIII-2 may now be written in the form of a working equation as:

$$h_m = \frac{F_x q_m (x_i/31.75) - 0.525(\theta_2 - \theta_0) + 0.263(\theta_{i+2} - \theta_{i-2})}{0.1634 \quad (x_i/12)\theta_m} - 0.1.$$

By Simpson's Rule, $\theta_m = (2/3x_i)(\theta_0 + 4\theta_2 + 2\theta_4 + \cdots + \theta_i)$ for an integration interval of two inches. Substitution for θ_m

yields the final working equation as:

$$h_m = \frac{3.47F_x q_M x_i - 57.8(\theta_2 - \theta_0) + 28.9(\theta_{i+2} - \theta_{i-2})}{(\theta_0 + 4\theta_2 + 2\theta_4 + \cdots + \theta_i)} \quad -0.1, \qquad \text{VIII-13}$$

where h_m is in B $hr^{-1}ft^{-2}F^{-1}$, x_i is in inches, and corresponding θ_i are from Table XIII.

A local surface coefficient of heat transfer may be computed also. The computation is based upon an approximation to Equation II-1 by finite differences over a thermal length of two inches.

Let three points as (x_{i-2}, θ_{i-2}), (x_i, θ_i), and (x_{i+2}, θ_{i+2}) be chosen. The heat gained at a section at x_i-1 inches may be approximated by:

$$q_{c,o} = -k_x A(\theta_i - \theta_{i-2})/(x_i - x_{i-2}),$$
$$= -6k_x A(\theta_i - \theta_{i-2}), \text{ B } hr^{-1} . \qquad \text{VIII-14}$$

The heat lost at a section at x_i+1 inches may be approximated by:

$$q_{c,2} = -6kA(\theta_{i+2} - \theta_i), \text{ B } hr^{-1} . \qquad \text{VIII-15}$$

The electrical heat energy released may be given by:

$$q_i = F_x' q_M(2/M), \text{ B } hr^{-1} , \qquad \text{VIII-16}$$

where M is in inches.

The heat transferred through the surface may be written as:

$$q = (h_r + h)C\theta_i(2/12), \text{ B } hr^{-1} . \qquad \text{VIII-17}$$

The heat balance for the portion of element may be written as:

$$q_{c,o} + q_i = q_{c,2} + q \qquad \text{VIII-18}$$

Substitution into Equation VIII-18 from Equations VIII-14 to VIII-17, inclusive, yields:

$$h = \frac{F_x' q_M (12/M) + 36kA(\theta_{i+2} - \theta_{i-2} - 2\theta_i)}{C\theta_i} - h_r$$

Substitution of previously determined constants gives the final working equation as:

$$h = \frac{2.305 F_x' q_M - 19.28(2\theta_i - \theta_{i+2} - \theta_{i-2})}{\theta_i} - 0.1, \quad \text{B hr}^{-1}\text{ft}^{-2}\text{F}^{-1}, \qquad \text{VIII-19}$$

in which F_x' is yet to be determined.

The factor F_x' is defined and determined as:

$$F_x' = \frac{\int_{x_i - 1}^{x_i + 1} hC\theta \, dx}{2hC\theta_m'}$$

$$= \frac{\theta_i}{\theta_m}$$

and,

$$F_x' = \frac{a_o - b_o x}{a_o - b_o M/2}$$

$$= \frac{1 - \frac{b_o}{a_o} x_i}{1 - \frac{b_o}{2a_o} M}$$

Substitution of the values previously determined yields:

$$F_x' = \frac{1 - 0.001192\, x_i}{0.981} \qquad \text{VIII-20}$$

The correction factors for determination of the local coefficient of heat transfer for the thermal lengths used are:

x_i	2	4	6	8	10	12	14	16
F_x	1.017	1.014	1.012	1.009	1.007	1.005	1.002	1.000

x_i	18	20	22	24	26	28	30
F_x	0.997	0.995	0.993	0.991	0.988	0.985	0.983

It is recalled from Chapter III that the Reynolds number offers a description of the flow configuration. The characteristic length is best chosen as the length upon which the boundary layer is formed whether heat is transferred or not. Therefore, the characteristic length is chosen as the total length and the kinematic viscosity is chosen at the undisturbed air stream temperature, t_o.

The choice of the total length may be arbitrary in this instance. If the intersection of the longitudinal axis of the heat transfer element with the tangent plane at the nosetip is called a pole, then the starting length is defined as the distance along a meridian from the pole to the nosepiece joint. The thermal length is chosen as the distance along the heat transfer element measured downstream from the nosepiece joint. With these definitions, the total length becomes the sum of the starting and thermal lengths.

The starting lengths may be computed as:

$$s = L_n - r + \frac{\pi r}{2}$$

$$s = L_n + r\left(\frac{\pi}{2} - 1\right)$$

$$= L_n + 0.18, \text{ inches.} \qquad \text{VIII-21}$$

The starting lengths used are given in Table XII.

TABLE XII

HYDRODYNAMIC STARTING LENGTHS

Run Series	Nosepiece length inches	Starting length inches	Starting length feet
A	0.31	0.49	0.0409
B	5.25	5.43	0.452
C	12.06	12.24	1.020
D	18.06	18.24	1.520
E	24.00	24.18	2.015
X	5.25	5.43	0.452
V	5.25	5.43	0.452

The concept of the Reynolds number as a fluid flow number may be applied to the Nusselt number. The Nusselt number becomes a heat transfer number. If the concept is continued, the total length in the Reynolds number is replaced by the thermal length in the Nusselt number. It may be noted that the characteristic length in both numbers becomes the same when the starting length is zero. Therefore, the characteristic length in the Nusselt number is chosen as the thermal length.

The choice of the physical properties of the fluid for the Nusselt number and the Prandtl number is based upon a film temperature. The film temperatures are defined as follows:

For computations with h_m,

$$t_f' = t_o + \frac{\theta_m}{2}, \ ^oF. \qquad \text{VIII-22}$$

For computations with h,

$$t_f = t_o + \frac{\theta}{2} \ , \ ^oF. \qquad \text{VIII-23}$$

The procedure described shows how Nusselt number and Reynolds number may be computed. The general pattern of further calculations is to develop an equation in the form of Equation II-8.

The Prandtl number for air in the range of the experiments may be assumed to be constant. The extreme values are 0.710 at 65°F and 0.708 at 84°F, with an average of 0.709. It is seen that the extreme variation of Prandtl number is in the order of one-third of one per cent.

With this result, Equation II-8 may be written as:

$$(N_{Nu})_x = C_o' \, (N_{Re})_L^n \, \phi^m \qquad \text{VIII-24}$$

The procedure for subsequent calculation may be:

(a) Establish regions of laminar and turbulent boundary layers,

(b) Find a suitable exponent for Reynolds number for each surface configuration,

(c) Find a function ϕ^m, and

(d) Establish C_o' and compare with values for other curvatures.

TABLE XIII

CORRECTED TEMPERATURE DISTRIBUTION DATA, SERIES A RUNS

(Body of table is $t_s - t_o$, F)

x, in.	Run No. 1	2	3	4	5	6	7	8	9
0	12.9	13.3	15.0	13.6	13.7	13.2	12.2	13.6	14.8
2	14.6	15.1	17.3	15.6	15.7	15.2	14.0	15.8	17.2
4	15.8	16.3	18.9	17.1	17.1	16.6	15.1	17.3	18.4
6	16.6	17.1	20.0	18.1	18.1	17.6	15.8	18.3	19.1
8	17.2	17.7	20.5	18.6	18.5	18.1	16.3	18.5	19.5
10	17.5	18.0	20.7	18.8	18.6	18.3	16.5	18.5	19.7
12	17.7	18.2	20.7	18.7	18.6	18.4	16.6	18.4	19.8
14	17.7	18.1	20.5	18.6	18.4	18.3	16.5	18.3	19.9
16	17.6	17.9	20.2	18.3	18.1	18.2	16.4	18.0	19.8
18	17.1	17.6	19.7	17.9	17.7	17.9	16.1	17.7	19.6
20	16.6	17.0	19.0	17.3	17.1	17.5	15.8	17.3	19.4
22	15.8	16.2	18.1	16.6	16.5	16.9	15.3	16.9	19.1
24	14.8	15.2	16.8	15.6	15.5	16.1	14.6	16.2	18.6
26	13.6	13.7	15.2	14.2	14.3	14.8	13.6	15.2	17.8
28	12.0	11.7	13.0	12.9	12.4	13.0	12.0	13.6	16.5
30	10.0	9.0	10.2	9.2	9.4	9.7	8.8	10.2	12.2

x, in.	Run No. 10	11	12	13	14	15	16
0	15.3	14.6	13.1	11.1	11.1	10.6	10.1
2	17.6	16.7	15.2	13.2	13.3	12.8	12.6
4	18.7	17.9	16.5	14.6	14.8	14.5	14.5
6	19.4	18.5	17.4	15.7	15.9	15.8	15.8
8	19.8	18.9	18.0	16.5	16.8	16.7	16.7
10	19.9	19.2	18.4	17.0	17.4	17.4	17.4
12	20.0	19.4	18.7	17.5	17.8	17.9	17.8
14	20.0	19.6	18.9	17.7	18.2	18.2	18.1
16	19.9	19.7	19.1	17.9	18.3	18.3	18.2
18	19.8	19.7	19.2	17.9	18.4	18.4	18.3
20	19.6	19.6	19.3	17.9	18.4	18.3	18.3
22	19.3	19.4	19.1	17.8	18.3	18.1	18.1
24	18.9	19.2	18.7	17.5	18.1	17.8	17.9
26	18.2	18.6	18.1	17.0	17.6	17.3	17.4
28	16.5	17.2	17.0	16.1	16.6	16.4	16.5
30	12.7	13.3	12.3	12.2	13.1	13.2	13.0

TABLE XIII, Continued

CORRECTED TEMPERATURE DISTRIBUTION DATA, SERIES B RUNS

(Body of table is $t_s - t_o$, F)

x, in.	Run No. 1	2	3	4	5	6	7	8	9
0	24.4	22.7	21.7	18.9	17.8	16.2	15.8	14.5	12.7
2	26.5	25.3	23.9	20.5	19.6	17.9	17.8	16.3	14.2
4	28.2	26.5	25.2	21.8	20.9	19.2	19.1	17.6	15.4
6	29.5	27.3	26.1	22.9	21.8	20.1	20.0	18.6	16.4
8	30.5	27.8	26.7	23.7	22.5	20.7	20.6	19.3	17.2
10	31.1	28.1	27.2	24.1	22.9	21.1	21.1	19.7	17.9
12	31.2	28.1	27.3	24.2	23.1	21.4	21.3	20.0	18.3
14	31.0	27.9	27.3	24.2	23.1	21.4	21.5	20.2	18.6
16	30.5	27.6	26.9	23.9	23.0	21.3	21.5	20.3	18.8
18	29.8	27.1	26.3	23.5	22.6	21.1	21.3	20.2	18.8
20	28.9	26.4	25.5	22.9	22.1	20.6	20.9	20.0	18.7
22	27.5	25.4	24.4	21.9	21.3	19.9	20.3	19.6	18.4
24	25.7	23.9	23.0	20.6	20.1	18.9	19.4	18.9	17.9
26	23.2	21.8	20.8	18.6	18.5	17.4	18.0	17.8	17.0
28	19.7	18.7	17.6	15.8	15.8	15.1	15.8	16.2	15.4
30	-	12.9	12.5	11.0	11.1	10.5	11.1	10.8	10.4

x, in.	Run No. 10	11	12	13	14	15	16
0	11.4	11.1	10.5	10.9	12.0	12.9	12.8
2	12.9	13.1	12.5	12.9	13.9	14.9	15.1
4	14.2	14.6	13.9	14.3	15.3	16.3	16.6
6	15.2	15.7	15.0	15.3	16.3	17.4	17.6
8	16.0	16.4	15.9	15.9	17.0	18.1	18.2
10	16.6	17.0	16.5	16.4	17.6	18.7	18.7
12	17.1	17.4	16.9	16.7	17.9	19.2	19.0
14	17.4	17.5	17.1	17.0	18.2	19.5	19.3
16	17.6	17.7	17.3	17.2	18.4	19.7	19.5
18	17.7	17.8	17.3	17.3	18.5	19.7	19.7
20	17.7	17.8	17.3	17.4	18.6	19.7	19.8
22	17.5	17.7	17.1	17.3	18.4	19.5	19.8
24	17.1	17.4	17.0	16.9	18.1	19.1	19.6
26	16.4	16.3	16.4	16.2	17.4	18.4	19.1
28	15.0	15.3	14.9	15.0	16.5	17.1	17.6
30	10.7	10.5	11.0	10.9	14.9	13.1	14.1

TABLE XIII, Continued

CORRECTED TEMPERATURE DISTRIBUTION DATA, SERIES C RUNS

(Body of table is $t_s - t_o$, F)

x, in.	Run No. 1	2	3	4	5	6	7	8	9
0	25.4	24.2	22.1	21.5	22.0	21.1	21.2	20.3	20.7
2	27.5	26.1	24.1	23.4	23.9	22.7	23.2	22.3	22.7
4	29.0	27.7	25.3	24.7	25.6	24.3	24.9	24.0	24.5
6	30.1	28.9	26.1	25.8	26.8	25.6	26.3	25.4	26.1
8	30.8	29.8	26.7	26.5	27.8	26.5	27.3	26.5	27.2
10	31.1	30.2	27.0	27.0	28.4	27.1	28.1	27.3	28.1
12	31.0	30.0	27.0	26.8	28.4	27.2	28.4	27.8	28.5
14	30.3	29.3	26.4	26.3	28.2	27.0	28.2	27.7	28.6
16	29.1	28.3	25.5	25.5	27.4	26.4	27.8	27.6	28.4
18	27.3	26.9	24.2	24.3	26.0	25.2	26.8	26.8	27.7
20	24.8	24.6	22.0	22.2	23.7	23.2	24.8	25.0	26.1
22	21.4	20.0	18.2	18.2	19.8	19.0	20.5	21.0	22.0

x, in.	Run No. 10	11	12	13	14	15
0	20.7	19.8	19.4	19.5	18.1	17.9
2	22.6	21.7	21.1	21.2	19.6	19.6
4	24.3	23.2	22.5	22.8	21.0	20.8
6	25.8	24.5	23.8	24.1	22.2	21.8
8	26.9	25.6	24.8	25.1	23.1	22.6
10	27.9	26.3	25.5	25.7	23.8	23.1
12	28.4	26.7	25.8	26.0	24.2	23.5
14	28.4	26.8	25.9	26.1	24.1	23.7
16	28.3	26.8	25.9	26.2	23.9	23.8
18	27.7	26.3	25.7	25.8	23.8	23.6
20	26.3	24.9	25.0	24.6	22.9	23.0
22	23.5	21.3	23.0	22.1	20.8	21.0

TABLE XIII, Continued

CORRECTED TEMPERATURE DISTRIBUTION DATA, SERIES D RUNS

(Body of table is $t_s - t_o$, F)

x, in.	Run No. 1	2	3	4	5	6	7	8	9
0	25.0	23.9	21.4	21.2	22.0	21.6	20.8	17.4	17.0
2	27.0	25.9	23.1	22.9	24.0	23.7	22.8	19.5	18.9
4	28.6	27.4	24.4	24.2	25.5	25.3	24.5	20.8	20.3
6	29.7	28.6	25.5	25.2	26.5	26.4	25.7	21.8	21.4
8	30.6	29.4	26.1	25.8	27.0	27.1	26.6	22.4	22.2
10	30.9	29.8	26.4	26.1	27.1	27.3	27.0	22.8	22.8
12	30.9	29.8	26.4	26.0	27.0	27.4	27.0	23.1	23.1
14	30.6	29.6	26.1	25.8	26.8	27.3	26.9	23.2	23.4
16	30.3	29.3	25.8	25.4	26.5	27.0	26.6	23.2	23.5
18	29.6	28.8	25.2	24.9	26.0	26.6	26.2	23.1	23.5

x, in.	Run No. 10	11	12	13	14
0	16.1	15.6	16.8	16.8	17.7
2	17.6	17.3	18.6	18.8	19.6
4	18.8	18.6	19.9	20.3	21.0
6	19.9	19.6	20.9	21.3	22.0
8	20.8	20.4	21.7	21.8	22.6
10	21.4	20.9	22.2	22.4	23.1
12	21.5	21.3	22.6	22.8	23.4
14	21.6	21.6	22.9	23.0	23.5
16	21.6	21.8	23.1	23.1	23.6
18	21.5	21.8	23.2	23.1	23.6

TABLE XIII, Continued

CORRECTED TEMPERATURE DISTRIBUTION DATA, SERIES E RUNS

(Body of table is $t_s - t_o$, F)

x, in.	Run No. 1	2	3	4	5	6	7	8	9
0	24.0	21.5	19.5	17.8	16.6	14.6	11.6	13.1	14.2
2	26.6	23.5	21.6	19.3	18.0	15.8	13.1	14.5	15.9
4	27.7	24.7	22.8	20.2	19.1	16.8	14.1	15.7	17.0
6	28.5	25.4	23.6	20.9	19.7	17.5	14.7	16.3	17.8
8	29.0	25.8	24.2	21.4	19.9	17.8	14.9	16.9	18.3
10	29.2	26.0	24.3	21.7	19.8	18.0	15.0	17.2	18.7
12	29.1	26.0	24.1	21.7	19.6	17.9	15.0	17.4	18.8
14	28.9	25.7	23.7	21.5	19.2	17.7	14.8	17.2	18.7
16	28.1	25.2	23.1	21.1	18.7	17.5	14.5	16.9	18.5
18	26.9	24.2	22.2	20.3	18.2	17.2	14.1	16.4	18.1

x, in.	Run No. 10	11	12	13
0	14.0	14.2	13.1	14.6
2	15.9	16.1	15.0	16.6
4	17.2	17.4	16.1	17.7
6	17.9	18.3	16.9	18.4
8	18.5	18.9	17.4	18.8
10	18.8	19.2	17.7	19.1
12	19.0	19.4	17.9	19.3
14	19.1	19.3	18.0	19.5
16	19.0	19.1	17.9	19.4
18	18.7	18.6	17.6	19.1

TABLE XIII, Continued

CORRECTED TEMPERATURE DISTRIBUTION DATA, SERIES X RUNS

(Body of table is $t_s - t_o$, F)

x, in.	Run No. 1	2	3	4	5	6	7	8	9
0	18.8	19.6	18.3	17.0	15.5	15.2	14.9	11.4	11.5
2	20.7	21.5	20.5	18.8	17.6	17.2	16.9	13.0	13.3
4	22.1	22.9	21.9	20.1	18.9	18.5	18.4	14.3	14.6
6	23.1	23.9	22.8	21.1	20.0	19.5	19.4	15.2	15.5
8	23.9	24.6	23.4	21.7	20.7	20.2	20.1	15.9	16.2
10	24.5	25.1	23.7	22.2	21.1	20.7	20.6	16.3	16.7
12	24.9	25.4	23.9	22.4	21.4	20.9	20.9	16.7	16.9
14	25.0	25.4	24.0	22.4	21.5	21.0	21.1	16.8	17.0
16	24.9	25.2	23.8	22.3	21.4	21.0	21.0	16.9	17.0
18	24.5	24.8	23.5	21.9	21.2	20.7	20.7	16.8	17.0
20	23.9	24.2	22.9	21.3	20.7	20.2	20.4	16.7	16.9
22	23.1	23.4	22.2	20.5	20.1	19.6	19.8	16.5	16.7
24	21.9	22.2	21.1	19.4	19.1	18.7	19.0	16.1	16.3
26	20.1	20.3	19.4	17.7	17.6	17.3	17.7	15.4	15.5
28	17.3	17.0	17.5	15.1	15.3	15.3	16.8	14.1	14.4
30	11.9	12.0	11.8	10.7	10.3	10.7	11.4	10.1	10.5

x, in.	Run No. 10
0	12.9
2	15.2
4	16.5
6	17.4
8	18.0
10	18.5
12	18.6
14	18.6
16	18.6
18	18.5
20	18.3
22	18.1
24	17.7
26	16.9
28	15.7
30	11.7

TABLE XIII, Continued

CORRECTED TEMPERATURE DISTRIBUTION DATA, SERIES V RUNS

(Body of table is $t_s - t_o$, F)

x, in.	Run No. 1	2	3	4	5	6	7	8
0	26.1	22.0	20.8	18.1	14.5	13.4	13.1	13.1
2	28.3	23.7	22.7	19.9	16.7	15.8	15.6	15.8
4	30.2	25.0	24.3	21.5	18.2	17.2	17.1	17.5
6	31.6	26.0	25.5	22.9	19.8	18.4	18.3	18.6
8	32.6	26.5	26.5	24.0	20.8	19.2	19.1	19.4
10	33.2	26.8	27.0	24.9	21.5	19.8	19.7	19.9
12	33.2	26.8	27.2	25.6	22.1	20.2	20.1	20.2
14	32.9	26.6	27.1	25.8	22.3	20.5	20.3	20.4
16	32.4	26.2	26.9	25.9	22.5	20.7	20.4	20.5
18	31.7	25.6	26.4	25.9	22.6	20.9	20.5	20.6
20	30.7	25.0	26.0	26.0	22.8	21.0	20.6	20.6
22	29.4	24.1	25.2	25.6	22.9	21.0	20.5	20.5
24	27.6	22.8	24.0	24.6	22.7	20.9	20.3	20.4
26	25.1	20.8	22.3	23.0	21.8	20.4	19.7	20.0
28	21.6	18.0	19.4	20.3	19.7	18.7	18.2	18.7
30	16.0	13.4	14.5	15.1	15.3	14.5	14.4	15.0

CHAPTER IX

EXPERIMENTAL RESULTS

The preliminary experimental results are developed by expressing Nusselt number in terms of h_m. It may be noted that Equations VIII-13 and VIII-19 offer a choice between h and h_m for calculations.

It was shown in Chapter III that all theoretical results and one experimental result for determining the function ϕ^m in which h is to be used have been presented. One experimental result is available in which h_m is used. This would indicate that calculations with h may be preferable, for better comparison may be possible.

Closer examination of Equation VIII-19 shows that errors of approximation may be appreciable. The equivalent of $(d^2\theta/dx^2)$ is required and the attainment of an accurate approximation is a formidable obstacle. The factor F_x' is of importance and should be known accurately. These considerations show that the calculation of h may be of acceptable status only near the place where the temperature gradient along the outer tube is near zero.

Examination of Equation VIII-13 shows that the equivalent of $(d\theta/dx)$ is required as well as the factor F_x. However, it has been shown how the effects of errors of approximation may decrease as thermal length is increased. As a consequence, h_m is chosen for calculations.

The experimental results are shown graphically in

Figures 13 to 28, inclusive. Nusselt number is plotted as a function of Reynolds number with logarithmic coordinates. The results illustrated in Figures 13 to 20, inclusive, were obtained with the air stream flowing parallel to the longitudinal axis of the heat transfer element. It is noted that laminar boundary layers may have been obtained for $(N_{Re})_L$ up to 10^5 and that turbulent boundary layers may have been obtained for $(N_{Re})_L$ at 3×10^5. It is also noted that the exponent for Reynolds number is verified to be 0.5 in the laminar range and to be 0.8 in the turbulent range; the lines drawn in the Figures have corresponding slopes.

Each of the Figures is drawn for a specific thermal length. Comparing Figures 13 to 19, inclusive, it is noted that at a given Reynolds number the values for the different starting lengths (Series A, B, C, D, and E,) come closer to each other as the ratio s/L becomes smaller. This effect is noted for both laminar and turbulent flows.

The effect of oblique cross flow, with an angle of three degrees between the stream and element axes, is partially shown in Figure 21. The starting and thermal lengths chosen for the illustration are 5.43 in. and 16 in., respectively. At Reynolds numbers greater than 5×10^5, the slope of a line drawn through the data corresponds to an exponent of unity. At Reynolds numbers less than 4×10^5, the slope corresponds to an exponent of 0.57.

The behavior at high Reynolds number may have been anticipated. The surface coefficient of heat transfer in

rectangular cross flow is independent of the length for given fluid velocity and properties, excluding end effects. If the distance along the surface is chosen as characteristic length for both Nusselt number and Reynolds number then the variation of Nusselt number with Reynolds number should become linear; that is, the exponent for Reynolds number should be unity.

A possible conclusion, therefore, is that data in the turbulent range suggesting an exponent greater than 0.8 for Reynolds number with respect to Nusselt number may have been influenced by oblique cross flow.

The behavior at lower Reynolds numbers, approximating the transition region, is unexplained and is of no importance in the present work.

Comparison of Figures 13 to 20, inclusive, with Figure 21 shows that centering of the heat transfer element in the air stream was accomplished with reasonable effectiveness. The exponent of Reynolds number remains at 0.8 in the runs with parallel flow.

The effect of vibrations of the heat transfer element is partially illustrated in Figure 22. It is seen that the exponent for Reynolds number remains at 0.8 for the vibrations measured in the turbulent range. The effect of vibrations in the laminar range is not clear.

Composite results comparing vibration data, cross flow, and parallel flow are illustrated in Figures 23 to 28, inclusive. At high Reynolds numbers, the exponent for

cross flow is seen to remain at unity and the exponent for vibration data remains at 0.8. It is noted further that the effect of vibration may not be appreciable.

The effect of vibrations in the turbulent range may be examined quantitatively. The data of each run may be expressed as:

$$(N_{Nu})_x = C_s(N_{Re})_L^{0.8}$$

for the turbulent range. Rearrangement yields:

$$C_s = (N_{Nu})_x/(N_{Re})_L^{0.8} \qquad \text{IX-1}$$

in which C_s may assume different values for different surface configurations.

The computations for the Series V runs are illustrated in Table XIV. The data for the table were selected so that Reynolds number is equal to or greater than 5×10^5.

A similar computation for the Series B runs may be used for comparison purposes for the surface configurations are the same for both series. The results are summarized in Table XV.

TABLE XV

COMPARISON OF VIBRATION AND PARALLEL FLOW RESULTS

s, in.	x, in.	Average Value of C_s Series V	Series B	Difference, per cent of Series B Values
5.43	8	0.0185	0.0191	3.1
5.43	12	0.0214	0.0218	1.8
5.43	16	0.0234	0.0238	1.7
5.43	20	0.0249	0.0253	1.6
5.43	24	0.0261	0.0263	0.8
5.43	28	0.0267	0.0269	0.7

These results suggest that the effects of vibration

are within the limits of experimental and approximation error and that results with respect to the vibrations encountered may not be significant.

Two conclusions are possible with respect to vibrations. It is possible that the combination of different frequencies and the respective amplitudes is such that the net result is the same for the present experiments. On the other hand, it is possible that the kinds of vibrations encountered were of negligible effect in comparison with a system that does not vibrate.

Eckert (10) has stated that the greatest resistance to heat transfer by forced convection with turbulent boundary layers is due to the laminar sublayer, and that this layer is very thin with respect to the overall boundary layer thickness. It may be concluded, therefore, that vibrations have little effect on the heat transfer unless they are of such a nature as to interfere with the laminar sublayer.

Examination of the data coupled with the premise of Eckert leads to the conclusion that the effects of the vibrations encountered in the turbulent range are negligible with respect to a steady system. In addition, the conclusion is reached that vibrations may have a greater effect in the laminar range because the whole boundary layer is postulated to be laminar.

Illustration (C) of Figure 1 may serve for illustrating these conclusions. If it is supposed that part of the boundary layer to the right of L_c is removed or washed

away, yet allowing the laminar sublayer to remain intact, then appreciable changes in the heat transfer may not be expected. On the other hand, if a part of the boundary layer to the left of L_c' is washed away, then appreciable changes in the heat transfer may be expected.

An additional effect may occur when vibrating and steady systems are compared. In the case of flow in pipes, for example, it is known that laminar flow may occur for large Reynolds numbers. If such a flow is disturbed, then the flow becomes turbulent and remains so. Further, if a flow is occuring for Reynolds number less than the lower critical, then disturbances may introduce a turbulent flow which returns to laminar upon cessation of the disturbance. Thus the effect of vibration may be to change the lower critical Reynolds number, an amount depending upon the nature of the vibrations.

The supporting results of calculations for the Figures presented in this chapter are given in Tables XVI to XXII, inclusive.

TABLE XIV

CALCULATION OF VIBRATION DATA, SERIES V RUNS

Run No.		Thermal Length, inches					
		8	12	16	20	24	28
4	$(N_{Re})_L \times 10^{-5}$	-	-	-	-	5.25	5.96
	$(N_{Re})_L^{0.8} \times 10^{-4}$	-	-	-	-	3.77	4.17
	$(N_{Nu})_x$	-	-	-	-	969	1100
	$C_s \times 10^2$	-	-	-	-	2.57	2.64
5	$(N_{Re})_L \times 10^{-5}$	-	-	5.34	6.34	7.34	8.33
	$(N_{Re})_L^{0.8} \times 10^{-4}$	-	-	3.82	4.39	4.93	5.45
	$(N_{Nu})_x$	-	-	892	1089	1288	1457
	$C_s \times 10^2$	-	-	2.34	2.48	2.62	2.67
6	$(N_{Re})_L \times 10^{-5}$	-	6.08	7.48	8.87	10.25	11.66
	$(N_{Re})_L^{0.8} \times 10^{-4}$	-	4.24	5.01	5.72	6.42	7.18
	$(N_{Nu})_x$	-	916	1182	1432	1685	1985
	$C_s \times 10^2$	-	2.16	2.36	2.50	2.62	2.64
7	$(N_{Re})_L \times 10^{-5}$	6.05	7.85	9.65	11.45	13.23	15.05
	$(N_{Re})_L^{0.8} \times 10^{-4}$	4.22	5.20	6.12	7.03	7.90	8.75
	$(N_{Nu})_x$	775	1107	1420	1725	2050	2360
	$C_s \times 10^2$	1.84	2.13	2.32	2.46	2.59	2.69
8	$(N_{Re})_L \times 10^{-5}$	8.22	10.67	13.12	15.53	18.00	20.45
	$(N_{Re})_L^{0.8} \times 10^{-4}$	5.39	6.68	7.83	8.99	10.06	11.18
	$(N_{Nu})_x$	1005	1428	1840	2280	2670	3000
	$C_s \times 10^2$	1.86	2.14	2.35	2.53	2.65	2.69
Average $C_s \times 10^2$		1.85	2.14	2.34	2.49	2.61	2.67

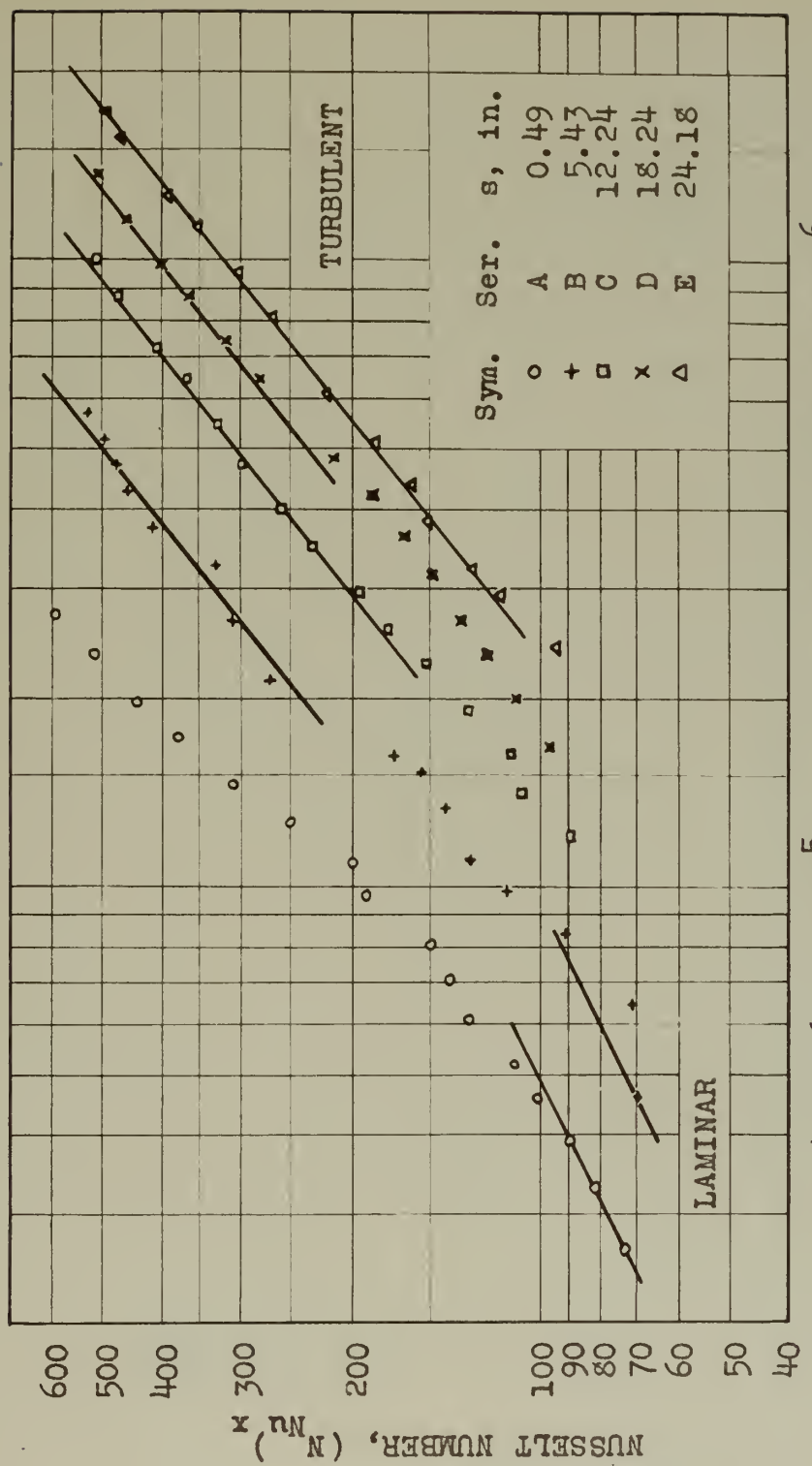


FIGURE 13. EXPERIMENTAL RESULTS FOR THERMAL LENGTH OF FOUR INCHES

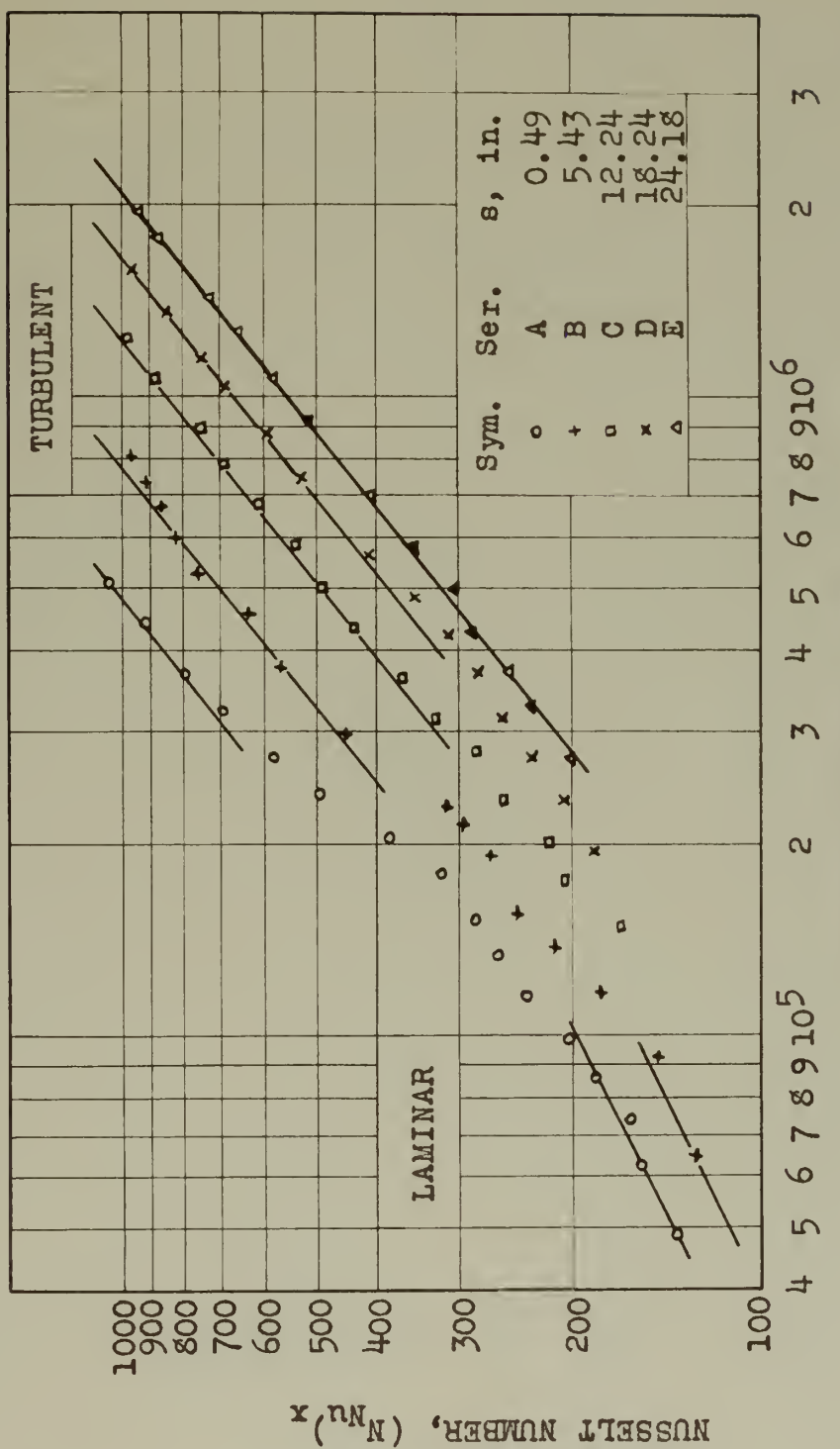


FIGURE 14. EXPERIMENTAL RESULTS FOR THERMAL LENGTH OF EIGHT INCHES

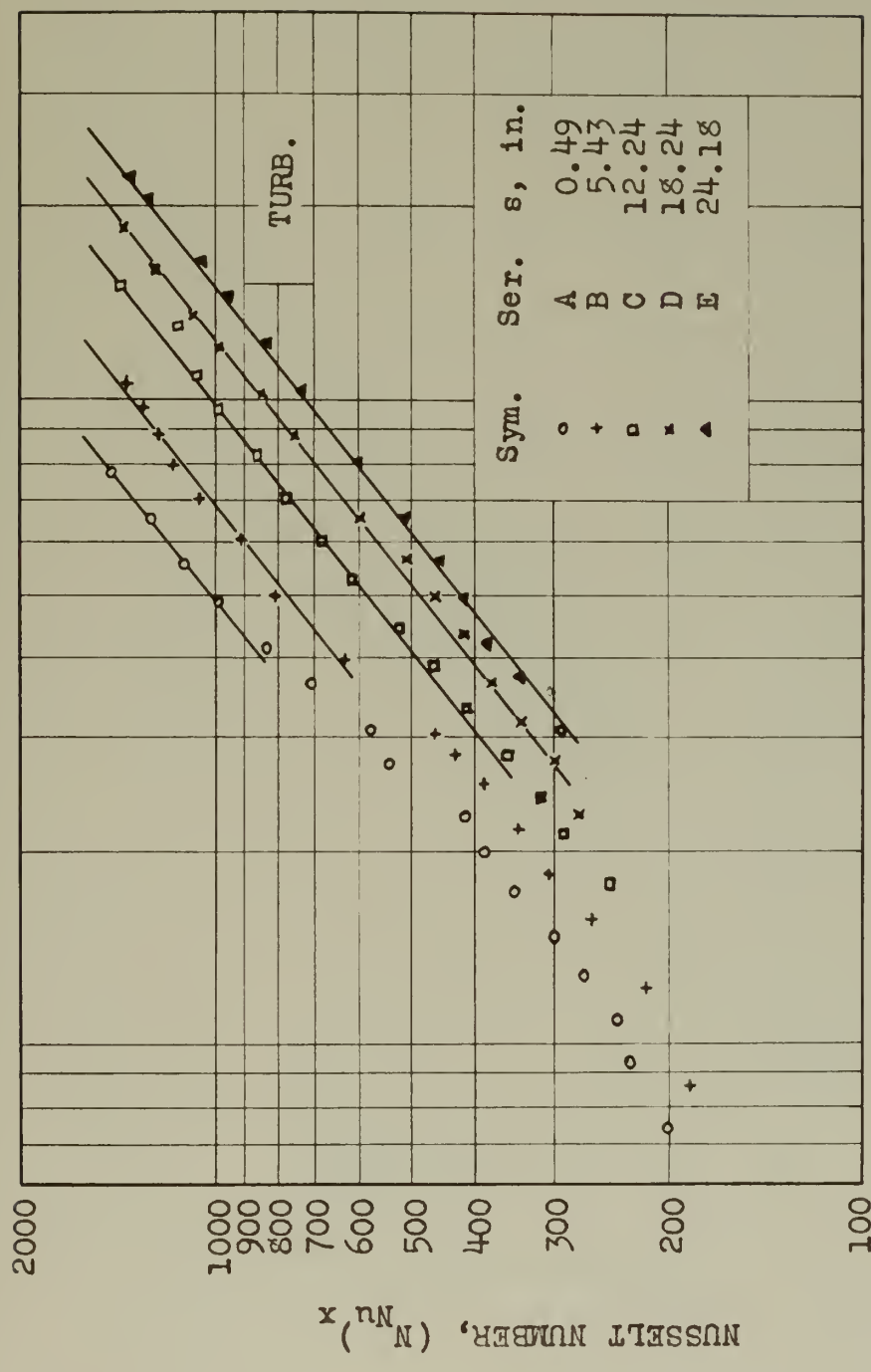


FIGURE 15. EXPERIMENTAL RESULTS FOR THERMAL LENGTH OF TWELVE INCHES

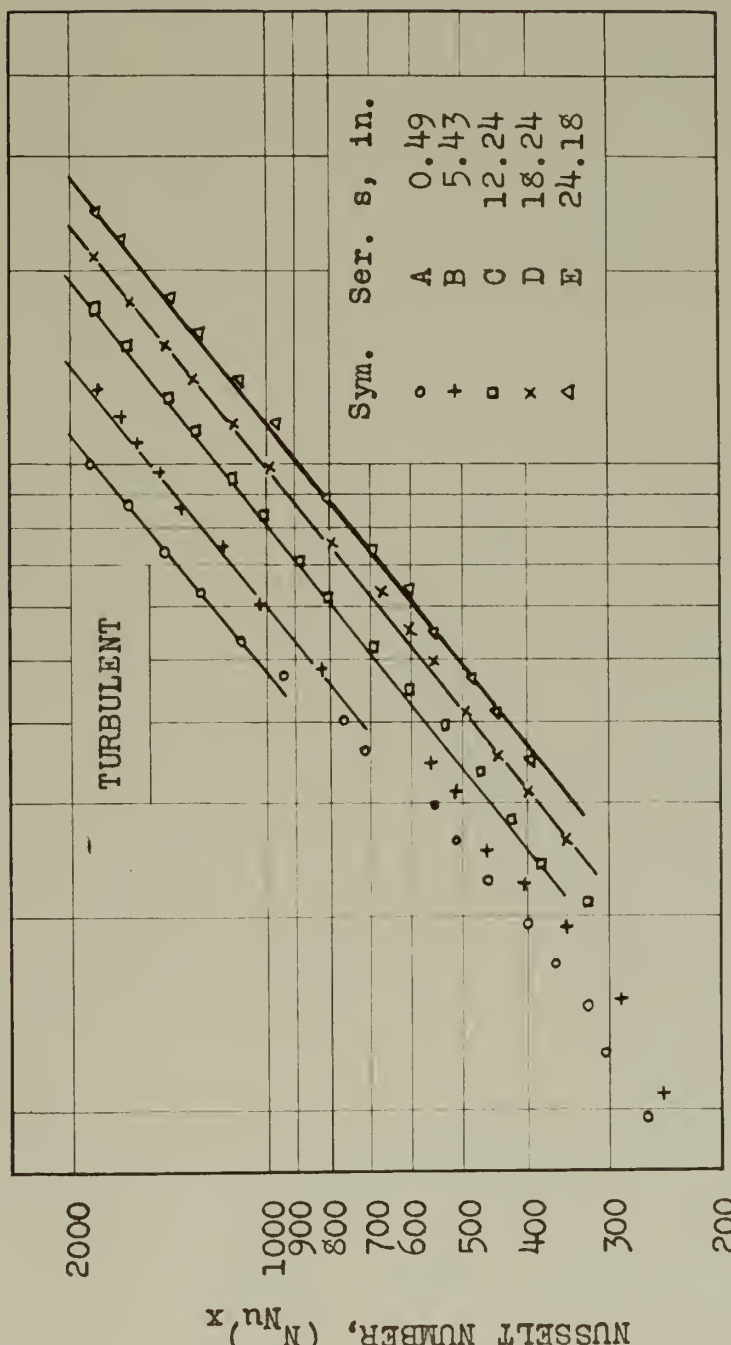


FIGURE 16. EXPERIMENTAL RESULTS FOR THERMAL LENGTH OF SIXTEEN INCHES

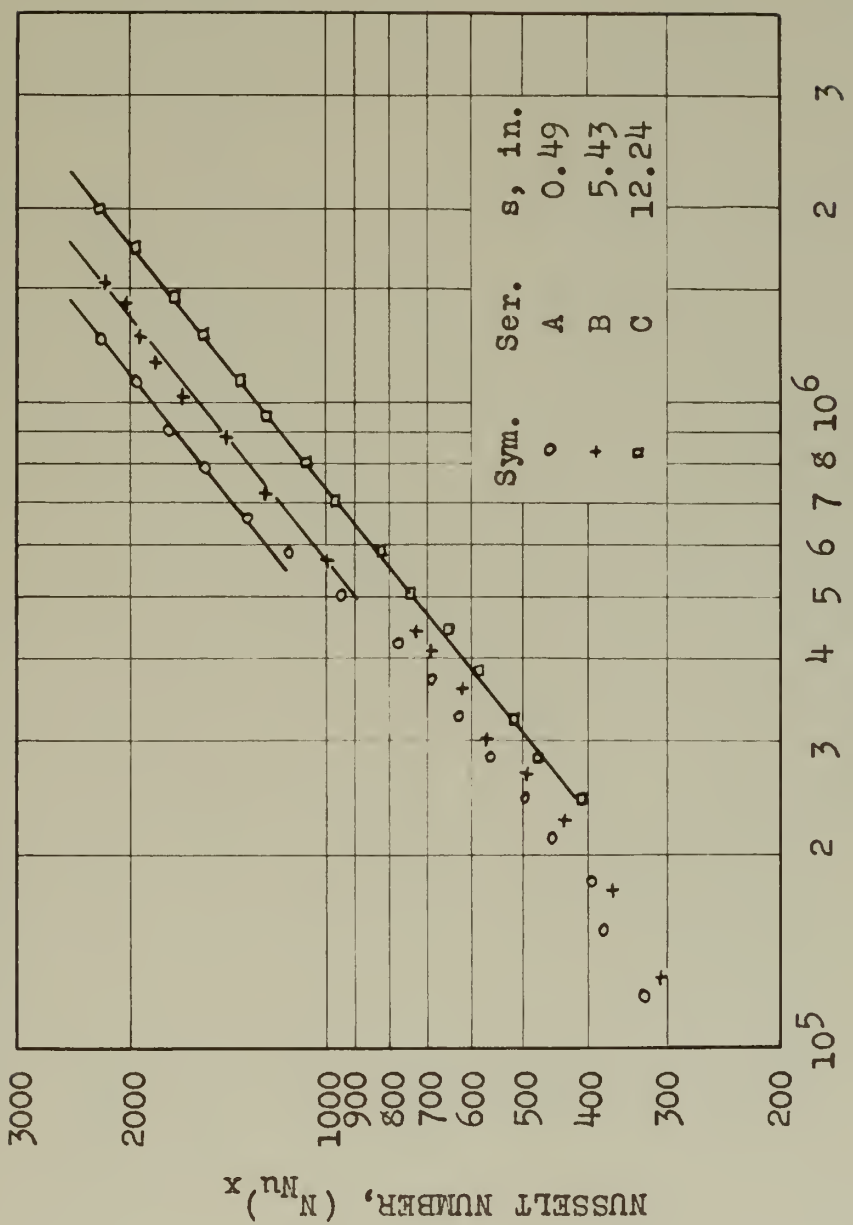


FIGURE 17. EXPERIMENTAL RESULTS FOR THERMAL LENGTH OF TWENTY INCHES

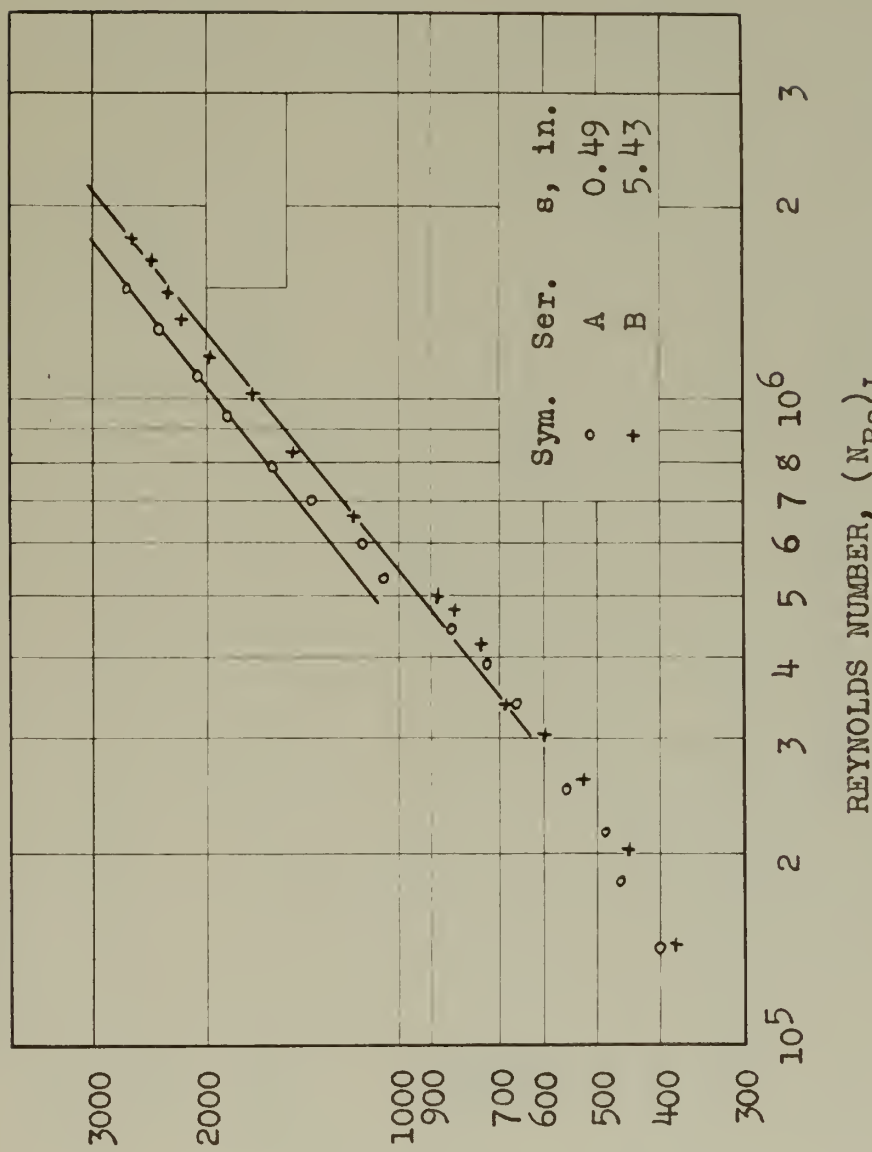


FIGURE 18. EXPERIMENTAL RESULTS FOR THERMAL LENGTH OF TWENTY-FOUR INCHES

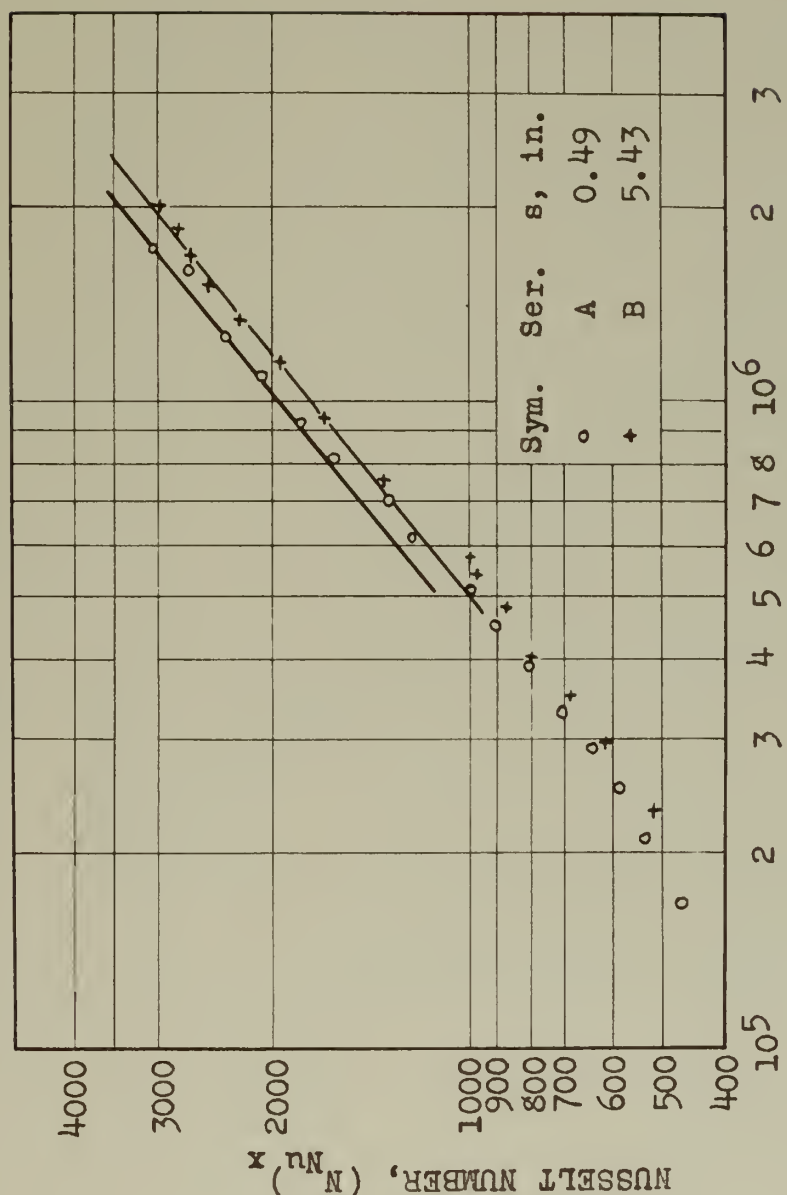


FIGURE 19. EXPERIMENTAL RESULTS FOR THERMAL LENGTH OF TWENTY-EIGHT INCHES

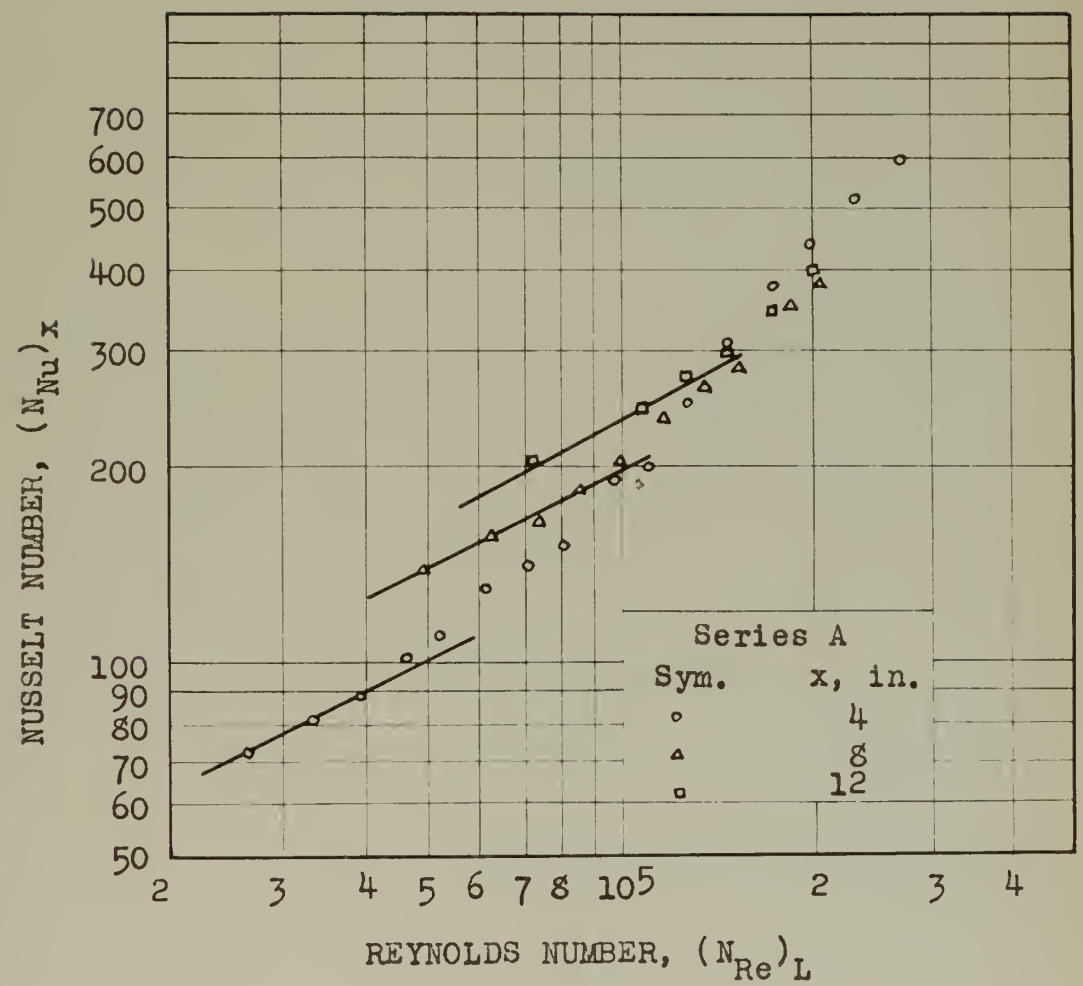


FIGURE 20. EXPERIMENTAL RESULTS FOR STARTING LENGTH OF 0.49 INCHES, LAMINAR FLOW

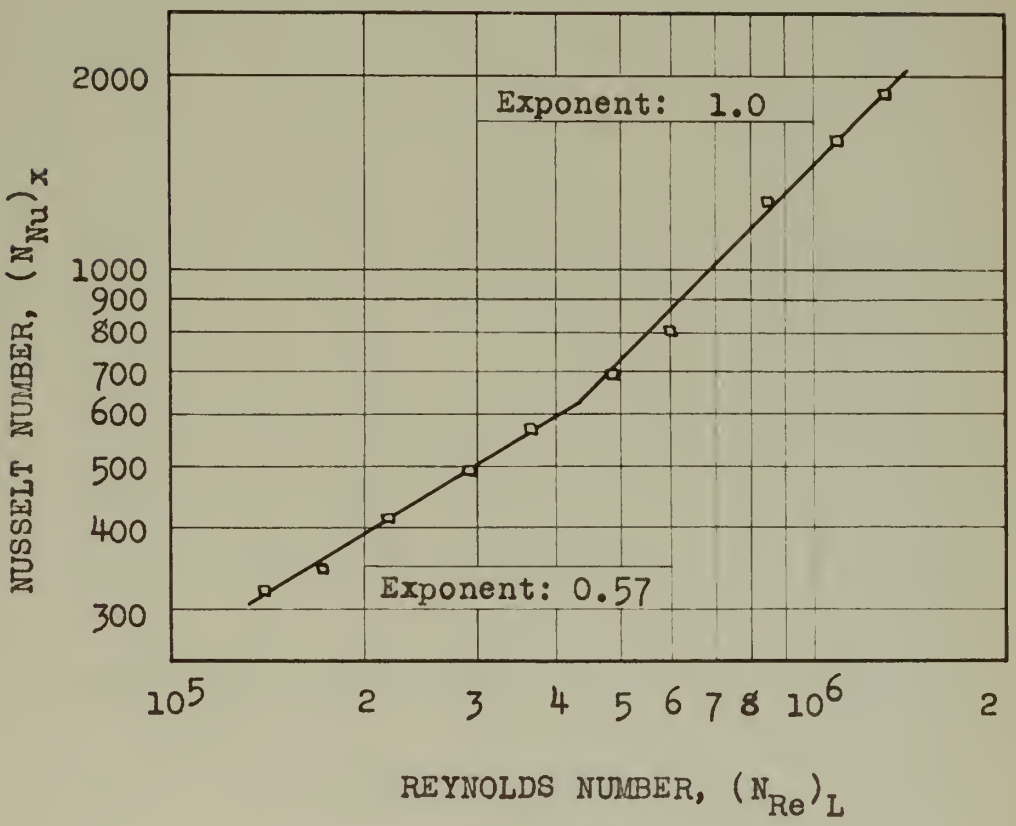


FIGURE 21. EXPERIMENTAL RESULTS FOR OBLIQUE CROSS FLOW FOR THERMAL LENGTH OF SIXTEEN INCHES. SERIES X RUNS. ELEMENT AXIS AT 3° TO JET AXIS.

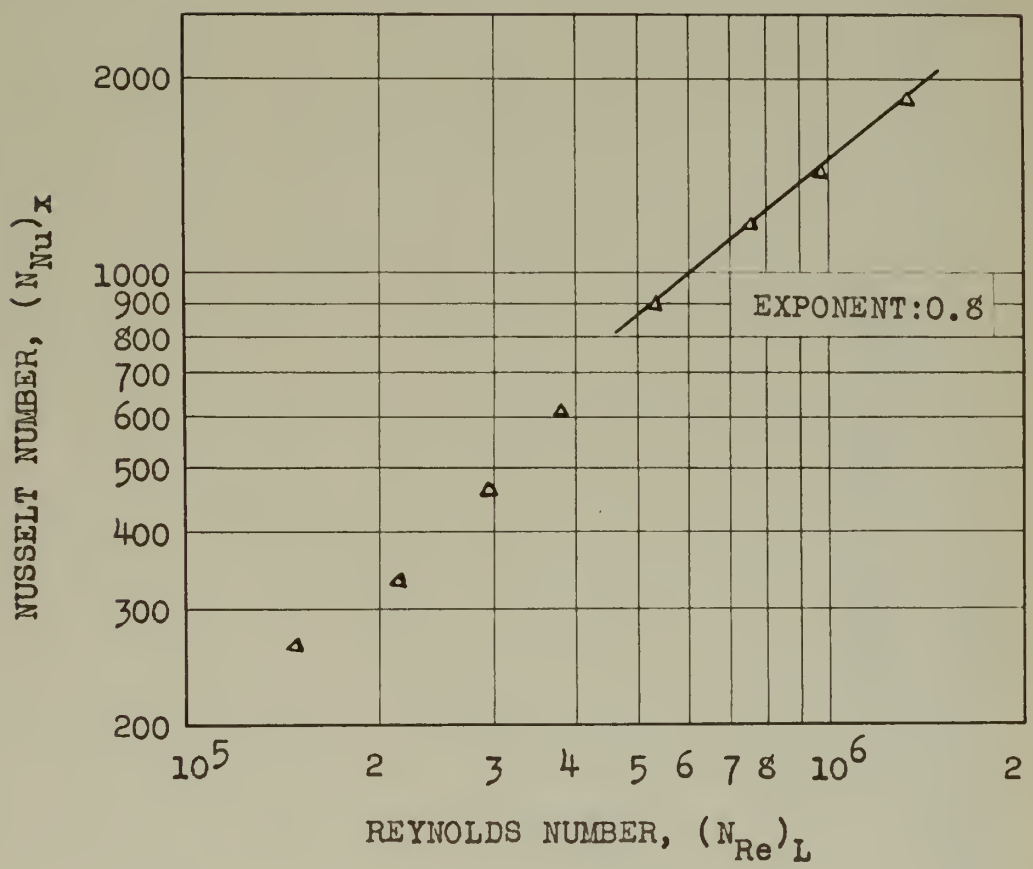


FIGURE 22. EXPERIMENTAL RESULTS FOR VIBRATION FOR THERMAL LENGTH OF SIXTEEN INCHES. SERIES V RUNS.

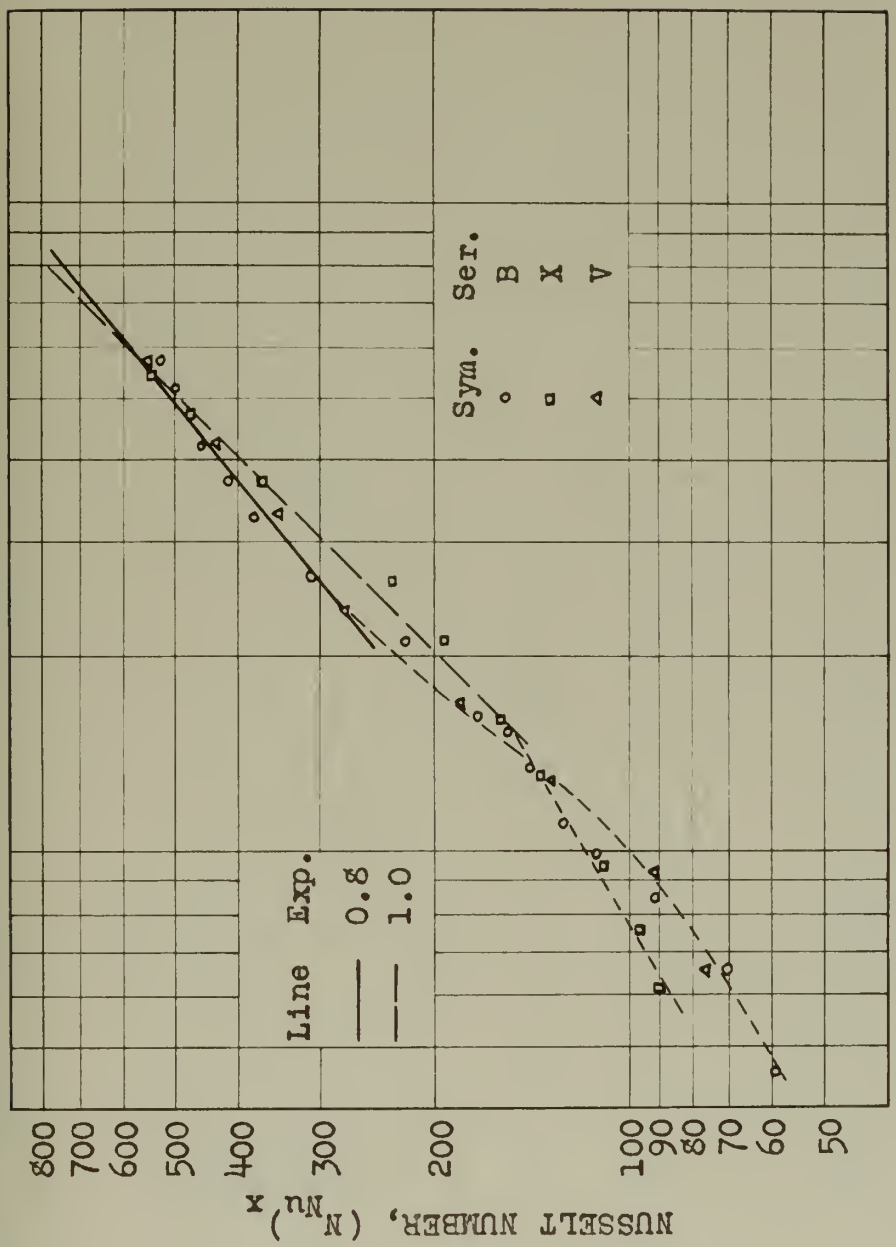


FIGURE 23. COMPARISON OF VIBRATION AND OBLIQUE CROSS FLOW DATA FOR THERMAL LENGTH OF FOUR INCHES.

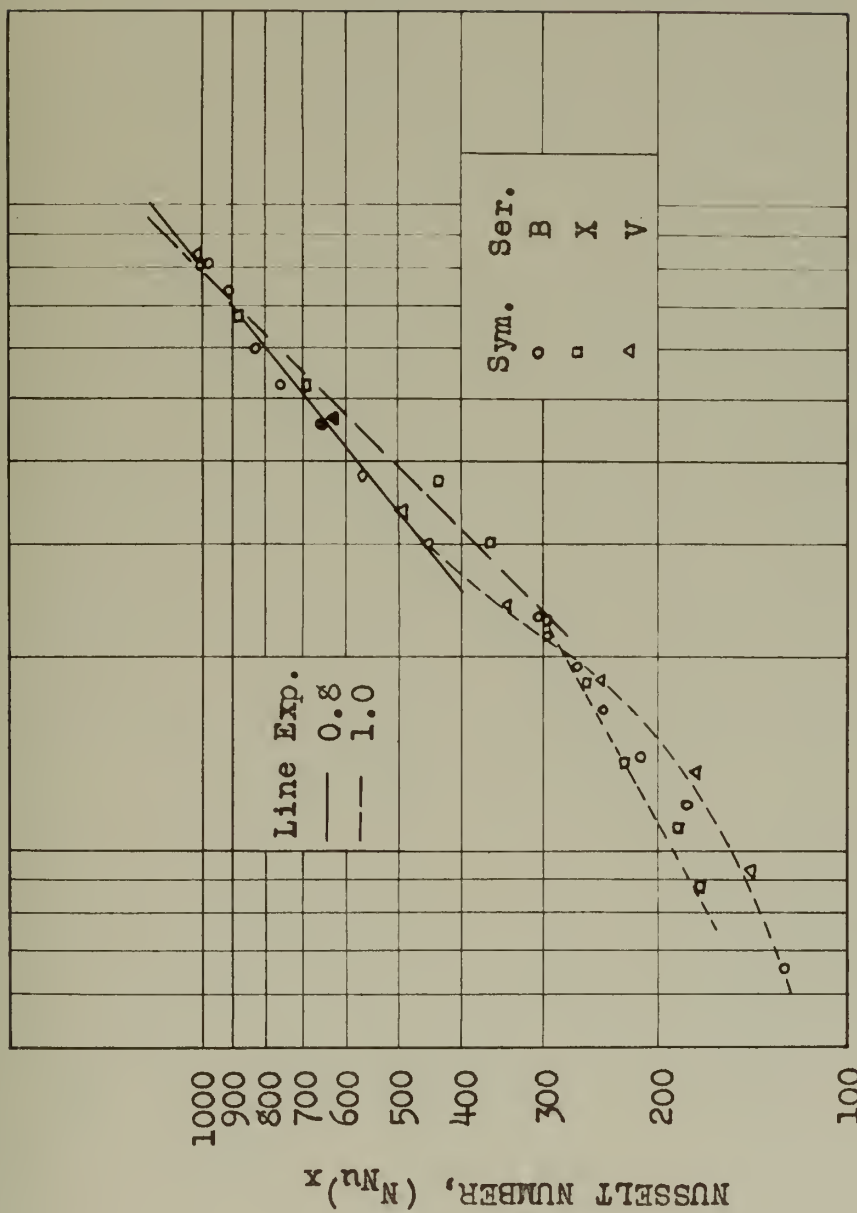


FIGURE 24. COMPARISON OF VIBRATION AND OBLIQUE CROSS FLOW DATA FOR THERMAL LENGTH OF EIGHT INCHES.

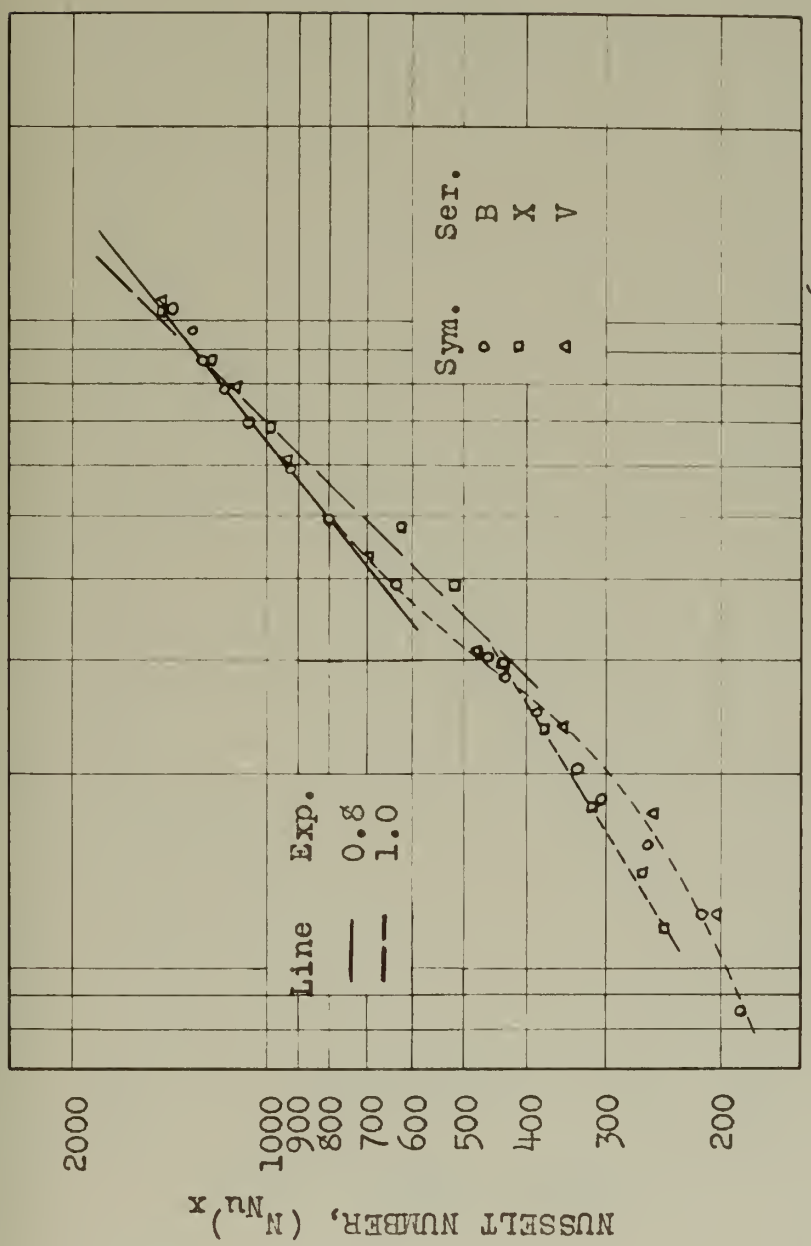


FIGURE 25. COMPARISON OF VIBRATION AND OBLIQUE CROSS FLOW DATA FOR THERMAL LENGTH OF TWELVE INCHES.

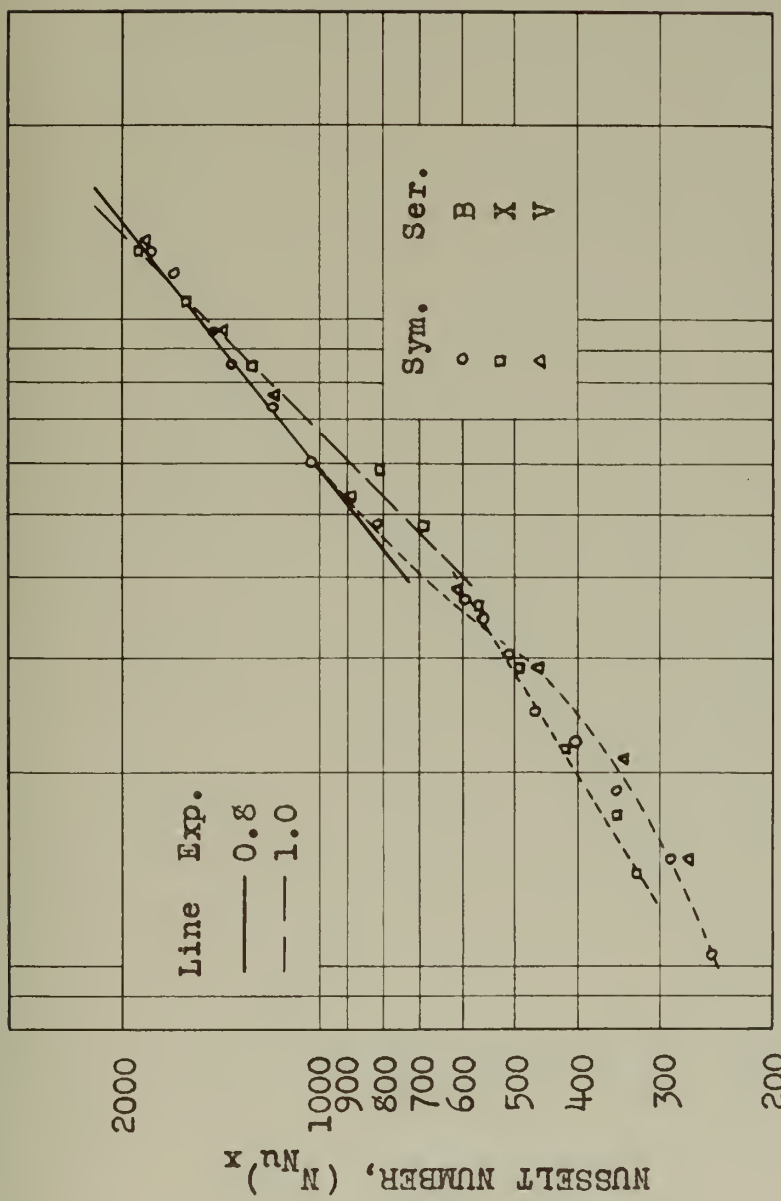


FIGURE 26. COMPARISON OF VIBRATION AND OBLIQUE CROSS FLOW DATA FOR THERMAL LENGTH OF SIXTEEN INCHES.

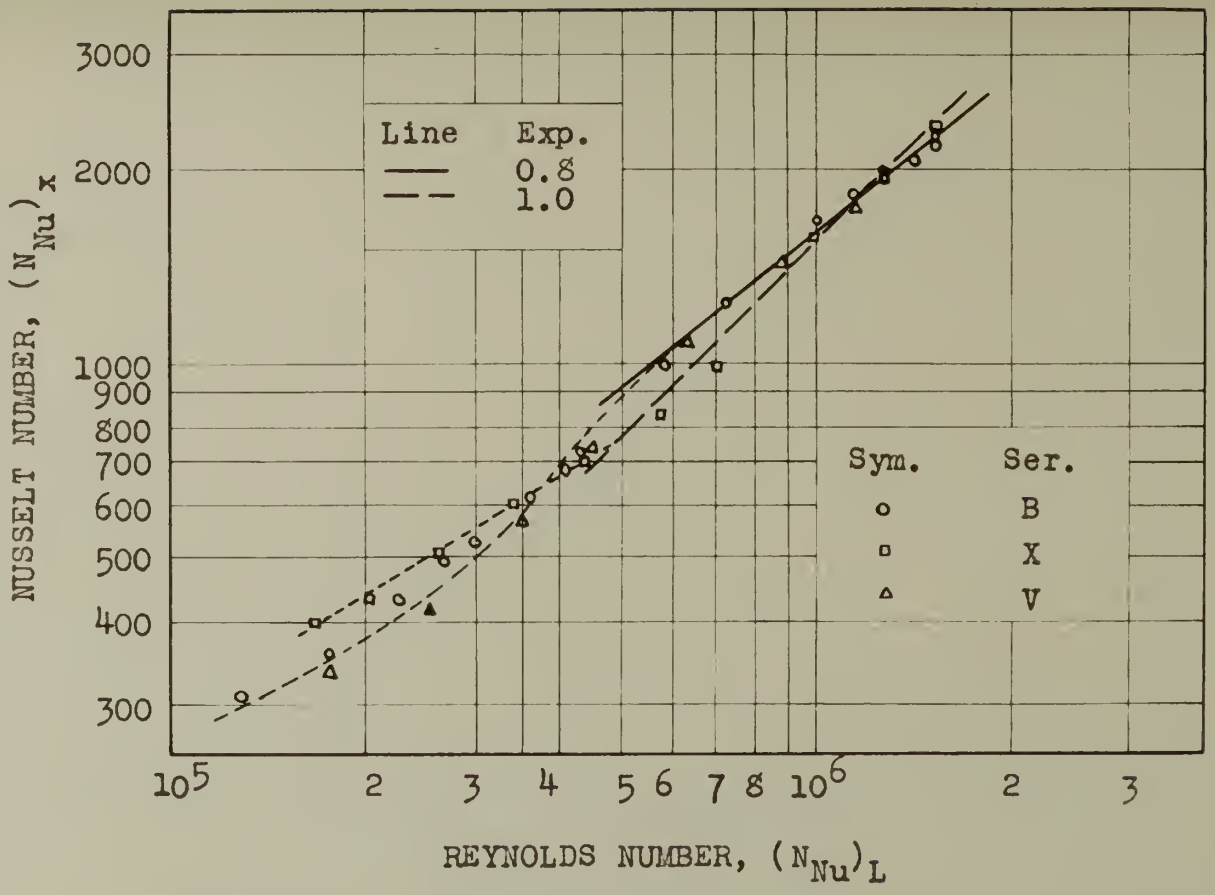


FIGURE 27. COMPARISON OF VIBRATION AND OBLIQUE CROSS FLOW DATA FOR THERMAL LENGTH OF TWENTY INCHES.

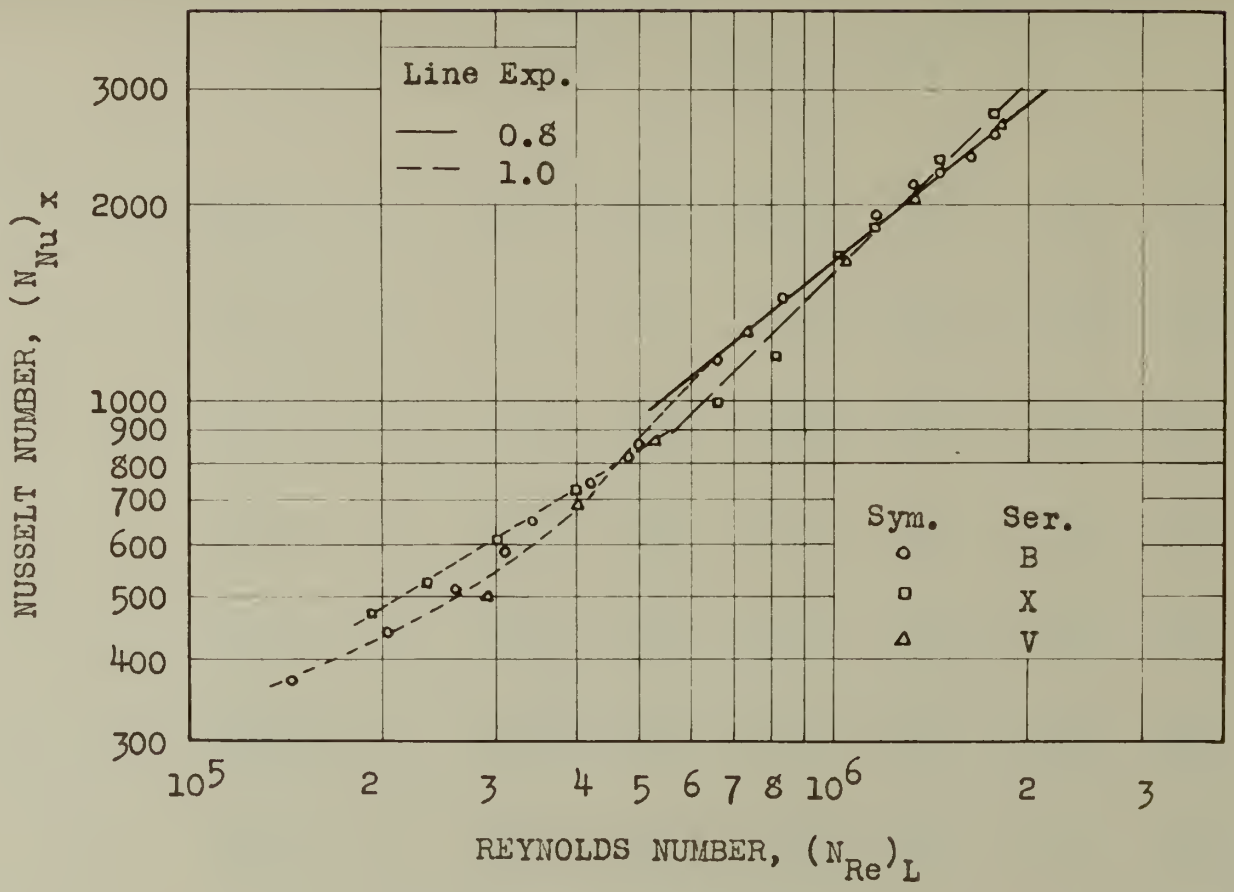


FIGURE 28. COMPARISON OF VIBRATION AND OBLIQUE CROSS FLOW DATA FOR THERMAL LENGTH OF TWENTY-FOUR INCHES.

TABLE XVI

EXPERIMENTAL RESULTS, SERIES A RUNS

Run No.	x, in.	4	8	12	16	20	24	28
1	$(N_{Re})_L \times 10^{-5}$	0.261	0.494	0.726	0.959	1.192	1.425	1.659
	$(N_{Nu})_x$	73	137	200	260	326	392	466
2	$(N_{Re})_L \times 10^{-5}$	0.330	0.625	0.919	1.211	1.510	1.800	2.10
	$(N_{Nu})_x$	82	155	227	299	373	451	528
3	$(N_{Re})_L \times 10^{-5}$	0.392	0.740	1.088	1.438	1.790	2.14	2.48
	$(N_{Nu})_x$	89	162	240	318	391	458	578
4	$(N_{Re})_L \times 10^{-5}$	0.456	0.861	1.268	1.672	2.08	2.49	2.90
	$(N_{Nu})_x$	101	184	270	358	452	545	640
5	$(N_{Re})_L \times 10^{-5}$	0.521	0.985	1.448	1.911	2.38	2.84	3.31
	$(N_{Nu})_x$	110	202	298	396	496	601	710
6	$(N_{Re})_L \times 10^{-5}$	0.606	1.164	1.711	2.26	2.81	3.36	3.91
	$(N_{Nu})_x$	128	235	344	454	562	678	794
7	$(N_{Re})_L \times 10^{-5}$	0.714	1.350	1.986	2.62	3.26	3.90	4.53
	$(N_{Nu})_x$	138	262	384	504	631	733	884
8	$(N_{Re})_L \times 10^{-5}$	0.806	1.527	2.24	2.96	3.68	4.41	5.12
	$(N_{Nu})_x$	152	278	415	550	688	830	976
9	$(N_{Re})_L \times 10^{-5}$	0.970	1.835	2.70	3.56	4.43	5.29	6.16
	$(N_{Nu})_x$	188	353	537	705	878	1053	1222

Run No.	x, in.	4	8	12	16	20	24	28
10	$(N_{Re})_L$ x 10^{-5}	1.094	2.07	3.05	4.02	5.00	5.98	6.96
	$(N_{Nu})_x$	199	386	573	758	945	1131	1312
11	$(N_{Re})_L$ x 10^{-5}	1.272	2.42	3.55	4.69	5.81	6.94	8.12
	$(N_{Nu})_x$	252	488	716	938	1156	1380	1602
12	$(N_{Re})_L$ x 10^{-5}	1.452	2.74	4.04	5.33	6.63	7.83	9.22
	$(N_{Nu})_x$	308	579	837	1090	1330	1572	1802
13	$(N_{Re})_L$ x 10^{-5}	1.724	3.25	4.78	6.32	7.85	9.38	10.92
	$(N_{Nu})_x$	380	696	984	1261	1541	1818	2085
14	$(N_{Re})_L$ x 10^{-5}	1.977	3.71	5.48	7.24	9.00	10.75	12.50
	$(N_{Nu})_x$	438	795	1120	1432	1735	2040	2350
15	$(N_{Re})_L$ x 10^{-5}	2.34	4.44	6.52	8.62	10.72	12.82	15.92
	$(N_{Nu})_x$	516	918	1281	1628	1980	2340	2680
16	$(N_{Re})_L$ x 10^{-5}	2.71	5.13	7.55	9.95	12.38	14.80	17.20
	$(N_{Nu})_x$	589	1038	1448	1838	2230	2630	3030

TABLE XVII

EXPERIMENTAL RESULTS, SERIES B RUNS

Run No.	x, in.	4	8	12	16	20	24	28
1	$\left(N_{Re}\right)_L x\ 10^{-5}$	0.461	0.656	0.850	1.047	1.270	1.435	-
	$\left(N_{Nu}\right)_x$	60	127	187	246	306	370	-
2	$\left(N_{Re}\right)_L x\ 10^{-5}$	0.651	0.926	1.202	1.480	1.756	2.03	2.31
	$\left(N_{Nu}\right)_x$	71	144	214	286	362	439	509
3	$\left(N_{Re}\right)_L x\ 10^{-5}$	0.835	1.190	1.542	1.895	2.25	2.61	2.96
	$\left(N_{Nu}\right)_x$	91	179	262	343	430	516	607
4	$\left(N_{Re}\right)_L x\ 10^{-5}$	0.981	1.396	1.810	2.24	2.65	3.07	3.48
	$\left(N_{Nu}\right)_x$	113	212	305	399	494	591	685
5	$\left(N_{Re}\right)_L x\ 10^{-5}$	1.098	1.562	2.02	2.50	2.96	3.42	3.90
	$\left(N_{Nu}\right)_x$	128	242	335	459	527	648	795
6	$\left(N_{Re}\right)_L x\ 10^{-5}$	1.340	1.912	2.47	3.06	3.62	4.19	4.76
	$\left(N_{Nu}\right)_x$	142	266	385	504	622	744	865
7	$\left(N_{Re}\right)_L x\ 10^{-5}$	1.519	2.16	2.80	3.44	4.09	4.75	5.38
	$\left(N_{Nu}\right)_x$	155	296	429	558	688	821	955
8	$\left(N_{Re}\right)_L x\ 10^{-5}$	1.610	2.29	2.98	3.66	4.34	5.03	5.72
	$\left(N_{Nu}\right)_x$	171	312	463	588	724	860	982
9	$\left(N_{Re}\right)_L x\ 10^{-5}$	2.12	3.01	3.92	4.82	5.73	6.62	7.53
	$\left(N_{Nu}\right)_x$	220	449	636	815	988	1170	1341

Run No.	x, in.	4	8	12	16	20	24	28
10	$\left(N_{Re}\right)_x^L \times 10^{-5}$	2.65	3.78	4.90	6.03	7.20	8.28	9.40
	$\left(N_{Nu}\right)_x^L$	310	564	804	1018	1230	1445	1655
11	$\left(N_{Re}\right)_x^L \times 10^{-5}$	3.24	4.61	5.98	7.36	8.75	10.10	11.50
	$\left(N_{Nu}\right)_x^L$	380	641	916	1166	1422	1677	1930
12	$\left(N_{Re}\right)_x^L \times 10^{-5}$	3.72	5.31	6.89	8.46	10.06	11.62	13.20
	$\left(N_{Nu}\right)_x^L$	417	759	1068	1361	1656	1952	2240
13	$\left(N_{Re}\right)_x^L \times 10^{-5}$	4.21	6.01	7.80	9.59	11.39	13.16	14.95
	$\left(N_{Nu}\right)_x^L$	452	825	1176	1448	1846	2170	2500
14	$\left(N_{Re}\right)_x^L \times 10^{-5}$	4.69	6.68	8.68	10.68	12.68	14.67	16.65
	$\left(N_{Nu}\right)_x^L$	473	867	1233	1590	1926	2270	2630
15	$\left(N_{Re}\right)_x^L \times 10^{-5}$	5.21	7.43	9.65	11.88	14.10	16.30	18.53
	$\left(N_{Nu}\right)_x^L$	495	912	1296	1665	2028	2390	2760
16	$\left(N_{Re}\right)_x^L \times 10^{-5}$	5.68	8.10	10.50	12.92	15.33	17.73	20.2
	$\left(N_{Nu}\right)_x^L$	525	967	1382	1796	2178	2580	2960

TABLE XVIII

EXPERIMENTAL RESULTS, SERIES C RUNS

Run No.	x, in.	4	8	12	16	20
1	$(N_{Re})_L$ x 10^{-5}	1.185	1.475	1.770	2.16	2.35
	$(N_{Nu})_x$	89	169	245	322	402
2	$(N_{Re})_L$ x 10^{-5}	1.400	1.746	2.09	2.43	2.78
	$(N_{Nu})_x$	108	202	289	381	468
3	$(N_{Re})_L$ x 10^{-5}	1.613	2.01	2.40	2.80	3.20
	$(N_{Nu})_x$	111	216	317	418	516
4	$(N_{Re})_L$ x 10^{-5}	1.900	2.36	2.83	3.30	3.76
	$(N_{Nu})_x$	129	256	355	469	578
5	$(N_{Re})_L$ x 10^{-5}	2.24	2.78	3.32	3.87	4.42
	$(N_{Nu})_x$	152	283	407	530	652
6	$(N_{Re})_L$ x 10^{-5}	2.54	3.16	3.79	4.42	5.05
	$(N_{Nu})_x$	176	325	463	598	740
7	$(N_{Re})_L$ x 10^{-5}	2.93	3.65	4.37	5.09	5.81
	$(N_{Nu})_x$	196	365	521	674	822
8	$(N_{Re})_L$ x 10^{-5}	3.50	4.36	5.22	6.08	6.95
	$(N_{Nu})_x$	233	434	617	799	970
9	$(N_{Re})_L$ x 10^{-5}	4.03	5.02	6.01	7.00	8.00
	$(N_{Nu})_x$	262	482	686	882	1076
10	$(N_{Re})_L$ x 10^{-5}	4.72	5.88	7.05	8.21	9.37
	$(N_{Nu})_x$	297	535	780	1000	1230
11	$(N_{Re})_L$ x 10^{-5}	5.42	6.75	8.09	9.42	10.75
	$(N_{Nu})_x$	324	603	860	1112	1354
12	$(N_{Re})_L$ x 10^{-5}	6.37	7.93	9.50	11.07	12.64
	$(N_{Nu})_x$	368	691	985	1274	1556
13	$(N_{Re})_L$ x 10^{-5}	7.23	9.01	10.78	12.56	14.35
	$(N_{Nu})_x$	406	755	1078	1398	1712
14	$(N_{Re})_L$ x 10^{-5}	8.65	10.78	12.90	15.04	17.16
	$(N_{Nu})_x$	473	880	1258	1626	1996
15	$(N_{Re})_L$ x 10^{-5}	9.97	12.43	14.88	17.34	19.80
	$(N_{Nu})_x$	516	975	1412	1820	2224

TABLE XIX

EXPERIMENTAL RESULTS, SERIES D RUNS

Run No.	x, in.	4	8	12	16
1	$(N_{Re})_L \times 10^{-5}$	1.668	1.966	2.26	2.58
	$(N_{Nu})_x$	98	182	273	347
2	$(N_{Re})_L \times 10^{-5}$	1.992	2.36	2.72	3.07
	$(N_{Nu})_x$	109	206	298	392
3	$(N_{Re})_L \times 10^{-5}$	2.32	2.73	3.14	3.54
	$(N_{Nu})_x$	122	230	335	442
4	$(N_{Re})_L \times 10^{-5}$	2.65	3.14	3.61	4.07
	$(N_{Nu})_x$	135	255	372	488
5	$(N_{Re})_L \times 10^{-5}$	3.16	3.74	4.31	4.87
	$(N_{Nu})_x$	148	280	412	544
6	$(N_{Re})_L \times 10^{-5}$	3.59	4.23	4.88	5.52
	$(N_{Nu})_x$	166	310	455	595
7	$(N_{Re})_L \times 10^{-5}$	4.19	4.84	5.57	6.31
	$(N_{Nu})_x$	187	351	505	661
8	$(N_{Re})_L \times 10^{-5}$	4.79	5.66	6.51	7.37
	$(N_{Nu})_x$	216	411	594	777
9	$(N_{Re})_L \times 10^{-5}$	6.36	7.51	8.65	9.79
	$(N_{Nu})_x$	279	521	755	969
10	$(N_{Re})_L \times 10^{-5}$	7.43	8.77	10.10	11.43
	$(N_{Nu})_x$	319	595	850	1108
11	$(N_{Re})_L \times 10^{-5}$	8.74	10.32	11.88	13.45
	$(N_{Nu})_x$	371	692	996	1282
12	$(N_{Re})_L \times 10^{-5}$	9.80	11.58	13.33	15.09
	$(N_{Nu})_x$	405	757	1092	1412
13	$(N_{Re})_L \times 10^{-5}$	11.58	13.68	15.75	17.83
	$(N_{Nu})_x$	459	854	1238	1606
14	$(N_{Re})_L \times 10^{-5}$	13.60	16.04	18.48	20.92
	$(N_{Nu})_x$	510	958	1389	1808

TABLE XX

EXPERIMENTAL RESULTS, SERIES E RUNS

Run No.	x, in.	4	8	12	16
1	$\left(N_{Re}\right)_L x\ 10^{-5}$	2.39	2.72	3.06	3.41
	$\left(N_{Nu}\right)_x$	95	199	296	391
2	$\left(N_{Re}\right)_L x\ 10^{-5}$	2.88	3.29	3.69	4.10
	$\left(N_{Nu}\right)_x$	117	228	337	446
3	$\left(N_{Re}\right)_L x\ 10^{-5}$	3.22	3.68	4.14	4.61
	$\left(N_{Nu}\right)_x$	128	247	364	482
4	$\left(N_{Re}\right)_L x\ 10^{-5}$	3.78	4.31	4.85	5.40
	$\left(N_{Nu}\right)_x$	152	285	415	550
5	$\left(N_{Re}\right)_L x\ 10^{-5}$	4.38	5.00	5.61	6.25
	$\left(N_{Nu}\right)_x$	162	305	451	598
6	$\left(N_{Re}\right)_L x\ 10^{-5}$	5.07	5.79	6.51	7.24
	$\left(N_{Nu}\right)_x$	185	350	511	678
7	$\left(N_{Re}\right)_L x\ 10^{-5}$	6.11	6.98	7.85	8.73
	$\left(N_{Nu}\right)_x$	218	407	602	797
8	$\left(N_{Re}\right)_L x\ 10^{-5}$	8.06	9.20	10.32	11.50
	$\left(N_{Nu}\right)_x$	272	510	735	958
9	$\left(N_{Re}\right)_L x\ 10^{-5}$	9.46	10.80	12.15	13.52
	$\left(N_{Nu}\right)_x$	306	577	832	1085
10	$\left(N_{Re}\right)_L x\ 10^{-5}$	11.18	12.78	14.36	15.97
	$\left(N_{Nu}\right)_x$	352	663	960	1250
11	$\left(N_{Re}\right)_L x\ 10^{-5}$	12.61	14.40	16.20	18.05
	$\left(N_{Nu}\right)_x$	395	733	1054	1380
12	$\left(N_{Re}\right)_L x\ 10^{-5}$	15.62	17.85	20.1	22.3
	$\left(N_{Nu}\right)_x$	469	880	1281	1668
13	$\left(N_{Re}\right)_L x\ 10^{-5}$	17.11	19.55	22.0	24.5
	$\left(N_{Nu}\right)_x$	489	940	1371	1792

TABLE XXI

EXPERIMENTAL RESULTS, SERIES X RUNS

Run No.	x, in.	4	8	12	16	20	24	28
1	$\left(\frac{N_{Re}}{N_{Nu}}\right)_{L}^{x}$ 10^{-5}	0.610	0.869	1.140	1.402	1.663	1.918	2.18
		90	171	245	320	395	471	544
2	$\left(\frac{N_{Re}}{N_{Nu}}\right)_{L}^{x}$ 10^{-5}	0.747	1.071	1.400	1.713	2.03	2.34	2.66
		97	184	267	344	435	523	602
3	$\left(\frac{N_{Re}}{N_{Nu}}\right)_{L}^{x}$ 10^{-5}	0.953	1.372	1.761	2.18	2.58	2.99	3.39
		110	224	311	410	507	609	685
4	$\left(\frac{N_{Re}}{N_{Nu}}\right)_{L}^{x}$ 10^{-5}	1.303	1.810	2.33	2.88	3.42	3.95	4.49
		138	257	372	489	604	729	933
5	$\left(\frac{N_{Re}}{N_{Nu}}\right)_{L}^{x}$ 10^{-5}	1.592	2.27	2.94	3.62	4.30	4.97	5.66
		159	296	430	564	695	832	965
6	$\left(\frac{N_{Re}}{N_{Nu}}\right)_{L}^{x}$ 10^{-5}	2.10	2.98	3.88	4.77	5.66	6.55	7.45
		192	358	516	687	833	1000	1163
7	$\left(\frac{N_{Re}}{N_{Nu}}\right)_{L}^{x}$ 10^{-5}	2.58	3.68	4.77	5.86	6.96	8.06	9.15
		231	427	615	801	988	1180	1375
8	$\left(\frac{N_{Re}}{N_{Nu}}\right)_{L}^{x}$ 10^{-5}	3.68	5.25	6.81	8.37	9.93	11.50	13.08
		367	691	981	1275	1561	1850	2130
9	$\left(\frac{N_{Re}}{N_{Nu}}\right)_{L}^{x}$ 10^{-5}	4.70	6.70	8.70	10.70	12.70	14.70	16.70
		474	865	1230	1602	1962	2330	2700

Run No.	x, in.	4	8	12	16	20	24	28
10	$\left(N_{Nu}\right)_x \times 10^{-5}$	5.66	8.06	10.48	12.89	15.30	17.70	20.10
	$\left(N_{Re}\right)_L$	541	1000	1431	1892	2320	2760	3220

TABLE XXII

EXPERIMENTAL RESULTS, SERIES V RUNS

Run No.	x, in.	4	8	12	16	20	24	28
1	$\left(N_{Re}\right)_x^L \times 10^{-5}$	0.648	0.925	1.200	1.477	1.752	2.03	2.30
	$\left(N_{Nu}\right)_x^L$	77	142	203	267	334	403	463
2	$\left(N_{Re}\right)_x^L \times 10^{-5}$	0.931	1.326	1.721	2.12	2.52	2.91	3.31
	$\left(N_{Nu}\right)_x^L$	92	173	252	333	416	501	586
3	$\left(N_{Re}\right)_x^L \times 10^{-5}$	1.280	1.828	2.37	2.92	3.46	4.01	4.55
	$\left(N_{Nu}\right)_x^L$	132	246	354	462	572	687	798
4	$\left(N_{Re}\right)_x^L \times 10^{-5}$	1.681	2.38	3.09	3.82	4.54	5.25	5.96
	$\left(N_{Nu}\right)_x^L$	182	336	473	606	740	969	1100
5	$\left(N_{Re}\right)_x^L \times 10^{-5}$	2.34	3.34	4.34	5.34	6.34	7.34	8.33
	$\left(N_{Nu}\right)_x^L$	272	496	695	892	1089	1288	1457
6	$\left(N_{Re}\right)_x^L \times 10^{-5}$	3.28	4.68	6.08	7.48	8.87	10.25	11.66
	$\left(N_{Nu}\right)_x^L$	346	633	916	1182	1432	1685	1985
7	$\left(N_{Re}\right)_x^L \times 10^{-5}$	4.24	6.05	7.85	9.65	11.45	13.23	15.05
	$\left(N_{Nu}\right)_x^L$	422	775	1107	1420	1725	2050	2360
8	$\left(N_{Re}\right)_x^L \times 10^{-5}$	5.76	8.22	10.67	13.12	15.53	18.00	20.45
	$\left(N_{Nu}\right)_x^L$	545	1005	1428	1840	2280	2670	3000

CHAPTER X

CORRELATION FOR THE MEAN SURFACE COEFFICIENT

The computation shown in Table XIV suggests a method to determine the effect of surface configuration. The subsequent calculations are limited to the data for turbulent boundary layers. The data available for laminar boundary layers are not sufficient for detailed conclusions and the effect of vibrations in the laminar region was not explored.

Data for correlations are, therefore, only chosen from Tables XVI to XX, inclusive, so that Reynolds number is equal to or greater than 5×10^5. The procedure for computation was the same as that outlined in Table XIV.

A summary of the results of computation is given in Table XXIII. These results suggest a relationship between C_s of Equation IX-1, and the dimensionless ratio of thermal length to total length, (x/L). The existence of such a relationship is shown in Figure 29.

It is noted that the results shown in Figure 29 offer a strong correlation. The range of thermal lengths considered is in the proportion 7:1, the range of starting lengths is in the proportion 55:1, and the range of the ratio (x/L) is in the proportion 7:1.

An equation for the line shown in Figure 29 was obtained from the data of Table XXIII by the method of least squares. The result of the computation yields:

$$C_o' = 0.0307 \, (x/L)^{0.91}. \qquad \text{X-1}$$

By definition, Equation IX-1 :

$$C_o' = (N_{Nu})_x / (N_{Re})_L^{0.8}$$

therefore:

$$(N_{Nu})_x = 0.0307\ (x/L)^{0.91} (N_{Re})_L^{0.8} \qquad X\text{-}2$$

This result may be put into the form of Equation II-8 as:

$$(N_{Nu})_L = (N_{Nu})_x\ (L/x)$$
$$= 0.0307\ (x/L)^{-0.09} (N_{Re})_L^{0.8}, \text{ for air.} \qquad X\text{-}3$$

If it is assumed that the Prandtl number for the air conditions as encountered in these experiments has the value 0.709 and an exponent of 1/3 for the Prandtl number, then

$$(N_{Nu})_x = 0.0344\ (x/L)^{0.09}\ (N_{Re})_L^{0.8} (N_{Pr})^{1/3} \qquad X\text{-}4$$

is a general equation.

By analogy with Equation II-8, it is seen that:

$$C_o'' = 0.0344$$
$$\phi^m = (x/L)^{-0.09} \qquad X\text{-}5$$

The results of correlation are illustrated in Figures 30 to 37, inclusive. For purposes of illustration, a dimensionless parameter is defined as:

$$Y = (N_{Nu})_x / (x/L)^{0.91}, \qquad X\text{-}6$$

and for the turbulent region:

$$Y = 0.0307\ (N_{Re})_L^{0.8} \qquad X\text{-}7$$

Figures 30 to 36, inclusive, may be compared with Figures 13 to 19, inclusive, as follows:

Before correlation		After correlation
Figure 13	compares with	Figure 30
" 14	" "	" 31
" 15	" "	" 32
" 16	" "	" 33
" 17	" "	" 34
" 18	" "	" 35
" 19	" "	" 36

Correlation of all data is illustrated in Figure 37. It may be noted that correlation is strong for Reynolds number greater than 5×10^5. The result of Jakob and Dow (2) for the laminar range is included for comparison purposes. Those points lying below the Jakob and Dow line are based on low velocities which cannot be measured exactly.

It is of interest to compare the results for the function ϕ^m with another observer. A direct comparison may be made with Equation III-1, that of Jakob and Dow (2). The present result in the form given in Equation X-5 is convenient and the comparison is made neglecting the small effect of the different definition of starting and total lengths as used in Equation III-1. The comparison is made in Table XXIV.

Equation X-5 was obtained with (x/L) having extreme values of 0.141 and 0.983. Equation III-1 was obtained with (x/L) having extreme values of 0.394 and 0.899. The data given in Table XXIV for (x/L) in the interval 0.4 to 0.9 show a maximum deviation in the comparison of 1.5 per cent. This is a most satisfactory agreement, considering that the influence of surface curvature (to be considered in Chapter XII) cannot change much in the longitudinal direction.

TABLE XXIV

COMPARISON OF SURFACE CONFIGURATION FUNCTION VALUES

(x/L)	(s/L)	Equ. X-5	Equ. III-1	Diff., per cent, based on Equ. X-5
0.0	1.0	∞	1.400	
0.1	0.9	1.230	1.299	5.4
0.2	0.8	1.157	1.216	5.1
0.3	0.7	1.114	1.150	3.2
0.4	0.6	1.086	1.098	1.1
0.5	0.5	1.064	1.059	0.5
0.6	0.4	1.048	1.032	1.1
0.7	0.3	1.032	1.015	1.3
0.8	0.2	1.020	1.005	1.5
0.9	0.1	1.010	1.001	0.9
1.0	0.0	1.000	1.000	0

TABLE XXIII

CALCULATED RESULTS FOR CORRELATION PURPOSES

Data selected for Reynolds number equal to or greater than 5×10^5

Run Series	s, in.	x, in.	(x/L)	Average value of C_s
A	0.49	8	0.942	0.0280
		12	0.961	0.0287
		16	0.970	0.0290
		20	0.976	0.0290
		24	0.980	0.0295
		28	0.983	0.0305
B	5.43	8	0.595	0.0192
		12	0.689	0.0218
		16	0.746	0.0238
		20	0.786	0.0253
		24	0.815	0.0263
		28	0.837	0.0269
C	12.24	4	0.246	0.00835
		8	0.395	0.0131
		12	0.495	0.0163
		16	0.566	0.0186
		20	0.620	0.0204
D	18.24	4	0.181	0.00650
		8	0.305	0.0105
		12	0.397	0.0135
		16	0.468	0.0158
E	24.18	4	0.141	0.00510
		8	0.249	0.00870
		12	0.332	0.0115
		16	0.396	0.0137

$$C_s = (N_{Nu})_x/(N_{Re})_L^{0.8}$$

$L = s + x$, inches

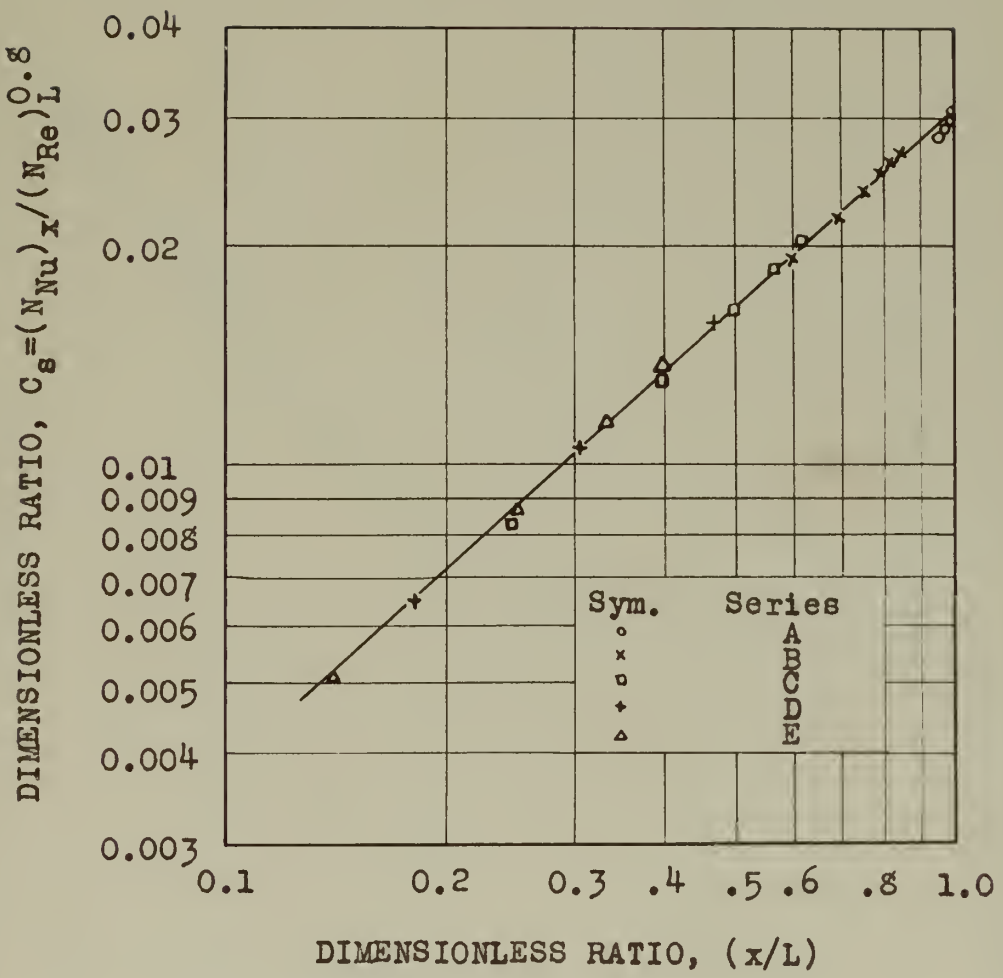


FIGURE 29. SURFACE CONFIGURATION DATA

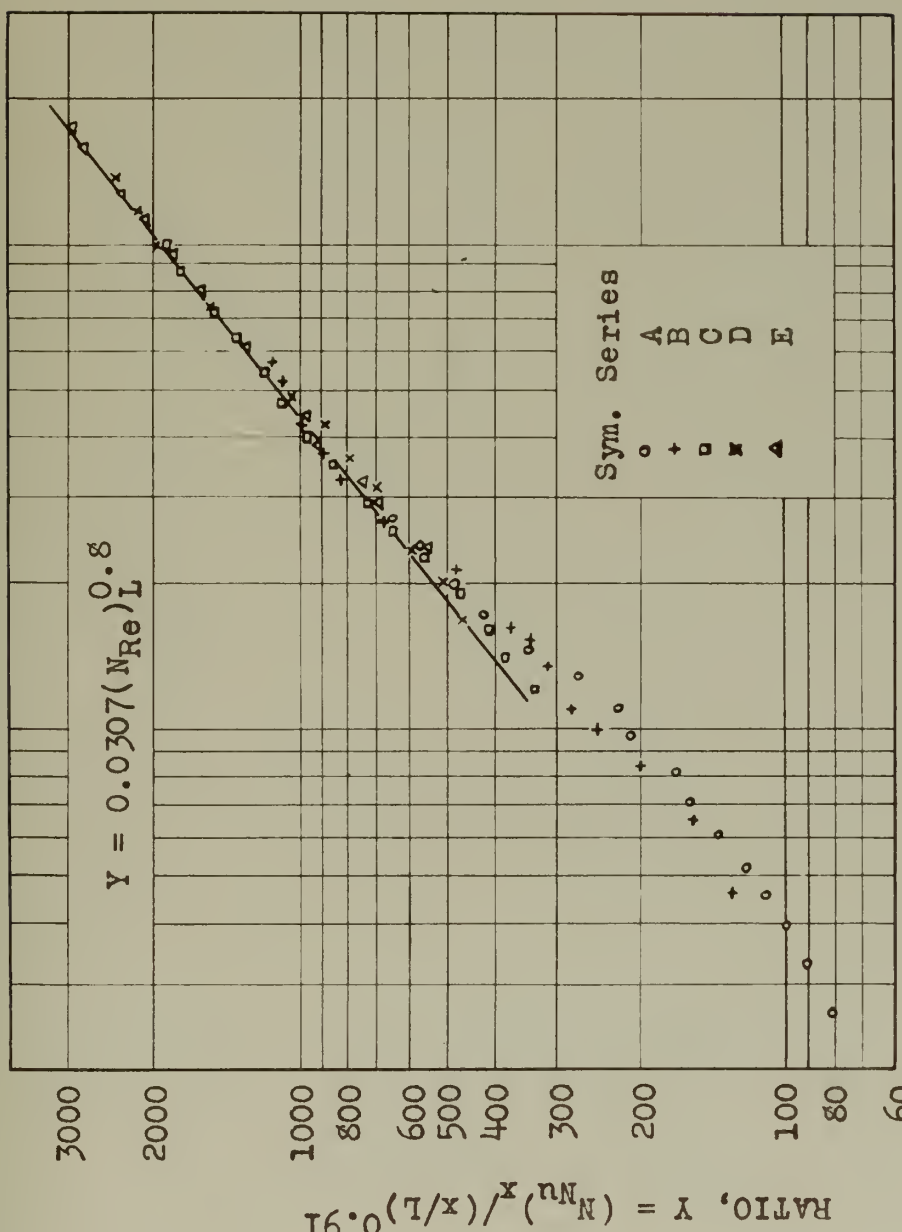


FIGURE 30. CORRELATION RESULTS FOR THERMAL LENGTH OF FOUR INCHES.

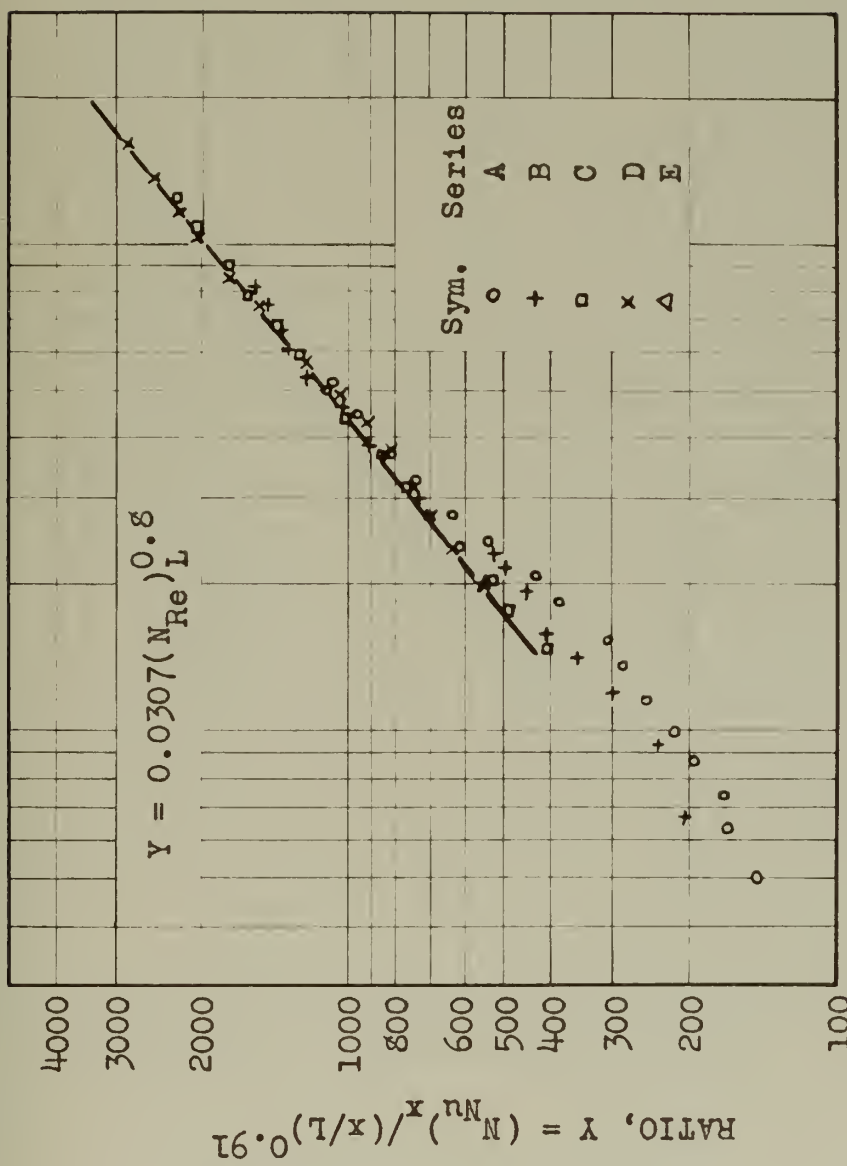


FIGURE 31. CORRELATION RESULTS FOR THERMAL LENGTH OF EIGHT INCHES.

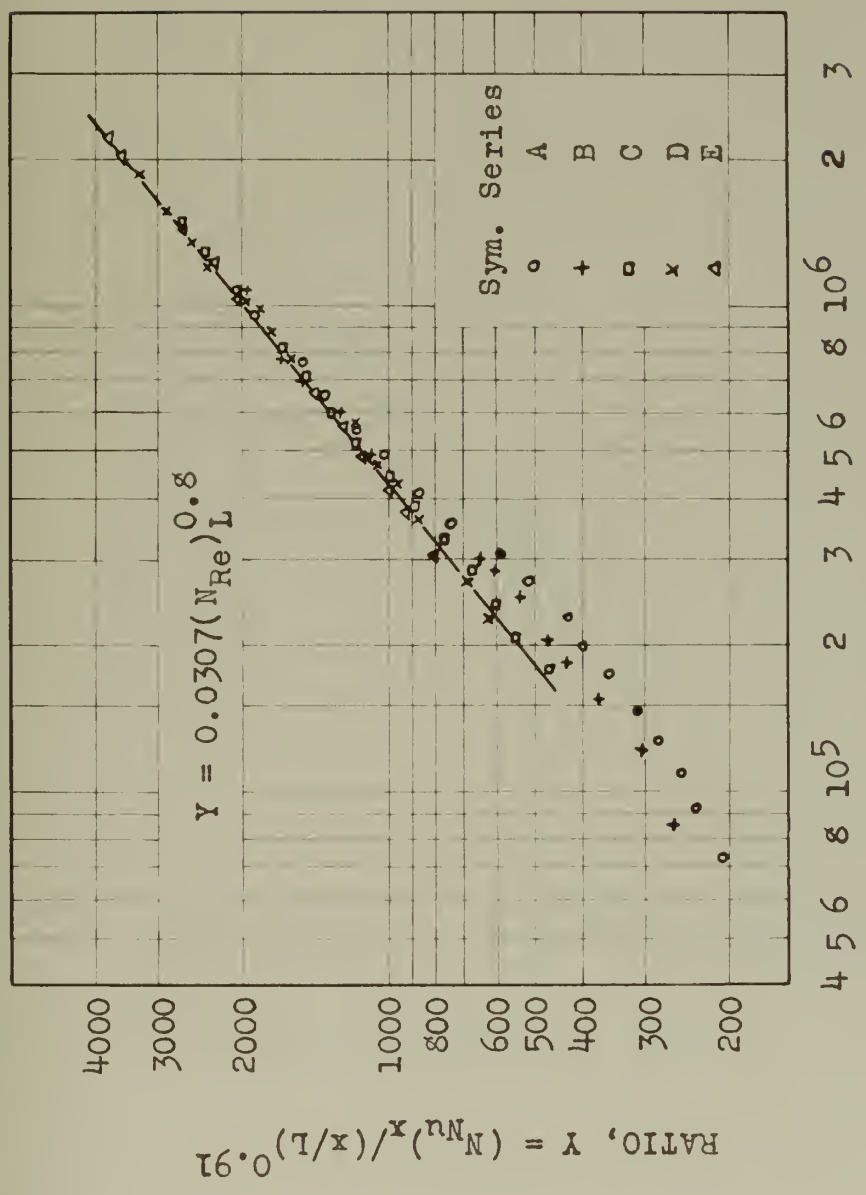


FIGURE 32. CORRELATION RESULTS FOR THERMAL LENGTH OF TWELVE INCHES.

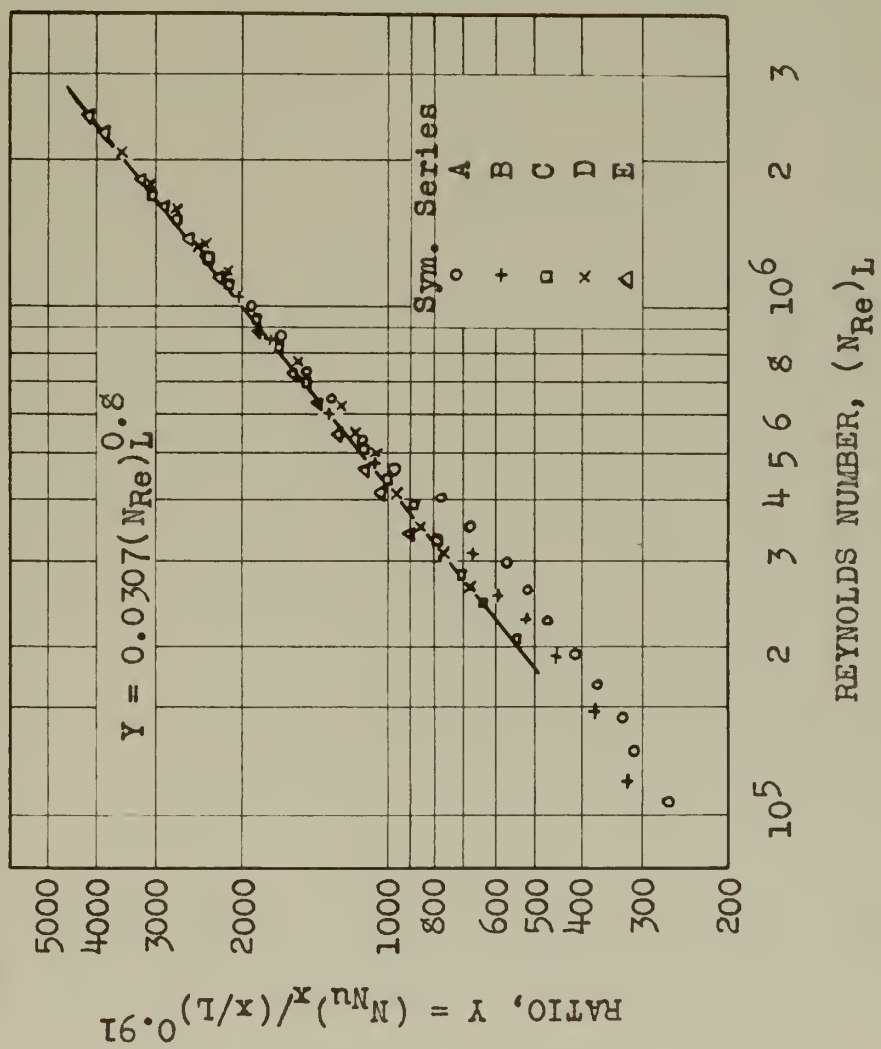


FIGURE 33. CORRELATION RESULTS FOR THERMAL LENGTH OF SIXTEEN INCHES.

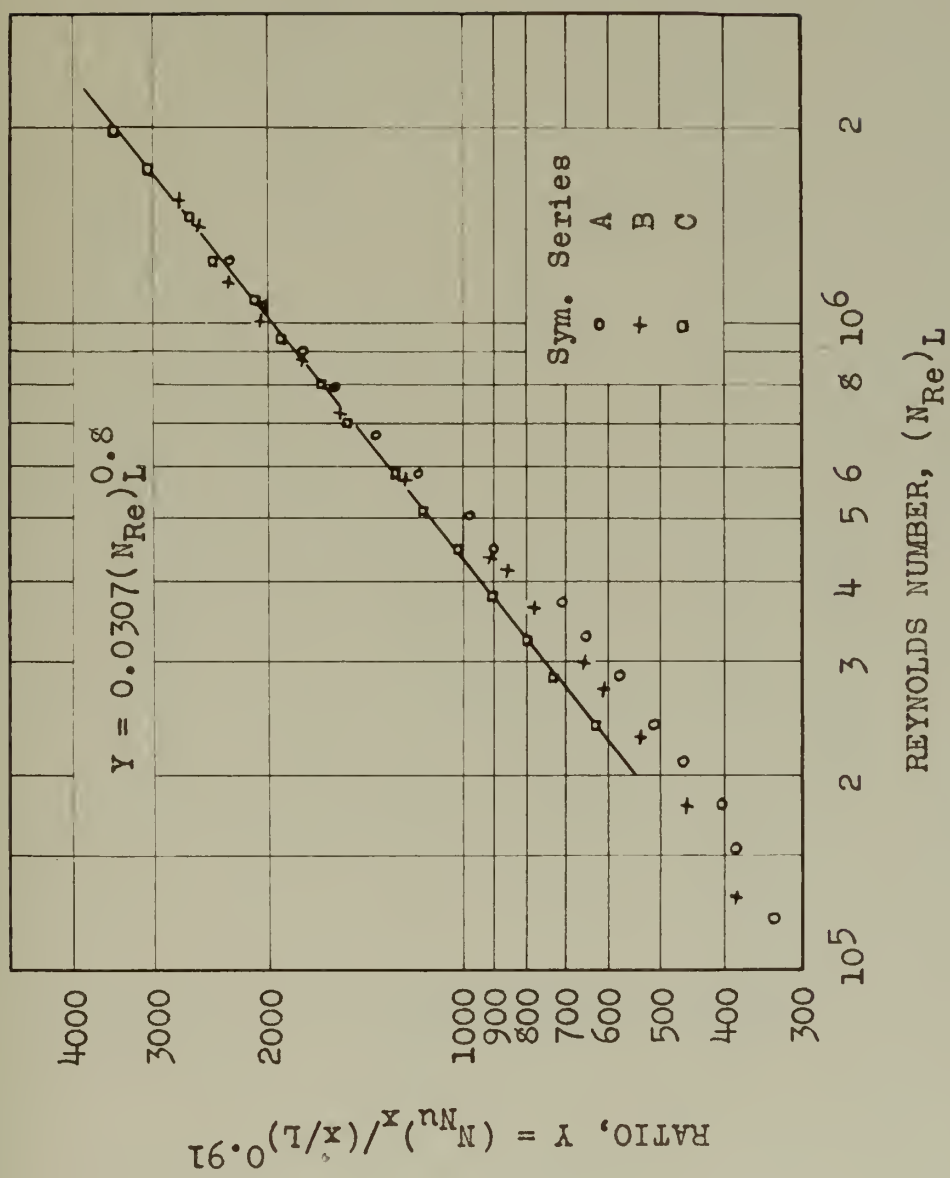


FIGURE 34. CORRELATION RESULTS FOR THERMAL LENGTH OF TWENTY INCHES.

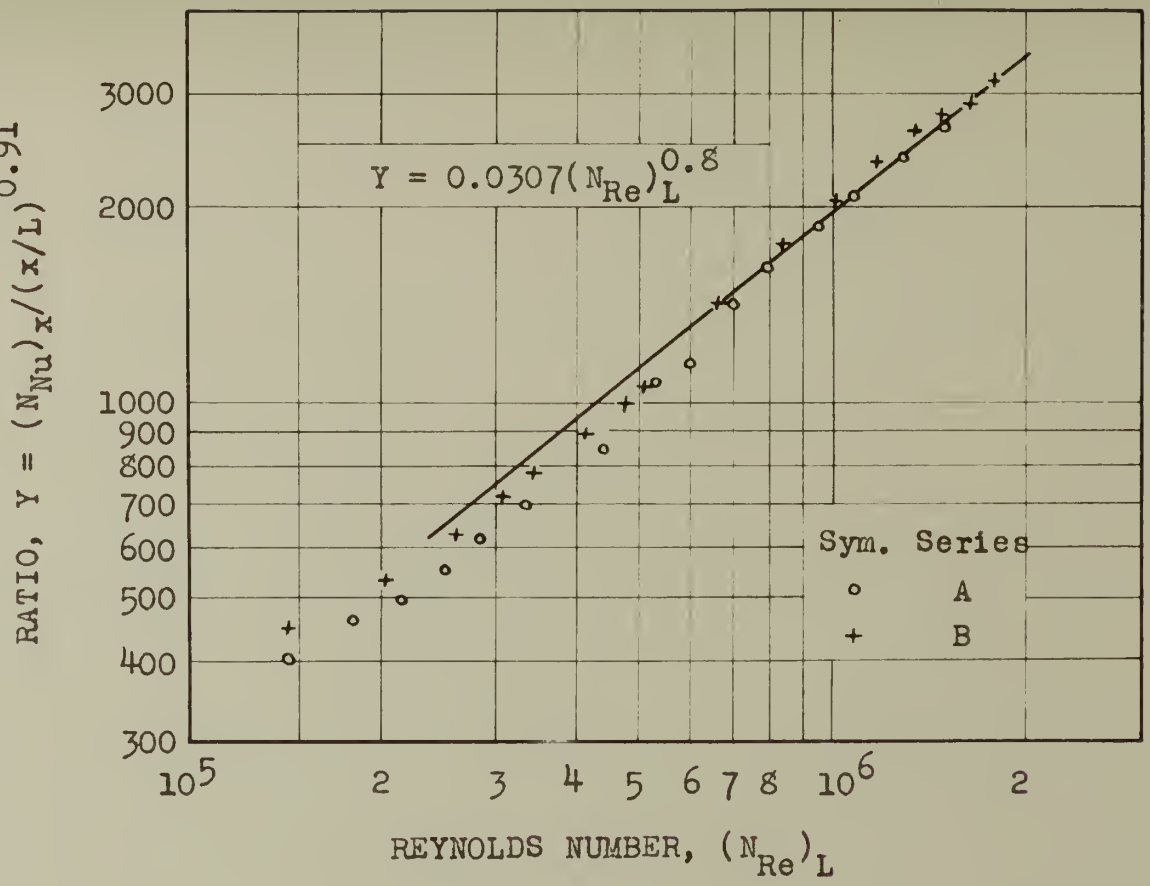


FIGURE 35. CORRELATION RESULTS FOR THERMAL LENGTH OF TWENTY-FOUR INCHES.

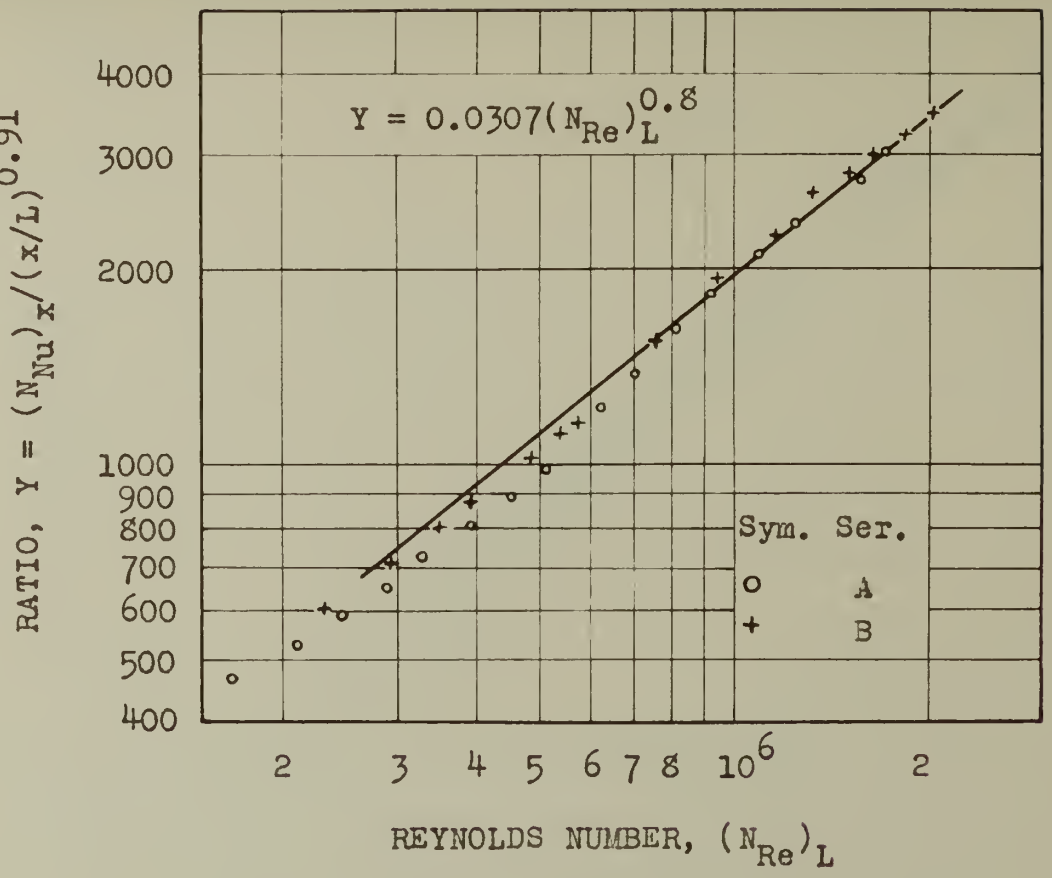


FIGURE 36. CORRELATION RESULTS FOR THERMAL LENGTH OF TWENTY-EIGHT INCHES.

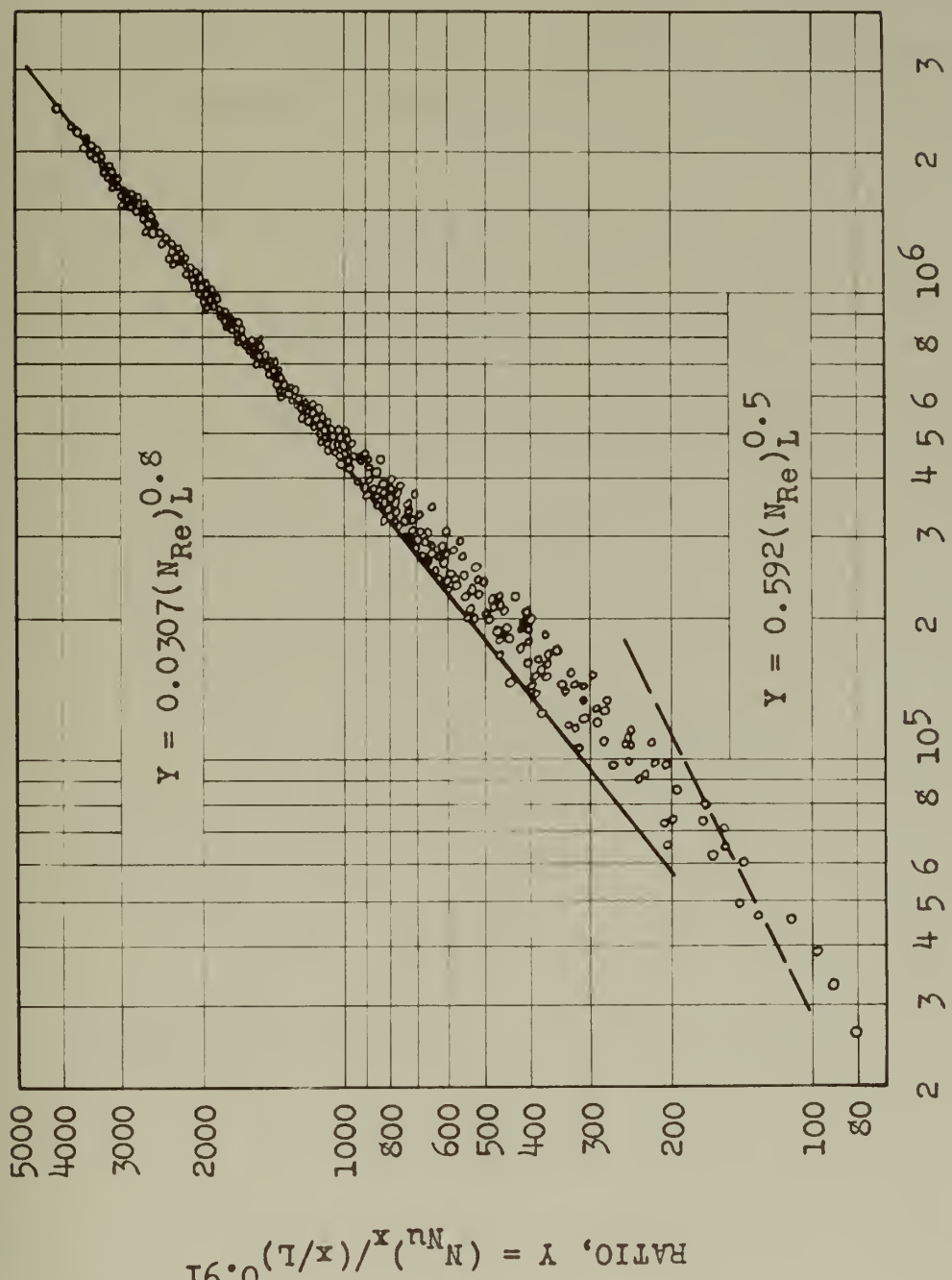


FIGURE 37. CORRELATION OF ALL RESULTS. THE JAKOB AND DOW RESULT FOR LAMINAR FLOW IS SHOWN FOR COMPARISON.

CHAPTER XI

THE LOCAL SURFACE COEFFICIENT

Previous discussions have been concerned with the mean surface coefficient of heat transfer. An expression for the local surface coefficient may be developed from the foregoing results.

Equation II-4 may be written as:

$$h_m \theta_m x = \int_0^x h\theta \, dx \qquad \text{XI-1}$$

Differentiation of Equation XI-1 yields:

$$\frac{d}{dx}(h_m \theta_m x) = \frac{d}{dx} \int_0^x h\theta \, dx$$

and,

$$h\theta = \frac{d}{dx}(h_m \theta_m x)$$

or,

$$h = h_m \frac{\theta_m}{\theta} + \frac{h_m x}{\theta} \frac{d\theta_m}{dx} + \frac{x\theta_m}{\theta} \frac{dh_m}{dx} \qquad \text{XI-2}$$

Equation II-5 may be written as:

$$\theta_m x = \int_0^x \theta \, dx \qquad \text{XI-3}$$

Differentiation of Equation XI-3 yields:

$$\theta = \theta_m + x \frac{d\theta_m}{dx}$$

or,

$$\frac{d\theta_m}{dx} = \frac{\theta - \theta_m}{x} \qquad \text{XI-4}$$

Equation X-2 may be written as:

$$(N_{Nu})_x = C_o' \left(\frac{x}{s + x}\right)^m \left(\frac{v_o(s + x)}{\nu_o}\right)^n$$

$$\text{or,} \qquad h_m = \frac{C_o' k}{x} \left(\frac{v_o}{\nu_o} \right)^n \left(\frac{x}{s + x} \right)^m (s + x)^n , \qquad \text{XI-5}$$

which is a function of x only. Terms may be combined as:

$$\frac{h_m}{C_o' \left(\frac{v_o}{\nu_o} \right)^n} = k (s + x)^{n-m} x^{m-1} \qquad \text{XI-6}$$

Differentiation of XI-6 yields:

$$\frac{dh_m}{dx} = C_o' \left(\frac{x}{s + x} \right)^m \left(\frac{v_o (s + x)}{\nu_o} \right)^n \left[\frac{1}{x} \frac{dk}{dx} + \frac{(m-1)k}{x^2} + \frac{(n-m)k}{x(s + x)} \right]$$

$$\text{or,} \quad \frac{dh_m}{dx} = \frac{C_o' k}{x} \left(\frac{x}{s + x} \right)^m \left(\frac{v_o (s + x)}{\nu_o} \right)^n \left[\frac{1}{k} \frac{dk}{dx} + \frac{(m-1)}{x} + \frac{(n-m)}{(s+x)} \right] \qquad \text{XI-7}$$

Substitution from Equation XI-5 into Equation XI-7 yields:

$$\frac{dh_m}{dx} = h_m \left[\frac{1}{k} \frac{dk}{dx} + \frac{(m-1)}{x} + \frac{(n-m)}{(s+x)} \right] \qquad \text{XI-8}$$

The term $\frac{dk}{dx}$ may be written as:

$$\frac{dk}{dx} = \frac{dk}{d\theta_m} \frac{d\theta_m}{dx}$$

and with the aid of Equation XI-4, there results:

$$\frac{dk}{dx} = \frac{\theta - \theta_m}{x} \frac{dk}{d\theta_m} \qquad \text{XI-9}$$

Substitution from Equations XI-4, XI-8 and XI-9 into Equation XI-2 yields:

$$h = h_m \left(1 + \frac{\theta_m}{\theta} \left[\frac{\theta - \theta_m}{k} \frac{dk}{d\theta_m} + (m-1) + (n-m) \frac{x}{(s+x)} \right] \right)$$

$$\text{or,}\quad \frac{h}{h_m} = 1 + \frac{\theta_m}{\theta}\left[\frac{\theta - \theta_m}{k}\frac{dk}{d\theta_m} + m - 1 + (n-m)\left(\frac{x}{s+x}\right)\right] \qquad \text{XI-10}$$

This is a startling result. If the surface is isothermal and lacks a hydrodynamic starting length, the substitution of previously determined values for m and n with turbulent boundary layers, yields:

$$\frac{h}{h_m} = 0.80 \qquad \text{XI-11}$$

This expression shows that the local coefficient at a point x is eighty per cent of the value of the mean coefficient to the point.

A comparison with Latzko's theoretical results for the flat plate and turbulent boundary layers may be made. Latzko's result for the local surface coefficient is:

$$q'' = 0.0285\,\gamma c v_o \theta_o \left(\frac{\nu_o}{v_o\, x}\right)^{0.2} \qquad \text{XI-12}$$

$$= h\theta_o$$

Latzko's result for the mean surface coefficient is:

$$q' = 0.0356\,\gamma c v_o \theta_o x \left(\frac{\nu_o}{v_o\, x}\right)^{0.2} \qquad \text{XI-13}$$

$$= h_m \theta_m x$$

The ratio of Equation XI-12 to Equation XI-13 yields:

$$\frac{h}{h_m} = \frac{0.0285}{0.0356} = 0.80, \qquad \text{XI-14}$$

which is the same as Equation XI-11.

Equation XI-10 may be put into a more useful form. For a small change in the fluid temperature, it may be assumed

that:

$$k = a_k + b_k\,(t_f')$$

where t_f' comes from Equation VIII-22 as:

$$t_f' = t_o + \theta_m/2$$

so that:

$$k = a_k + b_k(t_o + \theta_m/2) \qquad \text{XI-15}$$

Differentiation of Equation XI-15 yields:

$$\frac{dk}{d\theta_m} = \frac{b_k}{2}$$

Reference to the NBS-NACA Tables (27) permits evaluation of b_k. The data may be given as:

Temperature, °F	k, B $hr^{-1}ft^{-1}F^{-1}$
62	1.472×10^{-2}
98	1.562×10^{-2}

These data give b_k to be 2.5×10^{-5} B $hr^{-1}ft^{-1}F^{-2}$.

The minimum value of k in the experiments is not less than that at 62°F. Examination of the data shows that the maximum value of $\theta - \theta_m$ may be 5 F, approximately. With these extremal values, evaluation of the term $\frac{\theta - \theta_m}{k}\frac{dk}{d\theta_m}$ yields 0.004 as a maximum. Therefore, the term may be neglected when compared with the developed value for h/h_m in Equation XI-11.

Insertion of other known values into Equation XI-10 yields:

$$h/h_m = 1 - \theta_m/\theta(0.09 + 0.11x/L) \qquad \text{XI-16}$$

It is of interest to test Equation XI-16 with

experimental data. The comparison between calculated values and experimental results may be made in Table XXV. Examination of the table shows that the experimental result is greater than the calculated value in almost all cases. The maximum difference between the experimental value and the calculated value is about 12.9 per cent, based on the experimental value. Thus Equation XI-16 would give conservative results for h.

The agreement between experimental and calculated results is very good for values of s/L smaller than 0.95. The majority of differences between experimental and calculated results are of the order of five percent of the experimental result.

When consideration is given to the nature of the approximations required for the calculation of the surface coefficients from the basic data, the agreement between experimental and calculated results is considered to be satisfactory.

A surface configuration function for the local surface coefficient may be obtained. If it is assumed that the surface is isothermal, then Equation XI-16 yields.

$$(N_{Nu})'_x = (N_{Nu})_x \, (0.91 - 0.11 \, x/L)$$

Substitution for $(N_{Nu})_x$ from Equation X-2 yields:

$$(N_{Nu})'_x = 0.0307 \, (N_{Re})_L^{0.8} \left[0.91(x/L)^{0.91} - 0.11(x/L)^{1.91}\right] \qquad \text{XI-17}$$

This equation may be put into a form wherein the term in the brackets becomes unity when x is made equal to L, if

the constants in the brackets are multiplied and the equation constant is divided by 1.25. The result is:

$$(N_{Nu})'_x = 0.0246\ (N_{Re})_L^{0.8}\ \left[1.138(x/L)^{0.91} - 0.138(x/L)^{1.91}\right] \qquad \text{XI-18}$$

and,

$$(N_{Nu})'_L = 0.0246\ (N_{Re})_L^{0.8}\ \left[1.138(x/L^{-0.09} - 0.138(x/L)^{0.91}\right] \qquad \text{XI-19}$$

A comparison of surface configuration functions is made in Tables XXVI and XXVII. Equation II-8 in combination with Equation III-2 remains unchanged if C_o' is divided and $\emptyset$ is multiplied by 1.25. In this way the configuration function of Jakob and Dow may be made comparable to the present configuration function. The method has been shown in passing from Equation XI-17 to Equation XI-18. This procedure has the effect of permitting the function to assume the value of unity when x becomes equal to L.

Examination of the tables in which extrapolated values are given in parenthesis shows that agreement among the various surface configuration functions is satisfactory for values of x/L greater than 0.3. Greater discrepancies occur for the smaller values of x/L. Except for x/L equal to zero, the functions of Rubesin, Jakob and Dow, and the present work yield acceptable results for small values of x/L. Obviously, extrapolation of Jakob and Dow's empirical form to very small values of x/L is not possible because this form does not consider that the function will become infinity as x/L approaches zero.

TABLE XXV

COMPARISON OF LOCAL SURFACE COEFFICIENTS

Data selected for $(N_{Re})_L$ equal to or greater than 5×10^5.

Series A Runs

Run No.	x, in.	h/h_m Calc.	h/h_m Exp.	Difference, per cent of experimental value
13	16	0.825	0.879	6.2
	20	0.820	0.907	9.8
	24	0.813	0.933	12.9
14	12	0.829	0.869	4.6
	16	0.825	0.885	6.8
	20	0.822	0.903	9.0
	24	0.815	0.916	11.0
15	12	0.832	0.851	2.2
	16	0.828	0.883	6.1
	20	0.822	0.897	8.3
	24	0.813	0.929	12.5
16	8	0.835	0.845	1.2
	12	0.833	0.859	3.0
	16	0.828	0.875	5.4
	20	0.823	0.894	8.0
	24	0.815	0.914	10.8

Series C Runs

8	12	0.871	0.865	-0.7
	16	0.859	0.884	2.8
9	8	0.881	0.889	1.0
	12	0.871	0.889	2.0
	16	0.859	0.902	4.8
10	8	0.880	0.916	3.9
	12	0.872	0.875	0.5
	16	0.860	0.899	4.3
11	4	0.890	0.938	5.1
	8	0.881	0.881	0
	12	0.870	0.896	2.9
	16	0.859	0.901	4.7

TABLE XXV, Continued

Series C Runs, continued

Run No.	x, in.	h/h_m Calc.	h/h_m Exp.	Difference, per cent of experimental value
12	4	0.891	0.934	4.6
	8	0.880	0.904	2.7
	12	0.870	0.907	4.1
	16	0.859	0.929	7.5
13	4	0.891	0.919	3.1
	8	0.880	0.898	2.0
	12	0.869	0.894	2.8
	16	0.859	0.905	5.1
14	4	0.891	0.926	3.8
	8	0.879	0.879	0
	12	0.870	0.894	2.7
	16	0.854	0.894	8.7
15	4	0.890	0.941	5.4
	8	0.877	0.908	3.4
	12	0.869	0.909	4.5
	16	0.860	0.914	5.9
		Series E Runs		
7	4	0.903	0.913	1.1
	8	0.892	0.925	3.6
	12	0.881	0.945	6.8
8	4	0.903	0.943	4.3
	8	0.893	0.909	1.7
	12	0.884	0.904	2.2
9	4	0.902	0.932	3.2
	8	0.892	0.919	2.9
	12	0.884	0.923	4.2
10	4	0.903	0.901	0
	8	0.894	0.913	2.1
	12	0.884	0.923	4.2
12	4	0.903	0.925	2.4
	8	0.894	0.911	1.9
	12	0.885	0.913	3.1
13	4	0.903	0.930	2.9
	8	0.892	0.941	5.2
	12	0.883	0.936	5.7

TABLE XXVI

COMPARISON OF SURFACE CONFIGURATION FUNCTIONS

For Local Surface Coefficients and Turbulent Boundary Layers
Extrapolated values in Parentheses

(x/L)	Rubesin Equ. III-5	Maisel and Sherwood Equ. III-3	Jakob and Dow Equ. III-2	Present Work Equ. XI-19	(s/L)
0.0	∞	(∞)	(1.750)	(∞)	1.0
0.1	1.518	1.318	(1.490)	1.383	0.9
0.2	1.341	1.220	(1.311)	1.281	0.8
0.3	1.246	1.166	(1.200)	1.223	0.7
0.4	1.183	1.128	1.130	1.176	0.6
0.5	1.136	1.098	1.090	1.138	0.5
0.6	1.099	(1.075)	1.069	1.103	0.4
0.7	1.069	(1.057)	1.053	1.077	0.3
0.8	1.042	(1.036)	1.042	1.049	0.2
0.9	1.021	(1.019)	1.025	1.023	0.1
1.0	1.000	(1.000)	(1.000)	1.000	0.0

TABLE XXVII

DEVIATION OF SURFACE CONFIGURATION FUNCTIONS

For Local Surface Coefficients and Turbulent Boundary Layers

Body of table is the deviation in per cent, based on Rubesin's result.
Extrapolated values in Parentheses

(x/L)	Present Work	Jakob and Dow	Maisel and Sherwood	(s/L)
0.0	(0)	(100)	(0)	1.0
0.1	- 8.9	(- 1.8)	- 13.2	0.9
0.2	- 4.5	(- 2.2)	- 9.0	0.8
0.3	- 1.8	(- 3.7)	- 6.5	0.7
0.4	- 1.6	- 4.5	- 4.8	0.6
0.5	+ 0.2	- 4.1	- 3.4	0.5
0.6	+ 0.4	- 2.8	(- 2.2)	0.4
0.7	+ 0.8	- 1.5	(- 1.2)	0.3
0.8	+ 0.5	0	(- 0.7)	0.2
0.9	+ 0.2	+ 0.3	(- 0.3)	0.1
1.0	0	(0)	(0)	0.0

CHAPTER XII

THE EFFECT OF SURFACE CURVATURE

The experimental results with respect to curvature are conveniently compared by assuming unit Reynolds number, zero hydrodynamic starting length, and unit total length. This procedure serves to make Nusselt number equal to C_o' of Table IV and the influence of curvature is reflected therein.

The available experimental results for curved surfaces with air at atmospheric pressures and temperatures are:

Source	C_o'	K, ft^{-1}
Jakob and Dow	0.0280	18.46
Present Work	0.0307	38.46

Jakob and Dow have given a correction factor, a result of theoretical reasoning, which is a multiplier for Latzko's result for the flat plate. The factor is:

$$F = 1 + (3/10)\, bK \,. \qquad \text{XII-1}$$

It is noted that F is a linear function of the curvature. Therefore, it is assumed that C_o' may be given in the form:

$$C_o' = C_o + b_K K \,. \qquad \text{XII-2}$$

Substitution of the two experimental results enables solution of Equation XII-2. The solution yields:

$$C_o' = 0.0255 + 1.35 \times 10^{-4} K \,, \qquad \text{XII-3}$$

wherein C_o is 0.0255 and b_K is 1.35×10^{-4} ft.

Extrapolation of Equation XII-3 to zero curvature yields C_o' as equal to 0.0255. It may be recalled that Latzko's value for the flat plate is 0.0253. These results

are illustrated in Figure 38.

The theoretical reasoning of Jakob and Dow may be summarized as:

$$q = 2\pi r v_o c\, \theta_o b\, \gamma \left(\frac{n}{(n+1)(2n+1)}\right)\left(1 + \frac{b}{r}\,\frac{(n+1)(2n+1)}{(n+2)(2n+2)}\right) . \qquad \text{XII-4}$$

This equation comes from considering a heat and mass balance for an elemental slice through the boundary layer in which it is assumed that the velocity distribution is given by:

$$v = (y/b)^n v_o , \qquad \text{XII-5}$$

and that the temperature distribution is similar.

Jakob (30) has shown that the exponent n in Equation XII-5 may vary from 1/6 to less than 1/10 for flow inside tubes. It is of interest to determine how similar changes may affect Equation XII-4. The computation yields:

n	$\frac{n}{(n+1)(2n+1)}$	$\frac{(n+1)(2n+1)}{(n+2)(2n+2)}$
1/6	0.1071	0.308
1/7	0.0973	0.300
1/8	0.0889	0.294
1/9	0.0818	0.289
1/10	0.0758	0.286

This computation shows that a larger exponent yields greater heat transfer.

It is noted from Table IV that Colburn's correlation gives the smallest experimental result for the flat plate, in which the curvature is zero. Latzko's result is based upon the exponent n being 1/7, as suggested by von Kármán (31). Comparison of these two results shows that Colburn's

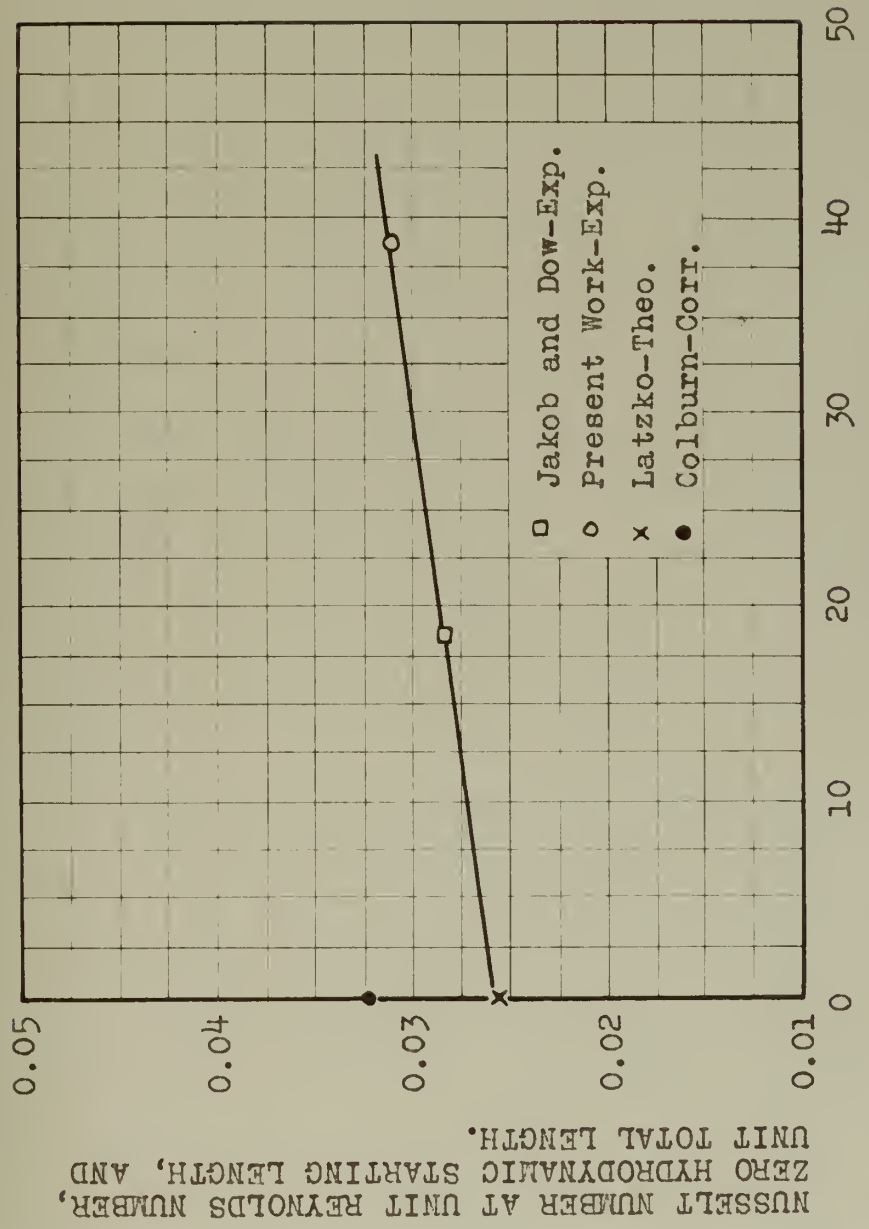


FIGURE 38. INFLUENCE OF CURVATURE.

value is 1.265 times greater than Latzko's value. Such a result requires the exponent n to be about 1/4.

On the other hand, the effect of the exponent on the factor F is seen to be small in comparison with the effect of the exponent on the flat plate result. The Jakob and Dow result for a cylinder 1.3 inches in diameter is about ten per cent higher than Latzko. If the curvature has no effect, then this increase is of the same order of magnitude given by n equal to 1/6.

The present result is about twenty-one per cent higher than that of Latzko. If the curvature has no effect, then n should be about 1/4 as with Colburn. Thus the results for the flat plate are not compatible with those for curved surfaces for any reasonable change in the value of the exponent.

Equation XII-4 shows that an increase in the boundary layer thickness causes an increase in the heat transfer. It is possible that the inter-relation between the boundary layer thickness and the exponent n is such that the net effect on the change in heat transfer between the plate and a cylinder is zero. However, by the Jakob and Dow result, it is seen that the inter-relation reaches a minimum value somewhere between the present result and that for the plate as given by Colburn. Such a condition may not occur for reasonable changes in the exponent because it has been shown that the exponent would have to change from 1/4 to 1/6 and back to 1/4 with corresponding changes in the boundary layer

thickness.

As a consequence of this discussion, it is concluded that the curvature is a variable of great importance. Reasonable changes in the value of the exponent or of the boundary layer thickness do not account for the experimental results with cylinders.

The influence of curvature may be added to previously determined results, yielding:

$$(N_{Nu})_x = (0.0255 + b_K/r)(N_{Re})_L^{0.8}(x/L)^{0.91} \qquad \text{XII-6}$$

and

$$(N_{Nu})_L = (0.0255 + b_K/r)(N_{Re})_L^{0.8}(x/L)^{-0.09} \qquad \text{XII-7}$$

in which b_K has the value 1.35×10^{-4} ft and r is 1/K ft.

CHAPTER XIII

SUMMARY AND CONCLUSIONS

1. A heat transfer element was constructed having a nominal diameter of 0.624 inches. Cylindrical nosepieces of various lengths having hemispherical nosetips were attached to the heat transfer element. The nosepiece lengths were varied in the proportion 55:1, and the thermal lengths were varied in the propertion 7:1, so that the ratio of thermal length to total length varied from 0.141 to 0.983.

2. The heat transfer element was placed in an air stream so that the surface generators were parallel to the flow. The stream velocity was varied from 9.9 ft sec^{-1} to 122.8 ft sec^{-1} corresponding to a variation in Reynolds number from 2.6×10^4 to 2.4×10^6 based on a defined total length as the characteristic length. Transition to turbulence started at Reynolds number of 50,000 and was completed for Reynolds number as low as 3×10^5 and as high as 6×10^5.

3. The result of measurements was obtained for turbulent boundary layers only. The result could be expressed as:

$$(N_{Nu})_x = 0.0307\ (N_{Re})_L^{0.8} (x/L)^{0.91}\ , \qquad \text{X-2}$$

where $(N_{Nu})_x$ is based on the mean surface coefficient of heat transfer and the thermal length $\hat{x}$ as characteristic length, and the Reynolds number based on a defined total length L as characteristic length. The above equation was found to be valid for variable thermal length as well as variable hydrodynamic starting length.

4. An equation for the Nusselt number based on the local surface coefficient of heat transfer was developed from Equation X-2 by differentiation. The developed equation was tested with experimental data. The developed equation gave results lower than the experimental measurements varying from zero to 12.9 per cent, with an average variation of five per cent.

5. The total length of the heat transfer element and attached nosepieces was such that an unsupported overhang of three feet occurred. Vibration and cross flow studies were made and it was concluded that the experimental results were not influenced by these factors.

6. The results of a previous investigation by Jakob and Dow were used in conjunction with the present results to determine the influence of curvature. The final result could be expressed as:

$$(N_{Nu})_x = (0.0255 + b_K/r)(N_{Re})_L^{0.8}(x/L)^{0.91} , \qquad \text{XII-6}$$

where $b_K = 1.35 \times 10^{-4}$ ft and r is the radius of a section of the surface perpendicular to the air stream.

7. Equation XII-6 coupled with the theory of Latzko for the flat plate leads to the conclusion that the experimental results for the flat plate reported by different previous sources are in error and that Latzko's result is more nearly correct for the flat plate.

8. The theoretical reasoning of Jakob and Dow coupled with the present result leads to the conclusion that the curvature may be increased to 70 ft^{-1} in Equation XII-6 without serious error.

APPENDIX I

VOLT BOX MODIFICATION

Modification of a Leeds and Northrup Co. volt box, No. 418271, was undertaken so that all direct current electrical potential differences likely to be encountered could be measured with a potentiometer. The portable precision potentiometer at hand was capable of measuring potential differences up to eighty millivolts, whereas the volt box was designed for use with a 1.5 volt potentiometer.

A volt box consists of a high resistance coil provided with taps to accomodate various impressed potential differences. An additional tap was provided so that the precision potentiometer could be used.

The volt box was provided with terminals for impressed voltages of 15, 150, and 300 volts. These terminals are designated as E_{15}, E_{150}, and E_{300}, respectively. The initial measuring terminal is designated as $e_{1.5}$ and the additional measuring terminal is designated as $e_{0.075}$.

After modification, the volt box was tested by measuring the various resistances with a Wheatstone bridge. These measurements were:

Coil Portion	Resistance, ohms
$R_{0.075}$	15.09
$R_{1.5}$	300.2
R_{15}	3000
R_{150}	30,000
R_{300}	60,000

where the subscripts correspond to the voltage terminals.

An additional test was made by connecting 1.5 volt dry cells in series to the volt box. Simultaneous observations were made at the measuring terminals.

The test data are given in Table I-1. These data show that the ratio $e_{1.5}/e_{0.075}$ may be 19.92. The probable error may be obtained from the formula[1]:

$$r_{\bar{m}} = 0.8453 \left[n^2(n-1)\right]^{-1/2} \sum_{i=1}^{n} X_i$$

where $r_{\bar{m}}$ is the probable error of the mean,

n is the number of independent observations,

X_i is the difference between the i^{th} observed value and the arithmetic mean,

The computation yields:

$$r_{\bar{m}} \approx 0.8453\ (256 \times 15)^{-1/2} \times 0.247$$
$$\approx 0.0034$$

The test data may be converted into a more useful form as:

$$E_{300} = 200e_{1.5} = 3984e_{0.075}$$
$$E_{150} = 100e_{1.5} = 1992e_{0.075}$$
$$E_{15} = 10e_{1.5} = 199.2e_{0.075}$$

where the e are the potential differences at the measuring terminals in volts.

These results may be compared with that obtained with

[1] Handbook of Engineering Fundamentals. Ovid W. Eshbach, Editor. Wiley Engineering Handbook Series. First ed. Eleventh printing. John Wiley and Sons, Inc. New York. 1947.

the Wheatstone bridge as:

$$e_{1.5}/e_{0.075} = 300.2/15.09$$
$$= 19.89 .$$

It may be noted that the maximum current that flows in the volt box at rated impressed potential differences is:

$$I = 300/60,000 = 150/30,000 = 15/3000$$
$$= 0.005 \text{ amperes.}$$

TABLE I-1

VOLT BOX TEST DATA

Number of Dry Cells in series	Terminal	$e_{1.5}$ mv	$e_{0.075}$ mv	Ratio $e_{1.5}/e_{0.075}$	Diff. from mean
1	300	7.923	0.398	19.907	0.017
1	300	7.925	0.398	19.912	0.012
2	300	15.740	0.790	19.924	0.0
2	300	15.740	0.790	19.924	0.0
3	300	23.53	1.182	19.907	0.017
3	300	23.53	1.181	19.924	0.0
4	300	31.35	1.575	19.905	0.019
4	300	31.35	1.575	19.905	0.019
4	150	62.70	3.149	19.911	0.013
4	150	62.69	3.149	19.908	0.016
3	150	47.06	2.363	19.915	0.009
3	150	47.07	2.363	19.920	0.004
2	150	31.46	1.578	19.937	0.013
2	150	31.46	1.579	19.924	0.0
1	150	15.840	0.792	20.000	0.076
1	150	15.845	0.792	19.956	0.032
			Totals.....	318.779	0.247
			Arithmetic mean..	19.924	

APPENDIX II

CALIBRATION OF WESTON SHUNT

A Weston Electrical Instrument Co. shunt, number 33958, was used to measure the flow of electric current where necessary. This shunt was provided with five-ampere, twenty-ampere, and fifty-ampere terminals. Of these, the five-ampere and the twenty-ampere portions were tested.

The method of testing used was to connect this shunt in series with a standard resistance and then allow an electric current to flow through them. The potential drop caused by each shunt was measured with a potentiometer at various flows of current. The source of current was a storage battery.

The standard resistance was a Siemens, number 2006346, rated for fifty amperes in air, made of Manganin, and having a resistance of 0.01 ohms at 20 deg. C.

For the five ampere range of the Weston shunt; using the formula[1]:

$$r_{\bar{m}} \approx 0.8453x \left[n^2(n-1)\right]^{-1/2n} \sum_{i=1} X_i$$

where $r_{\bar{m}}$ is the probable error of the mean,

n is the number of independent observations,

X_i is the difference between the i^{th} observed value and the arithmetic mean,

there results:

$$r_{\bar{m}} \approx 0.8453 \times \left[1600(39)\right]^{-1/2} \times 0.0097$$

[1]Handbook of Engineering Fundamentals. Ovid W. Eshbach, Editor. Wiley Engineering Handbook Series, first edition, eleventh printing. John Wiley and Sons, Inc. New York. 1947. pg 2-126.

or, $r_m \approx 0.00003$

The value of the ratio used is 0.4340.

For the twenty ampere portion, the value of the ratio used is 1.844.

Since the electric resistance of the standard shunt is 0.01 ohms, using Ohm's Law, it follows that:

for the five ampere portion of the Weston shunt,

$$I = 0.04340 \times E_w, \text{ and}$$

for the twenty ampere portion of the Weston shunt,

$$I = 0.1844 \times E_w$$

where I is the electric current in amperes, and

E_w is the potential difference across the Weston shunt in millivolts.

TABLE II-1

CALIBRATION OF WESTON SHUNT

E_w, in millivolts	E_s, in millivolts	Ratio E_s/E_w	Diff.
	Five ampere portion		
4.838	2.099	0.4339	0.00008
4.838	2.097	0.4334	0.00058
4.835	2.096	0.4335	0.00048
4.833	2.095	0.4335	0.00048
6.859	2.973	0.4334	0.00058
6.856	2.974	0.4338	0.00018
6.852	2.973	0.4339	0.00008
6.852	2.973	0.4339	0.00008
13.861	6.018	0.4342	0.00022
13.872	6.020	0.4340	0.00002
13.872	6.021	0.4340	0.00002
13.876	6.022	0.4340	0.00002
21.27	9.22	0.4335	0.00048
21.26	9.23	0.4331	0.00088
21.26	9.23	0.4331	0.00088
21.28	9.24	0.4342	0.00022
27.80	12.07	0.4342	0.00022
27.80	12.07	0.4342	0.00022
27.81	12.07	0.4340	0.00002
27.81	12.07	0.4340	0.00002
34.87	15.13	0.4339	0.00008
34.84	15.12	0.4340	0.00002
34.89	15.16	0.4345	0.00052
34.92	15.19	0.4350	0.00102
42.14	18.29	0.4340	0.00002
42.15	18.29	0.4339	0.00008
42.15	18.30	0.4342	0.00022
42.16	18.30	0.4341	0.00012
49.25	21.38	0.4341	0.00012
49.26	21.38	0.4340	0.00002
49.26	21.38	0.4340	0.00002
49.26	21.38	0.4340	0.00002
59.84	25.99	0.4343	0.00032
59.85	25.99	0.4343	0.00032
59.84	25.98	0.4342	0.00022
59.83	25.98	0.4342	0.00022
70.95	30.80	0.4341	0.00012
70.98	30.82	0.4342	0.00022
70.98	30.81	0.4341	0.00012
70.98	30.81	0.4341	0.00012
Totals		17.3590	0.00968
Arithmetic mean		0.43398	

TABLE II-1, Continued

CALIBRATION OF WESTON SHUNT

E_w, mv	E_s, mv	Ratio, E_s/E_w
	Twenty ampere portion	
16.96	31.27	1.844
16.96	31.27	1.844
11.13	20.54	1.845
11.13	20.52	1.844
5.971	11.012	1.844
5.972	11.014	1.844

Room temperature: (For both portions)
At start..... 73°F
At end..... 75°F

APPENDIX III

CALIBRATION OF THERMOCOUPLES

The seven thermocouples were calibrated simultaneously. The hot junctions were in an atmosphere of condensing steam in a hypsometer. The cold junctions were at the temperature of a mixture of melting ice and water at atmospheric pressure. The hypsometer, vented to the atmosphere, was supplied with the steam from distilled water and was equipped with a water manometer for indicating interior pressure excess.

The data and results are as follows:

Thermocouple No.	emf, millivolts	Equivalent temp., °F.
1	4.258	211.2
2	4.258	211.2
3	4.258	211.2
Four in series	17.00	211.0

The computed temperature of condensing steam for a corrected barometric reading of 743.1 mm of mercury is 210.9 °F, using the Keenan and Keyes formula (25)

APPENDIX IV

CALROD HEATER SURFACE TEMPERATURE EXPLORATION

The determination of the uniformity of heat generation along the length of the Calrod heater was most important. Direct measurements of this characteristic could not be made.

A convenient indirect method is provided by measurement of surface temperature. If a heated element, surrounded by still air at a uniform temperature, is supported horizontally, then heat is transferred by free convection and radiation. The surface assumes an equilibrium temperature when the steady state is reached.

If the heat generation is uniform, the surface temperature will be the same over the whole length. Likewise, the surface coefficient of heat transfer remains constant. Variations in surface temperature along the length may be expected if the heat generation is non-uniform.

Study of the theory of heat transfer by free convection shows that the error made by assuming that the coefficient of heat transfer remains constant for small surface temperature variations is negligible. Also, if the surface temperature is higher at one place than at another place on the element, then the heat transferred from the one place is greater than that from the other place. It follows, therefore, that the heat released from the coil is greater at the one place than at the other. Thus the measurement of the surface temperature becomes a means to determine the

uniformity of heat generation.

A knowledge of the specific surface temperature is not required. The temperature distribution along the element is sufficient.

The measurement of the surface temperature was accomplished by suspending a movable thermocouple from the heater. This procedure causes an interference with the heat transfer process at the point of application of the thermocouple, but it is reasonable to assume that the influence of the interference is the same at all points of application.

The thermocouple, non-standard, was made of:

Chromel P, No. 40 Brown and Sharp Gauge, 0.0031 inches diameter,

Alumel, No. 40 Brown and Sharp Gauge, 0.0031 inches diameter.

The calibration data[1] for a thermocouple made of these wires are:

Temperature, °F	Millivolts		Error, °F
	No. 40 ga.	No. 18 ga.	No. 40 ga.
77	0.998	0.998	0
161	2.977	2.915	+ 3
227	4.547	4.440	+ 4
668	14.450	14.430	+ 1

The No. 18 gauge thermocouple follows the Leeds and Northrup Co. tables, Standard 31031.

[1]Dr. M. Spielman, Associate Research Engineer, Department of Mechanical Engineering, Illinois Institute of Technology, was kind enough to furnish these data and to show me the method he evolved for butt-welding these wires.

In service, the hot junction was located so that the welded joint was at the top surface of the Calrod heater being in contact with the surface for a distance of one-half the circumference of the heater.

A block of wood suspended eighteen inches below the heater served as the site for the cold junction for this system. The chromel wire was soldered to a copper-constantan thermocouple and the alumel wire was soldered to a copper wire. These wires were fastened and glued to the wood block.

The temperature of melting ice in water was the cold junction reference temperature for the copper-constantan thermocouple.

Two series of runs were made with this thermocouple system. One series was made with an electrical energy input of 125 watts and the other at 41.2 watts.

The recommended method for compensating for the cold junction temperature when the cold junction is at a temperature different from standard is to convert the observed temperature at the cold junction to the millivolt equivalent of the thermocouple.[1] In the present case, the cold junction is at a higher temperature than the reference standard, hence the millivolt equivalent is added to the observed potential difference to obtain an argument for use of the

[1]Applications of Chemical Engineering. H. McCormack, Editor. First edition. Second printing. D. Van Nostrand Co., Inc. New York. 1940.

conversion tables.

It may be recalled that the cold junction temperature of the chromel-alumel thermocouple was measured with a copper-constantan thermocouple. To reduce the commission of errors of conversion, the data from the Leeds and Northrup Co. tables, Standard 31031 may be:

Temperature, °F	Millivolts, 32 °F reference	
	Copper-constantan	Chromel-alumel
100	1.52	1.52
90	1.29	1.29
80	1.06	1.06
70	0.83	0.84

Inspection of these data shows that the two kinds of thermocouples may be considered to be thermometrically equivalent for the range of temperature indicated.

The temperature at the wood block was considered to be the temperature of the air passing across the heater surface.

The observed data are given in Tables IV-1 and IV-2. It is seen that one end of the heater was hotter and that the heat release from the coil was non-uniform.

A reasonable estimate of the temperature distribution along the heater may be obtained by assuming that the temperature variation is a linear function of the length. This estimate may be obtained by computing a least squares line to fit the data with the middle twenty-four inches as a basis.

Computation yields the following:

$$\theta_A = 367.1 - 0.43\ z\ ,\ F, \text{ and} \qquad \text{(Part A)}$$

$$\theta_B = 160.4 - 0.19\ z\ ,\ F \qquad \text{(Part B)}$$

where z is the distance along the heater beginning at the hot end, in inches.

TABLE IV-1

CALROD HEATER SURFACE TEMPERATURE

Part A: 125 watts input

Distance along heater, in.	Surface temp. minus room temp., F		Variation from mean, F	
	Run 1	Run 2	Run 1	Run 2
7	316	316	- 38.0	- 43.7
8	354	353	0	- 6.7
9	365	362	+ 11.0	+ 2.3
10	366	366	+ 12.0	+ 6.3
11	365	367	+ 11.0	+ 7.3
12	362	359	+ 8.0	- 0.7
13	356	356	+ 2.0	- 3.7
14	356	356	+ 2.0	- 3.7
15	355	357	+ 1.0	- 2.7
16	361	361	+ 7.0	+ 1.3
17	363	365	+ 9.0	+ 5.3
18	362	369	+ 8.0	+ 9.3
19	362	366	+ 8.0	+ 6.3
20	357	368	+ 3.0	+ 8.3
21	360	362	+ 6.0	+ 2.3
22	357	364	+ 3.0	+ 4.3
23	351	360	- 3.0	+ 0.3
24	352	361	- 2.0	+ 1.3
25	349	355	- 5.0	- 4.7
26	348	355	- 6.0	- 4.7
27	351	360	- 3.0	+ 0.3
28	356	360	+ 2.0	+ 0.3
29	351	358	- 3.0	- 1.7
30	350	359	- 4.0	- 0.7
31	351	361	- 3.0	+ 1.3
32	351	360	- 3.0	+ 0.3
33	351	356	- 3.0	- 3.7
34	347	358	- 7.0	- 1.7
35	345	359	- 9.0	- 0.7
36	345	347	- 9.0	- 12.7
37	341	344	- 13.0	- 15.7
38	344	344	- 10.0	- 15.7
39	346	346	- 8.0	- 13.7
40	341	342	- 13.0	- 17.7
41	311	311	- 43.0	- 48.7
Arithmetic mean of middle twenty-four inches.....	354.0	359.7		

TABLE IV-2

CALROD HEATER SURFACE TEMPERATURE

Part B: 41.2 watts input

Distance along heater, in.	Surface temp. minus room temp., F		Variation from mean, F	
	Run 1	Run 2	Run 1	Run 2
7	132	130	- 25.0	- 24.7
8	150	148	- 7.0	- 6.7
9	157	156	0	+ 1.3
10	160	160	+ 3.0	+ 5.3
11	161	157	+ 4.0	+ 2.3
12	159	155	+ 2.0	+ 0.3
13	157	154	0	- 0.7
14	156	154	- 1.0	- 0.7
15	158	152	+ 1.0	- 2.7
16	157	154	0	- 0.7
17	158	158	+ 1.0	+ 3.3
18	159	159	+ 2.0	+ 4.3
19	161	159	+ 4.0	+ 4.3
20	162	158	+ 5.0	+ 3.3
21	161	158	+ 4.0	+ 3.3
22	159	156	+ 2.0	+ 1.3
23	159	153	+ 2.0	- 1.7
24	159	155	+ 2.0	+ 0.3
25	156	155	- 1.0	+ 0.3
26	154	155	- 3.0	+ 0.3
27	157	155	0	+ 0.3
28	155	155	- 2.0	+ 0.3
29	156	155	- 1.0	+ 0.3
30	155	154	- 2.0	- 0.7
31	155	154	- 2.0	- 0.7
32	155	153	- 2.0	- 1.7
33	154	153	- 3.0	- 1.7
34	155	151	- 2.0	- 3.7
35	154	151	- 3.0	- 3.7
36	153	151	- 4.0	- 3.7
37	152	150	- 5.0	- 4.7
38	150	148	- 7.0	- 6.7
39	150	147	- 7.0	- 7.7
40	147	144	- 10.0	- 10.7
41	134	131	- 23.0	- 23.7
Arithmetic mean of middle twenty-four inches.....	157.0	154.7		

BIBLIOGRAPHY

1. Koch, W., Ueber die Waermeabgabe geheitzer Rohre bei verschiedener Niegung der Rohrachse. Beihefte zur Gesundheitsing. Vol. I, No. 22. R. Oldenbourg, Munich and Berlin. 1927.

2. Jakob, M., and Dow, W.M., Heat Transfer from a Cylindrical Surface to Air in Parallel Flow with and without Unheated Starting Sections. Trans. A.S.M.E. Vol. 68, No. 2, Feb., 1946.

3. Prandtl, L., Motion of Fluids with Very Little Viscosity. Translated in NACA Tech. Memo. 452. Washington, D.C. March, 1928.

4. Nusselt, W., Der Waermeuebergang in Rohrleitungen. Forsch. Arb. Ingenieurwes. Vol. 89. 1910.

5. Jakob, M., Heat Transfer, Vol. I. John Wiley and Sons, Inc. New York. 1949.

6. McAdams, W.H., Heat Transmission. Second ed. Sixth imp. McGraw-Hill Book Co., Inc. New York. 1942.

7. Reynolds, O., An Experimental Investigation of the Circumstances Which Determine Whether the Motion of Water Will be Direct or Sinuous, and of the Law of Resistance in Parallel Channels. Phil. Trans. Royal Society. London. 1863.

8. Dodge, R.A., and Thompson, M.J., Fluid Mechanics, First ed. Fifteenth imp. McGraw-Hill Book Co., Inc. New York. 1937.

9. Élias, F., The Transference of Heat from a Hot Plate to an Air Stream. Translated in NACA Tech. Memo. 614. Washington, D.C. 1931.

10. Eckert, E.R.G., Introduction to the Transfer of Heat and Mass. First ed. McGraw-Hill Book Co., In. New York. 1950.

11. ten Bosch, M., Die Waermeuebertragung. Third ed. Julius Springer. 1936.

12. Pohlhausen, E., Der Waerme-austauch zwischen festen Koerpen und Flussigkeiten mit kleiner Reibung und kleiner Waermeleitung. Zeits. fur angew. Math. und Mech. Vol. 1. No. 2. 1921.

13. Latzko, H., Heat Transfer in a Turbulent Liquid or a Gas Stream. Translated in NACA Tech. Memo. 1068. Washington, D.C. 1944.

14. Colburn, A.P., A Method of Correlating Forced Convection Heat Transfer Data and a Comparison with Fluid Friction. Trans. A.I.Ch.Eng. Vol.29. 1933.

15. Rubesin, M.W., An Analytical Investigation of Convective Heat Transfer from a Flat Plate having a Stepwise Discontinuous Surface Temperature. Advance Copy A.S.M.E. Paper No. 48-A043.

16. Maisel, D.S., and Sherwood, T.K., Evaporation of Liquids into Turbulent Gas Streams. Chem. Eng. Prog. Vol. 46. 1950.

17. Johnson, H.A., and Rubesin, M.W., Aerodynamic Heating and Convective Heat Transfer-Summary of Literature Survey. Trans. A.S.M.E. Vol. 71. No. 5. July, 1949.

18. Fisher, W.W., and Norris, R.H., Supersonic Convective Heat Transfer Correlation from Skin Temperature Measurements on a V-2 Rocket in Flight. Trans. A.S.M.E. Vol. 71. No. 5. July, 1949.

19. Juerges, W., Der Waermeuebergang an einer ebenen Wand. Beihefte zum Gesundheits-Ingenieur. Reihe I. Beihefte 19. Munich and Berlin. 1924.

20. Griffiths, E., and Awberry, J.H., Heat Transfer between Metal Pipes and Air. Proc. Inst. Mech. Eng. Vol. 125. 1933.

21. Berman, K., Erosion by Heat Transfer and Diffusion. Unpublished thesis, Harvard Univ., Cambridge, Mass. March, 1950.

22. General Electric Co., Electric Heaters and Heating Devices. Catalog GEC-1005. 1949.

23. Ellison Draft Gage Co. Bulletin 9-F. Jan., 1948.

24. Prandtl, L., and Tietjens, O.G., Applied Hydro- and Aerodynamics. Translated by J.P. Den Hartog. First ed. McGraw-Hill Book Co., Inc. New York. 1934.

25. Keenan, J.H., and Keyes, F.G., Thermodynamic Properties of Steam. John Wiley and Sons, Inc. New York. 1949.

26. The NBS-NACA Tables of Thermal Properties of Gases, Table 2.93, Dry Air, Coefficients of Viscosity. Preliminary Issue. National Bureau of Standards. Washington. D.C. July, 1950.

27. The NBS-NACA Tables of Thermal Properties of Gases, Table 2.42, Dry Air, Thermal Conductivity. Preliminary Issue. National Bureau of Standards. Washington, D.C. July, 1950.

28. The NBS-NACA Tables of Thermal Properties of Gages, Table 2.44, Dry Air, Prandtl Number. Preliminary Issue. National Bureau of Standards. Washington, D.C. July, 1950.

29. Schack, A., Industrial Heat Transfer. Translated by H. Goldschmidt and E.P. Partridge. John Wiley and Sons, Inc. New York. 1933.

30. Bates, H.T., Velocity Distribution of Fluids in Turbulent Flow, discussion by M. Jakob. Trans A.I.Ch.Eng. Vol. 36. 1940.

31. von Kármán, T., Ueber laminaire und turbulente Riebung. Zeits. fur angew. Math. und Mech. Vol. 1. 1921.

32. Seibert, O., Heat Transfer of Airfoils and Plates. Translated in NACA Tech. Memo. 1044. Washington, D.C. 1943.

FEB 18
BINDERY
RECAT

14829

Thesis
T34 Tessin
AUTHOR

Influence of curvature upon the
TITLE heat transfer from cylinders
to gas streams parallel to the axis

DATE DUE | BORROWER'S NAME

Library
U. S. Naval Postgraduate School
Monterey, California

thesT34
Influence of curvature upon the heat tra
3 2768 002 03458 9
DUDLEY KNOX LIBRARY